Università Politecnica delle Marche
Scuola di Dottorato di Ricerca in Scienze dell'Ingegneria
Curriculum in Ingegneria Informatica, Gestionale e dell'Automazione

Modelling a Shoal of Marine Biomimetic Vehicles: a Max-Plus Algebra Approach

Ph.D. Dissertation of:
Veronica Bartolucci

Advisor:
Prof. David Scaradozzi

XXXVI edition - new series

Università Politecnica delle Marche
Scuola di Dottorato di Ricerca in Scienze dell'Ingegneria
Facoltà di Ingegneria
Via Brecce Bianche, 12 – 60131 Ancona (AN), Italy

Abstract

This thesis introduces a novel approach to model the coordinated behaviour of fish robots for underwater exploration. A shoal of three biomimetic vehicles is here considered, each one with distinct capabilities, to survey an area via predefined paths covering certain Points of Interest in a cyclical manner. Hence, this formulation involves diversified and repetitive tasks for each robot. The starting point is the knowledge of the practical context of marine vehicles, their technologies, and the theoretical foundations of their mathematical models. Within the theoretical framework, max-plus algebra emerges as a fundamental tool to manage tasks concatenation and synchronization, and thus to effectively model such coordinated activities during patrols. Among the theoretical basis, the notion of causal controlled invariance for max-plus linear systems is also explored, introducing a new algorithm, based on the concept of causal projection, to verify the sufficient conditions for a module to satisfy this property. In other words, it is thus possible to check whether there is a causal state feedback that makes a module invariant for the closed-loop system. Through a series of calculations, the representation of the plant as a max-plus linear system is then obtained, where all variables are based on task-driven rather than time-driven requirements. This approach also leads to the formalization of this synchronised patrol problem, defined as "Model Matching Problem (MMP)". An MMP consists in finding a suitable control law, that forces the obtained plant to behave in accordance with a preestablished model. In this way, the fish robots of the shoal can perform their repetitive tasks according to a predefined strategy. The model is tested in simulation and examples of the resolution of an MMP are given. Finally, the module resulting from the solution of the MMP is tested with the developed algorithm to determine whether it is causal controlled invariant.

Italian title and Abstract

Italian title

Modellazione di un Banco di Veicoli Biomimetici Marini: un Approccio basato sull'Algebra Max-Plus.

Sommario

Questa tesi introduce un nuovo approccio alla modellazione del comportamento coordinato di pesci robot per l'esplorazione subacquea. Si considera un branco di tre veicoli biomimetici, ognuno con capacità distinte, per ispezionare un'area con percorsi predefiniti che coprono dei punti di interesse in modo ciclico. Questa formulazione prevede quindi compiti diversificati e ripetitivi per ciascun robot. Il punto di partenza è la conoscenza del contesto pratico dei veicoli marini, delle loro tecnologie e delle basi teoriche dei loro modelli matematici. All'interno del quadro teorico, l'algebra max-plus emerge come strumento fondamentale per gestire la concatenazione e la sincronizzazione dei compiti e dunque per modellare efficacemente tali attività coordinate durante il pattugliamento. Tra le basi teoriche, si esplora anche la nozione di invarianza causale controllata per sistemi lineari max-plus, introducendo un nuovo algoritmo, basato sul concetto di proiezione causale, per verificare le condizioni sufficienti affinché un modulo soddisfi tale proprietà. In altre parole, è così possibile verificare se esiste una retroazione dello stato causale che renda un modulo invariante per il sistema ad anello chiuso. Tramite una serie di calcoli, si ottiene la rappresentazione del sistema come sistema lineare max-plus, in cui tutte le variabili sono basate su requisiti guidati dai tasks piuttosto che dal tempo. Tale approccio porta anche alla formalizzazione di questo problema di pattugliamento sincronizzato come “Model Matching Problem (MMP)”. Un MMP consiste nel trovare una legge di controllo che forzi il sistema a comportarsi secondo un modello prestabilito. In questo modo, i pesci robot possono eseguire i loro compiti secondo una determinata strategia. Il modello è testato in simulazione seguito da esempi di risoluzione di MMP. Infine, è testato anche il modulo risultante dalla soluzione del MMP per determinare con l’algoritmo sviluppato se è invariante causale controllato.

Acknowledgments

First of all, I would like to express my warmest gratitude to my supervisor, Professor D. Scaradozzi, and to Professor G. Conte from the Department of Information Engineering at Università Politecnica delle Marche. Their insightful discussions and valuable suggestions were greatly beneficial in the preparation of this thesis.
I am also profoundly thankful to the team at LS2N in France for the period spent there and for the constant support and availability during my research endeavors. Their guidance and assistance played a pivotal role in the success of my work.
My heartfel thanks goes also to my colleagues at LabMACS. Your support has been invaluable, and I am so happy to have shared this experience with such a dedicated and inspiring group. Your companionship has been a source of joy and inspiration, making the challenges more manageable and the successes more meaningful.
I extend my sincere gratitude to all those who have been part of this journey, including those not explicitly mentioned but who are well aware of their significance in my life. Your unwavering support, encouragement, and friendship have left a lasting impact, and I am truly grateful to each and every one of you.

Ancona, November 2023

Veronica Bartolucci

Contents

List of Figures

Chapter 1.

Introduction

Max-plus algebra has long been used to model a series of situations, events, and tasks. It represents a class of discrete algebraic systems, and is known as an efficient tool for modelling, as linear systems, and analysing timed discrete event systems. It is used also for performance evaluation and design of networked systems. In this context, the operations *max* and *plus* from conventional algebra are defined as addition and multiplication, respectively, when it does not introduce ambiguity.

The main focus of this thesis is the modelling of the coordinated behaviour of various robots within a team of vehicles. Specifically, the application of max-plus algebra to manage the coordination of vehicles tasked with patrolling specific areas is investigated.

The research hypothesis suggests then that the integration of max-plus algebra into the control framework of marine vehicles enhances the efficiency and effectiveness of patrolling missions, particularly in complex environments. To investigate this hypothesis, the following research questions are posed: How can max-plus algebra be employed to model coordinated activities of marine vehicles during patrolling operations? What novel algorithms and methodologies can be developed to optimize the use of max-plus algebra in enhancing the efficiency and effectiveness of marine vehicle patrolling missions?

The objectives of this work are then: (1) To analyse the applicability of max-plus algebra in modelling marine vehicles during coordinated patrolling operations; (2) To simulate the obtained plant considering a real scenario involving three fish robots; (3) To develop and solve a Model Matching Problem (MMP) for the considered plant, in order to force the max-plus linear plant to generate an output exactly equal to that of a given model of the same kind; (4) To verify if the MMP is actually feasible, testing the module resulting from the solution of the MMP, exploiting an algorithm developed to check its causal controlled invariance, i.e. to verify the existence of a causal state feedback, that makes a module invariant for a closed-loop system.

Considering the perspective of multi-agent exploration by patrolling vehicles, the challenges related to this situation in the context of max-plus algebra have been thoroughly explored. This exploration stems from the need to address two fundamental aspects: on one hand, there's the practical construction of precise models for vehicles themselves, represented here by fish-like biomimetic robots with Body and Caudal Fin (BCF) swimming locomotion, and the development of a theoretical framework to facilitate effective modelling of their behaviour. Regarding the latter aspect, max-plus algebra stands out as a crucial tool. In fact, the innovative aspect of this thesis is the application of max-plus algebra to effectively manage the coordination and synchronization of different vehicles' activities, wherein the patrolling fish robots become one of many case studies that can be considered.

This thesis represents the three-year doctoral work of the author, initially focused on a single fish robot's mathematical model and underwater technologies, to then apply max-plus algebra in the third year. For this reason, the structure of the thesis includes these two distinct aspects: the modelling and technologies of an individual marine vehicle, and the exploration of max-plus algebra and its application in the control of cooperative vehicles. In fact, in the "State of The Art (SoTA)" Chapter 2 and in "Materials and Methods" Chapter 3, the focus is both on marine vehicles and in max-plus algebra. This thesis has been structured in this way to clearly distinguish the theoretical part of these two chapters from the application of the max-plus algebra theory to the problem of patrolling, fully presented in Chapter 4.

An overview of the three-year PhD activities is presented in the Fig. 1.1.

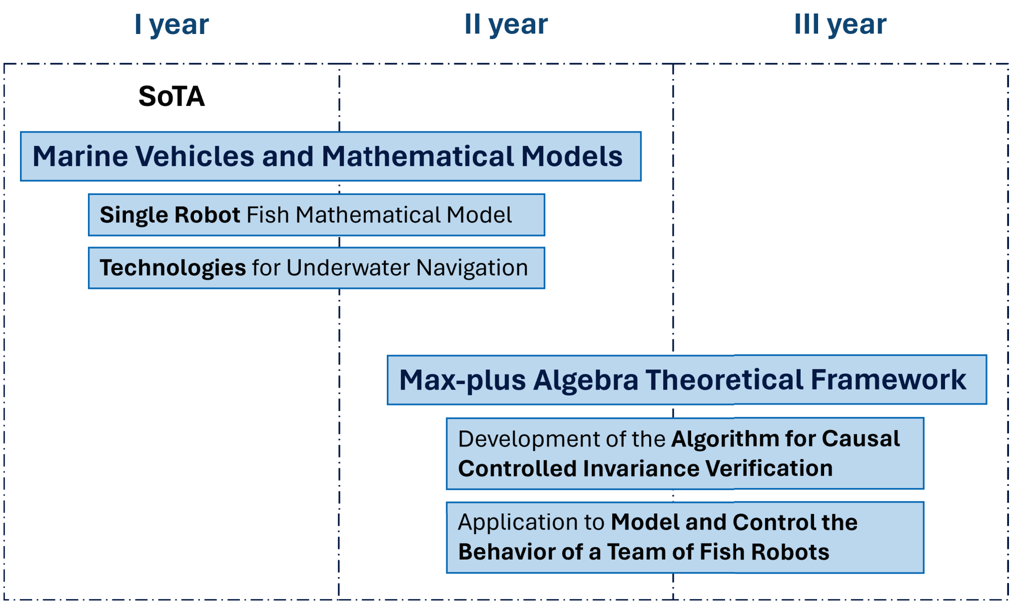

Figure 1.1.: Overview of the three-year PhD activities

This work aims to bridge the gap between practical and theoretical aspects, providing a precise model of patrolling vehicles and leveraging max-plus algebra to ensure coordinated and efficient behaviour. This combination leads to real-world environments through sensors providing precise positioning information. Sensors, like Inertial Measurement Units (IMU), are crucial for subsequent verification processes determining the vehicles' locations. The modelling aspect serves then a dual purpose: firstly, it can enhance sensor quality through techniques that use a combination of IMU, AHRS (Attitude and Heading Reference System), FOG (Fiber Optic Gyroscope), etc. Secondly, in simulation scenarios, it aids in predicting and analysing vehicle displacements, employing mathematical models such as the Fossen model, presented in Chapter 3.1.2.

The resolution of coordination challenges using max-plus algebra is here faced in terms of Model Matching Problem (MMP) and starting from it, the subsequent steps can be the verification and validation of this solution, either in real marine environments or simulated scenarios. In this way, the role of this work becomes evident in connecting theoretical concepts of mathematical models with the practical implementation in simulations and real environment. This integration is crucial, as without it, the two facets might seem disconnected, emphasizing the need for a comprehensive approach to effectively handle the complexities of coordinated behaviour in multi-agent patrolling frameworks.

The starting point of this thesis is represented by Chapter 2, that serves as a comprehensive review of the State of The Art (SoTA), laying the groundwork for the subsequent research. It examines the current landscape of marine biomimetic vehicles, delving into their applications, to then address the concept of agent-based exploration within confined areas. Additionally, it explores the theoretical and practical underpinnings of max-plus algebra, with focused insights into its modelling and applications, controlled invariance, and the MMP. Then, following the SoTA contextualization, Chapter 3 delves into the practical aspects of the research. It outlines various marine vehicles, categorizing their types and focusing on monofin devices. The mathematical model of the latter is introduced, followed by an overview of the main navigation technologies for underwater navigation and localization, such as the already-mentioned IMU and AHRS. The chapter then transitions to the exploration of max-plus algebra: the basic results concerning this algebra are reported, covering key theories such as max-plus linear systems, controlled invariance, the MMP and causality-related concepts. A novel approach with new sufficient conditions of causal controlled invariance of a module is also presented, through the development of an algorithm, used for the verification of such conditions. In other words, with this algorithm, the existence of a causal state feedback, that makes a module invariant for a closed-loop system, can be checked.

The crux of the thesis unfolds in Chapter 4, where the problem of patrolling is addressed. The modelling process is detailed, in order to obtain the representation of the plant as a max-plus linear system. Simulations of the model are also incorporated to enhance the comprehension of the behaviour of the modelled marine vehicles. The chapter further presents the formalization of the synchronised patrol problem as Model Matching Problem, with an example of its resolution. Consequently, the module resulting from the solution of this MMP is tested with the developed algorithm to determine whether it is causal controlled invariant.

The thesis concludes in Chapter 5, where a synthesis of the concepts explored throughout the work is presented, providing a summary of key findings, contributions, and implications for the fields of marine biomimetics, agent-based exploration, and max-plus algebra. A reflection on the results achieved and potential avenues of future research are also outlined.

Summarizing the novelty and contributions of this PhD thesis, it contributes to the advancement of knowledge in the following ways:

- It integrates max-plus algebra into the control framework of marine vehicles, paving the way for enhanced efficiency and effectiveness in patrolling missions.
- The research presents a novel algorithm and methodologies designed to optimize the use of max-plus algebra in marine vehicle patrolling missions, offering innovative solutions to coordination challenges.
- A solution to the MMP is proposed and tested, providing insights into the feasibility and effectiveness of leveraging max-plus algebra in real scenarios.
- The development of an algorithm for verifying causal controlled invariance offers a practical tool for ensuring the stability and reliability of the found solutions for marine vehicle control systems.

These contributions lay the groundwork for future research and application in the field of marine robotics and multi-agent systems.

In conclusion, this work has so far resulted in two publications, one for a French conference, the “Modélisation des Systèmes Réactifs (MSR ’23)”, outcome of the period spent abroad, focusing on the algorithm for causal controlled invariance verification [1], and one publication for “The 34th International Ocean and Polar Engineering Conference (ISOPE-2024)” for the modelling part of the cooperating fish robots [2]. Moreover, the work of this thesis will now be continued within the Project “MAXFISH: Multi agents systems and Max-Plus algebra theoretical frameworks for a robot-fish shoal modelling and control” 20225RYMJE, funded by the MUR Progetti di Ricerca di Rilevante Interesse Nazionale (PRIN) Bando 2022.

Chapter 2.

State of The Art

2.1. State of The Art of Marine Biomimetic Vehicles

Biomimetic robots and vehicles represent a burgeoning field at the intersection of biology, engineering, and technology and they draw inspiration from nature's designs to create devices that mimic the remarkable capabilities of living organisms. This approach has revolutionized various industries, including transportation, manufacturing, and healthcare, and holds immense promise for future advancements. At the current state of the art, there exist different robots that mimics, for example, various animals among them quadrupeds, insects, birds, fishes, etc [3,4]. Biomimetic robots, with their integration of biological characteristics, offer more powerful motor abilities, cognitive abilities, and delicate control processes. Overall, biomimetic robots and vehicles hold great potential in various applications, such as narrow space navigation and eco-friendly environment monitoring [5]. Focusing in this section on fish-like underwater robots, the starting point is the aim of developing solutions that mimic the swimming mechanisms of fishes.

An interesting review is the [6], where the characteristics of aerial-aquatic animals are presented, including an overview of the current marine bioinspired robots that are both aerial and aquatic, and with a comparison between each bioinspired robot and its corresponding animal. The design of biomimetic robotic fishes have evolved over time, with a focus on simplicity and robustness to achieve better swimming performances [7]. Fish swimming capabilities, achieved through millions of years of evolution, have inspired the development of Autonomous Underwater Vehicles (AUVs), capable of moving similar to biological swimmers. By imitating fish swimming, the vehicles can improve their flexibility, efficiency, propulsion efficiency, acceleration, and maneuverability [8, 9]. Most fishes generate thrust by bending their bodies into a backwards-moving propulsive wave that extends to their caudal fin: Body and Caudal Fin (BCF) locomotion. In fact, a classification that is widely employed to diversify the motion of fish is based on the locomotion of the BCF and the median and paired fin (MPF). The initial form of locomotion entails the fish bending its body to create a backward propulsive wave, which extends from its tail up to its caudal fin. The second form of locomotion is similar to BCF locomotion, but the bending motion is restricted to the median and paired fins. Both locomotion mechanisms are further categorized based on the type of movement observed in the propulsive structure. The motion is considered undulatory when there is a visible waveform along the propulsive structure, while the motion is oscillatory when thrust is generated solely by the oscillation about a fixed point of the propulsive structure [8]. Within this thesis, the focus will be placed on robots that use BCF locomotion, since they will be involved for the development of some aspects of the work. Starting with the ancestor of almost all biomimetic swimmers, the RoboTuna [10], created in 1994 by the Massachusetts Institute of Technology (MIT), has to be mentioned. The reason for choosing tuna fish is that it is one of the fastest-swimming fish in nature and it can swim at high speeds for a long time. Another important reason for choosing tuna as a biological inspiration is that different subspecies of tuna have similar morphology, allowing for easy scalability of any design for future use as an autonomous underwater vehicle (AUV). It was also thought that the tuna would allow for a large payload because a large portion of the body would remain rigid due to its swimming mode. MIT and Draper Laboratories developed then the vorticity control unmanned underwater vehicle (VCUUV) based on the success of the RoboTuna project [11]. The VCUUV is an AUV with its own power supply, designed to resemble a real blue fin tuna but scaled up to 2.4 meters in length. Then the RoboPike represents the next generation of robotic swimmers from MIT [12], inspired by the rapid manoeuvring and acceleration abilities of the pike. Moreover, the Japanese National Maritime Research Institute (NMRI) developed a series of simplified link-based robotic fish, including the PF-300 sea bream [13]. The sea bream was chosen for its large side profile area and carangiform swimming style. The two joints of the sea bream were actuated directly by brushless D.C. servomotors housed in small pressure vessels. The tail was left in a skeletal state as the propulsive force was thought to be generated by the caudal fin. Furthermore, the Tokyo Institute of Technology created two robotic dolphins as prototypes for a biomimetically propelled AUV. The first dolphin was powered by a pneumatic system, while the second one used a D.C. servomotor [14, 15]. The Istanbul Technical University also developed a robotic dolphin AUV prototype to improve propulsion efficiency in conventional AUVs [16]. Moreover, the University of Essex has implemented a series of multi-link carangiform and subcarangiform robot swimmers, with the latest being the G9 [17]. The Bei hang University Robotics Institute also developed robotic fishes for underwater vehicles. The fishes had a two-joint propulsion module and were actuated by brushless motors: SPC-II had a fish-like morphology and was useful for underwater archaeology, whereas SPC-III was constructed like a traditional AUV but had a BCF tail instead of a propeller [18, 19]. Furthermore, MIT has recently developed a Soft Robotic Fish called SoFi [20]: this robot has a hydraulic propulsion system that allows it to move its tail and swim at different speeds. The robot can also change direction by adjusting the deflection of its tail and the swimming mode is achieved by pumping water into balloon-like chambers in the fish's tail. When one chamber expands, the tail bends to one side, and when water is pushed to the other channel, the tail bends in the opposite direction. Another interesting work is represented by a bioinspired underwater prototype [21], together with an optimization algorithm to establish its dimensions, considering certain constraints. In that paper, a simulation is also carried out in a fluid to obtain an estimate of forces and drag coefficient. As regards more recent developments, the work of D. Costa et al. can be highlighted, in which the authors designed and experimentally validated [22] a series of bio-inspired vehicles for research purposes: the robot in [23] is driven by an oscillating plate-shaped such as a caudal fin and hinged to the rigid fore-body. Since the number of moving parts is minimal, the system is inexpensive and easy to fabricate and seal. The search for higher propulsive efficiency has improved the design by moving to the undulating tail presented in [24]. Two alternative oscillatory movement types can also be identified [25, 26], improving locomotion.

2.2. State of The Art of Agent-based Exploration

Agent-based exploration of confined areas has been a topic of significant interest in recent research. The scenario under consideration pertains to the collaboration and/or coordination among robots, wherein various vehicles must engage in exchanging and sharing information in order to execute a collective mission. Within the existing body of literature, the management of this particular complexity is achieved through the implementation of Multi-Agent System (MAS) theory, which is acknowledged as a tool possessing the capability to effectively address this matter. This is accomplished by modelling independent components (commonly referred to as agents) that, when combined, are able to carry out tasks that would otherwise be unattainable by a solitary entity or would yield inferior results. The so-called MAS have therefore received considerable attention due to their broad application domain and flexibility, potential robustness to faults, and the capacity to accomplish complex tasks that a single vehicle cannot efficiently address. Since their inception in the 1980s, MAS have been seen as a collection of agents that interact to coordinate their behaviour. The complexity of the environment in which agents operate necessitates a modular and distributed approach. There are three approaches to address these issues: applying principles from software engineering, using cognitive architecture, or employing MAS [27]. Due to computational and knowledge limitations, no single agent can successfully manage tasks, making cooperation necessary [28]. Modularity and abstraction are useful concepts in overcoming these difficulties. MAS offers modularity by developing specialized agents to solve specific problem aspects. Several state-of-the-art methods and strategies related to MAS have been proposed in the past years. Starting with Yan et al., a lidar-based multi-agent exploration approach was developed to balance the robustness of sub-map merging and exploration efficiency [29]. Examples of the utilization of the MAS theory can be observed in the context of energy, as stated in [30] and [31]. These references highlight specific applications that pertain to the restoration [32] and protection [33] of power systems. A significant focus has been placed on the development of tailored solutions for microgrids, as depicted in references [34] and [35]. The utilization of Multi-Agent Systems in these scenarios enables the attainment of various advantages, including but not limited to increased autonomy, reactivity, proactivity, and social ability. Moreover, the extensive utilization of the MAS theory is closely associated with automation. Two significant applications can be identified: home automation and robotics. In the first scenario, MAS has been widely employed to imbue home apparel with intelligence, enabling the distribution and management of diverse resources. For instance, in the work by [36], the authors effectively harnessed a MAS with a suitable model to define and oversee a Home Automation System (HAS). Similarly, in [37], a BACnet intelligent home supervisor system was implemented through the use of BDI agents. Furthermore, the management and orchestration of energy requirements in smart homes have been explored using a multi-agent approach in [38–40]. In the second scenario, MAS are extensively utilized to coordinate the behaviour of various components or robots in order to achieve a shared objective that cannot be satisfactorily accomplished by a single entity. Notable tasks in this regard include navigation [41–43], localization [44,45], exploration and mapping [46,47], search and rescue [48, 49]. The marine environment is one example of an environment that has benefited from the application of this theory. In truth, there have been numerous studies conducted to create Multi-Agent Systems (MAS) specifically tailored for underwater and surface vehicles, which typically collaborate with a ground station in order to navigate this challenging environment. Indeed, these systems must consider various factors among them the reduced visibility, slow communication, and the highly variable nature of the marine environment. Certain studies have focused on specific tasks such as mine countermeasures and marine surveillance [50]. Additionally, specific algorithms have been developed to manage various controls that are applicable in a multi-agent environment, such as fault detection and robot formation [51, 52]. Therefore, also referring to underwater missions, various approaches have been proposed to address the challenges of exploring marine environments. AUVs (Autonomous Underwater Vehicles) are becoming critical in challenging and potentially dangerous sea operations. Everyday activities in which groups of AUVs are employed include, e.g., monitoring, search, exploration, and data collection of hydrogeology or marine biology. Having a look at the literature, an interesting work is the [53], in which researchers have designed swarm intelligent systems that draw inspiration from natural swarms such as bees and slime mould to form integrated underwater swarm robotic exploration systems. These systems utilize decentralized control inspired by swarm intelligence to explore interesting locations, allocate robots, and handle failures [54]. A topic related to these aspects is also the path planning: an interesting review is [55] that deals with the concept of fully autonomy of underwater devices in dynamic uncertain conditions, presenting the different approaches and methods to optimize this autonomous path planning problems, with focus on game-theoretic approaches. A recent work that also needs to be mentioned is the [56], where the topic of swarm robotics is deeply presented, focusing on understanding how to use robot swarms for real-world problems. Another very interesting paper in this regard is that of A. Marino et al. [57], in which a decentralized coordinated strategy for multirobot patrolling (sampling) missions is presented, considering three autonomous marine surface robots that, based only on local information, compute the next point to visit according to a given performance criteria. Coming back to the main problem of this work, fish robots as state of the art can be easily implied to create MAS shoal and study robots team cooperation. The primary purposes of employing a MAS are to improve the overall capabilities and reduce the system's cost exploiting cooperation and coordination among the robots. This can be used to improve robotic shoal intervention in cases of intrusion detection and monitoring. Two recent projects are the EU-funded project WiMUST [58], which aims at developing a system of cooperative AUVs for geotechnical surveying, and the PNRM (National Military Research Project) DAMPS [59], which focuses on the employment of an underwater MAS for locating acoustic sources. Deploying multiple robots presents challenges, such as communication, localization, perception, and coordination, requiring specific methodological approaches. Underwater acoustic signals exhibit high latency and low bandwidth compared to other communication devices. Coordination algorithms need to take this into account, properly managing the exchanged data [60]. When the communication is used for locating a shoal as a unit, model and actuation of each tasks can be seen as a MAS or considering the predefined intervention aims. Overall, these advancements in agent-based underwater exploration contribute to the development of efficient and effective systems for exploring confined areas. In this context, starting with the problem of multi-agent exploration, it was decided to investigate the max-plus algebra framework, presented in the next section, given its potential applications in this field as well.

2.3. State of The Art of Max-Plus Algebra

Max-plus algebra is a class of discrete algebraic systems, that offers the capability to analyse, and model Timed Discrete Event Systems (TDES) as linear systems, particularly in scenarios involving synchronization without concurrency. It is known as an efficient tool for modelling such systems, for performance evaluation and design of networked systems. In this algebraic system, the operations *max* and *plus* from conventional algebra are defined as addition and multiplication, respectively, when it does not introduce ambiguity. The inclusion of the *max* operation should emphasize the non-linearity inherent in these systems, in a traditional sense. However, having a specialized algebra that employs these two operations $\oplus$ (sum) and $\otimes$ (product) redefined as *max* and $+$, it is possible to effectively model Dynamic Event-Driven Systems (DEDS) as linear systems. As it will be presented in section 3.2, the max-plus algebra, which is appropriately named given its operations, does not possess the same properties as the conventional algebra. Linear systems defined over the max-plus algebra were introduced by Cohen and co-authors in the middle of the eighties to model a special class of discrete event systems [61]. Then, the authors presented further developments in the book [62]. A survey on current and future perspectives of the max-plus algebra approach in systems and control theory at the end of the nineties is found in [63], whereas a more recent paper in this regard is the [64], in which the history of max-plus algebra is presented focusing on the field of discrete event systems.

2.3.1. Modelling and Application

Although the introduction of the formalism of the max-plus algebra dates back to the middle eighties, its application has always remained limited to the context of industrial and manufacturing application - notably, production planning and model predictive control (e.g., [65–67]). The current application area is new and promising due to the specific features of the field addressed, related to the modelling for exploration purposes. From the theoretical point of view, the formalism of the max-plus algebra has been exploited in connection with the structural approaches to system and control theory stemming from the geometric approach of [68] and [69]. It has led to exciting results, particularly the model matching problem [70]. The systems simulated using the max-plus algebra formalism constitute generally man-made systems wherein finite resources such as processors, communication channels, or production machinery are shared among multiple “users”, that can be processes, packets, or semi-finished products. The purpose is to achieve common objectives, such as parallel computation, packet transmission, or completion of a finished product on the production line. The lack of concurrency suggests that the available resources are not equal, or alternatively, that the users have been assigned to specific resources in advance, so as to prevent a situation in which a user can be served indiscriminately by multiple resources. One notable application of max-plus algebra is its use of as a foundational technique to develop software capable of analysing and simulating the evolution of production plants. For instance, the software introduced in [71] features a graphical interface enabling the composition of a manufacturing plant by concatenating elementary blocks. The goal is to define the necessary workforce at each production line stage, aiding designers in the reengineering of production lines. Another paper, [72], presents simulation and analysis software for electronic card production lines. The program allows the definition of the whole production line model by connecting machine models present in a software library. This tool has been applied by industrial partners to identify bottlenecks and predict human resource and component supply requirements for real production plants. Additionally, [73] has exploited this algebra to model a Kanban control policy as a linear system. The Kanban control system, a well-known pull control policy for manufacturing systems, employs authorization cards, called Kanbans, to trigger production when demand arises. The authors employ max-plus algebra to model the control policy and synthesize a regulator, reducing work-in-process without compromising performances. In fact, it has to be said that the application of this framework to model discrete event systems has primarily found utility in extrapolating useful metrics and conducting computations to analyse the expected behaviour of a system in various scenarios [74]. In urban transportation, instead, [75] developed a suitable max-plus formalism for urban bus networks, coupled with a procedure to compute timetables maximizing connections between buses from different lines. In the realm of semiconductor manufacturing plants, max-plus linear systems can serve to define schedules and control processes effectively [76–79]. In these cases, time constraints are crucial for the wafer's permanence within a processing chamber, as its quality is significantly impacted by delays after completing processing in high-temperature and high-pressure conditions. Moreover, the authors of [80] have modelled a networked automation system with a client-server architecture, computing the system response time through the produced mathematical model and comparing it with data taken from a laboratory. Furthermore, methodologies for identifying and localizing faults within a plant, which can be modelled as a max-plus linear system, have been presented in [81–83]. Additionally, the paper [84] has delved into the analysis of the performance of these linear systems when additive inputs are present. This evolution of max-plus algebra application from traditional manufacturing contexts to diverse and specialized domains reflects its versatility and adaptability to address complex system behaviours and requirements.

Another paper with a recent application of max-plus algebra is presented in [85], in which the scheduling of production systems is considered, with the goal to minimize the total production time. In that work, a result is also expressed in terms of a switching max-plus linear system.

Switching Max-Plus Linear Systems

Switching max-plus linear systems come into play when considering changes in event order or alterations in the system structure. This becomes crucial when factors like resource processing time or user allocation policies are variable. With these systems it is possible to overcome limitations in stationary max-plus linear systems, where concurrency is not possible. If the system structure varies arbitrarily, the plant can be described as a switching system; whereas, if the variation follows a predetermined periodic schedule, periodic systems provide a more precise formalization. Although these concepts are not directly addressed in this thesis, they hold potential for future advancements.

Expanding the max-plus formalism to the event-varying scenario enables the consideration of more intricate situations involving conflicts resolved based on the current event's index. It also allows for the exploration of scenarios where subsequent inputs need to follow different paths within the plant. Various approaches, each with its advantages and limitations, have been proposed for modelling such situations. In [86], a formalism based on the height of heaps of pieces efficiently compares the evolution of safe jobshops for different working sequences. Other works adopt a distinct approach by introducing switching max-plus linear systems. The initial application of this formalism can be traced back to [87] for modelling systems that can switch between different modes of operation, accommodating changes in structure, breaking synchronization, or modifying the order of events. Since then, switching max-plus linear systems have found diverse applications. In [88], the Dutch railway network is modelled as such a system to determine optimal dispatching actions using model predictive control. The model's flexibility allows for changes in train order, breaking connections, splitting joined trains, and changing tracks.

Recently, these systems have been employed to model cube-packing systems in [66], where different manipulators can be selected for resource handling, considering possible faults. The study proposes a fault-tolerant control compared to a simpler model predictive control strategy. Addressing the problem of controlling a switching max-plus linear system to meet strict time constraints between certain events, [89] proposes a causal state feedback. The authors also provide an example applying this theory to a crossing railway system. In contrast to this, the work of D. Animobono [90], focuses on studying the structural properties of systems, independent of specific resource allocation policies treated as exogenous decisions. This approach leads to control techniques applicable across various resource allocation decisions, facilitated by the development of a structural geometric approach for switching max-plus linear systems [91].

Periodic Max-Plus Linear Systems

Talking about periodic max-plus linear systems, they are characterized by event-varying structural variations occurring periodically, in the event domain, with a period denoted as ω. These systems offer a valuable formalism for modelling dynamic scenarios. One notable application is in resolving conflicts for shared resources through a periodic allocation scheme. This becomes particularly pertinent in cases like periodic scheduling of productive plants. In the latter context, the concept of the Minimal Part Set (MPS) plays a crucial role [92]. This approach proves advantageous in scenarios with negligible setup times, offering simplicity, predictability, low work-in-process inventory, and high machine use [93]. Various techniques, incorporating the max-plus algebra, have been developed for computing efficient periodic schedules across different applications [94]. Practical interest in modelling discrete event systems subject to periodic structural variations has spurred research in formalizing the structure of such systems. Early attempts utilized Petri nets instead of max-plus algebra, [95], even though it is now pretty feasible to convert a Timed Event Graphs (TEGs) into a max-plus linear system. The max-plus formalism gained prominence with Lahaye et al.'s work [96], providing tools for modelling repetitive manufacturing systems as periodic max-plus linear systems. Transformation procedures into equivalent stationary systems, focusing on time instants that are multiples of the system period, were there proposed, whereas in [97], the transformation from periodic max-plus linear systems into Weight-Balanced Timed Event Graphs (WBTEG) was presented. Other contributions introduced operators for event-varying and time-varying max-plus linear systems with a cyclic structure [98, 99]. These operators extended the theory of modelling and control of max-plus systems based on transfer functions to the periodic case, demonstrating the decomposition of event-varying systems into stationary and cyclic subsystems. It's crucial to differentiate these systems from those with partial synchronization introduced by David et al. [100] and studied under the hypothesis of periodic synchronization in [101]. The latter systems have integer daters as input, output, and internal variables, and importantly, they are time-varying rather than event-varying.

Control Problems

In recent years, control problems related to systems over the max-plus algebra have gained prominence, particularly in industrial engineering. Various analysis and control techniques have been developed, with a structural geometric approach for max-plus linear systems identified as a promising direction [63]. Subsequent efforts by different authors have produced noteworthy results in this direction [102–105]. Control challenges in max-plus algebra systems, particularly in industrial engineering, have spurred the development of various techniques, as comprehensively reviewed in [106]. One prevalent objective is optimizing input times, determining when to supply raw components to production machines, to align or pre-empt a predefined reference signal on the plant's output. The just-in-time criterion is commonly applied, aiming to delay the input signal as much as possible without exceeding the output schedule [107]. Prominent methods originate from the residuation theory and Model Predictive Control (MPC). Residuation seeks the largest solution to max-plus inequalities, widely used in the literature for optimal input date computations [108, 109]. MPC, initially designed for discrete-time linear systems over conventional algebra, minimizes a specific cost function (usually tracking error) within a prediction horizon. This approach extends to max-plus linear systems [110], providing the advantage of easily incorporating constraints on input and output daters. MPC has found practical applications, leading to many variants [111, 112]. Efficient MPC implementation for output tracking is detailed in [113], where the reference is based on a P-timed event graph. The max-plus algebra optimally divides computations into offline and online phases, enhancing performance compared to similar implementations. Addressing uncertainties in the time required for internal tasks, [114] proposes an approach analysing and improving the critical chain of tasks. A significant distinction in control techniques for max-plus linear systems lies in the need for an accessible state. Observer-based methods, estimating the internal state, are employed when knowledge of the internal state is crucial [104, 115]. However, their effectiveness is limited, offering only upper and lower bounds for the state vector. A different method, considered by some authors [116], involves estimating a linear function of the state $Wx(k)$ without knowing the exact value of the state $x(k)$. This information informs the computation of system feedback. Observer usage proves valuable when the system faces unmeasurable disturbances, such as human interventions or process failures [117]. For scenarios with strict time constraints, like a maximum time distance between two events, [118] proposes a control strategy not requiring full system state knowledge. This strategy proves applicable under suitable and non-restrictive hypotheses for real-world manufacturing systems. In [67], the authors implemented software generating a SCADA system based on the model of a max-plus linear plant and a specified control objective, such as disturbance decoupling, model matching, or observer-based control.

2.3.2. Controlled Invariance

In the last decades, the concept of controlled invariance, not necessarily causal, has been extensively studied in the field of dynamic systems within the realm of systems and control theory. This concept, also known as (A, B)-invariance, has proven its effectiveness in solving a wide range of classical control problems. For dynamic systems over a field, the (A, B)-invariance of a subspace is equivalent to its invariance with at least one static state feedback [68, 69]. However, for systems with coefficients over rings or semirings, this property is generally not valid, since in this case, state feedback invariance implies (A, B)-invariance, but the converse is not always true [103, 119].

The notion of (A, B)-invariance has been a cornerstone of the geometric approach for designing control laws for linear systems since the 1970s [120, 121].

Over the years, different authors have extended the application of this geometric approach to systems over rings [119, 122] and semirings, such as max-plus systems [103]. Significant work has been done by Conte and Perdon [122] with the concept of dynamic state feedback invariance for modules over principal rings. Additionally, in the work by Cardenas et al. [123], inspired by the work of Ito and Inaba [124], the authors obtained various results for the semiring $\mathbb{R}_{\max}$, introducing applications for controlling systems with discrete events subject to time constraints.

Several studies have focused on finding static state feedback to solve problems defined in terms of constraints or asymptotic behavior [103, 118, 125–131]. Other works have also addressed observability problems in similar terms [102,104,132–134].

Therefore, controlled invariance has also been addressed in the context of max-plus linear systems and has proven to be very useful and applicable to various control problems in such systems, which find applications in several fields, including graph theory, integer linear programming, production and planning systems, etc. A notable work is [104], in which the concepts of conditioned and controlled invariant spaces are extended to linear dynamic systems over max-plus or tropical semirings.

A duality theorem is there established and used to construct dynamic observers applied to a manufacturing system. Another paper related to this topic concerns the synchronization problem of max-plus linear systems, formulated in terms of controlled invariance and coreachability [135], while other works have examined static state feedback control laws, but they may not necessarily be linear [130, 136].

A particular consideration is that, in the max-plus algebra, static functions are not necessarily causal, as analyzed by T. Bousch [137] and B. Cottenceau et al. [138]. However, ensuring causality is essential to implement online control laws, as pointed out in [136], where the double description method by Allamigeon et al. [139, 140] is employed. Another significant contribution, which may provide another perspective on causality, is the work of Declerk [141], which deals with causal constraints and proposes different techniques using predictive control. Finally, another work worth mentioning is [142], which applies the structural geometric approach to the Model Matching Problem for positive linear systems, introducing a notion of positive controlled invariance.

Extension of the Geometric Approach

The geometric approach, rooted in controlled and conditioned invariance, represents a foundational paradigm within the domain of systems and control theory. The essence of this approach lies in its foundation on the representation of system properties through appropriate vector spaces. Initially developed for linear systems over conventional algebras [68, 69], this approach has provided solutions to various control problems, especially the disturbance decoupling problem and the model matching problem. The geometric approach extended to systems over the max-plus semiring has been identified as a promising field of research [63]. However, this generalization is not straightforward due to the distinct properties of max-plus semimodules compared to vector spaces. Some challenges that emerged have been addressed by researchers extending the geometric approach to linear systems over rings [119, 122, 143]. A pivotal step in extending geometric concepts to max-plus semirings was taken in [102], introducing reachable and observable semimodules for max-plus linear systems with coefficients in $\mathbb{Z}_{max}$. While these semimodules are not finitely generated in general, they belong to the class of rational semimodules with the integrity assumption. The geometric approach has traditionally excelled in solving the Disturbance Decoupling Problem (DDP) over conventional algebra. However, its transposition to max-plus linear systems [105], presents a different practical interpretation. In the max-plus algebra, controllers can only slow down the plant's operation, and this same effect is also given by disturbance. As a result, effective compensation for the disturbance becomes challenging, but at most, the system can be slowed down more than the disturbance would do. Other formulations of the DDP for systems over the max-plus algebra have been proposed and addressed in [144–149].

2.3.3. Model Matching Problem

The Model Matching Problem (MMP) is a significant problem that also finds a solution in the geometric approach for linear systems over the conventional algebra. This problem involves finding a control law that ensures a given plant behaves in accordance with a specified model. Different authors have proposed various formulations of this problem for max-plus linear systems, with the shared control objective of generating an output sequence for the plant that anticipates (smaller output than the model output) or equals that of the model. In other words, the output of the model is interpreted as a deadline. This perspective has been explored using concepts such as transfer matrices and formal power series over a dioid. Adaptive output feedback control [150] and other alternative representations, as the [151] based on the $(min, +)$ diod, have also been proposed. Another formulation of the model matching problem is considered in [109], where the matching condition involves minimizing the distance between the plant's output and a reference model while delaying the control action. This problem is addressed using residuation theory and the Kleene star operator. Similar considerations are explored in [152], introducing a three-block control structure with a precompensation and a feedback action, and in the context of temporal constraint meeting [125], where the goal is to ensure that the time between internal events does not exceed a certain threshold.

The approach presented in [90] introduces a new perspective on the solution of a MMP in which the applied control forces a plant, modelled as a max-plus linear system, to generate an output exactly equal to that of a given model. The same approach will be followed in this thesis. This formulation has generalized the classical MMP [153] to systems with coefficients in an idempotent semiring, rather than a field, and it has led to new correspondences between max-plus linear systems and linear systems over the conventional algebra, established through a non-trivial generalization process. Sufficient conditions for checking the problem's solvability and algorithms for computing solutions, if they exist, have been developed for stationary [70], switching [91], and periodic [154] max-plus linear systems. These advancements represent a significant contribution to the current state of the art, particularly for switching and periodic systems where a structural geometric approach was lacking [91, 154].

Chapter 3.

Materials and Methods

The use of max-plus algebra as a theoretical framework in this research stems from the unique challenges posed by confined underwater exploration scenarios. Specifically, the focus of this study revolves around biomimetic marine vehicles, represented by fish-like robotic devices. To address the challenges related of underwater exploration involving patrolling fish robots, two main aspects are required: on one hand, a practical aspect is the construction of the model on the fish robot, while the other is a theoretical infrastructure that allows the behaviour of the vehicles to be modelled. Consequently, the need arises for advanced technologies and mathematical formalization, where the latter is the core of the work. Therefore, this chapter deals with the practical components that support the research, primarily in the context of marine vehicles and their associated technologies, recognizing their importance in the broader context of the work. Within the domain of marine vehicles, the research relies on mathematical models, starting with the classic Fossen model, and modern devices for navigation, communication and positioning. The Fossen model serves as a foundational framework to understand marine vehicle dynamics, to be applied to a monofin fish, that contributes significantly to the understanding of the different types of monofin devices, that can be used in practice. An example of monofin device is presented in Fig. 3.1.

Figure 3.1.: Example of a monofin device (credits: *ANcybernetics*)

Various navigation technologies need also to be employed, including IMU (Inertial Measurement Unit), AHRS (Attitude and Heading Reference System), DVL (Doppler Velocity Log), and FOG (Fiber Optic Gyroscope), which are instrumental for practical implementations. Furthermore, the implementation has to incorporate vision systems and USBL (Ultra-Short Baseline) technology, essential for data collection, communication, and positioning, in order to perform tests in real-world scenarios, such as pools, lakes and open sea. However, while these components are vital for the practical dimension of the research and the implementation of the work, it is important to note that the primary focus of this thesis is on theoretical aspects. For this reason, the second part of this chapter is devoted to the presentation of the basic concepts and results related to the max-plus algebra.

3.1. Marine Vehicles

Marine vehicles are mechatronic devices specially designed to operate in aquatic environments, exploring places that often escape human access. Their versatility allows them to perform a wide range of tasks, from complex seabed mapping operations to the delicate collection of biological samples. The presence of these robots is vital in the field of marine exploration and scientific research, as they are able to reach depths and corners that would otherwise remain unexplored. An interesting development in the field of underwater robotics is the creation of *fish robots*, inspired by the movements and morphology of real fishes. These robots are designed to move smoothly and naturally through water, allowing for gentle exploration of the marine environment. The inspiration taken from nature and marine biology, known as biomimetics, plays a crucial role in the development of innovative robotic solutions and robots modelled on the characteristics and behaviour of sea creatures can lead to more efficient and effective solutions.

3.1.1. Type of Vehicles

To perform underwater explorations, there exist different types of marine vehicles: the most used are briefly presented here. Starting with the Autonomous Underwater Vehicles (AUVs), as their name suggests, they are autonomous vehicles without the need for direct control and can perform pre-programmed missions, such as ocean mapping or scientific data collection. Another type of devices are the Remotely Operated Vehicles (ROVs): they are controlled by human operators through cables and can be used for specific missions, such as monitoring underwater structures or retrieving objects. Then, there exists also Autonomous Surface Vehicles (ASVs) represent another important component in marine robotics. They are autonomous vehicles designed to operate on the water surface. They can be used to support underwater operations, communicating with AUVs and ROVs, to coordinate complex tasks. In addition, they can perform monitoring missions from the surface, surveying the marine environment or providing logistical support for other operations. In this context, fish robots are considered as AUVs, since they are autonomous during their patrolling activities.

3.1.2. Mathematical Model of a Monofin Fish

As a starting point, the understanding and implementation of a dynamic model for marine vehicles' and their propulsion system, is crucial. A comprehensive model also allows to create a simulation environment and implement control algorithms effectively. The Fossen model [155, 156] stands as a significant contribution in this regards and it provides a mathematical foundation for analyzing and simulating the behavior of underwater vehicles. This model forms the basis for further developments in biomimetic vehicles, enabling a more accurate representation of their movements in aquatic environments [7]. Inspired by nature, the mathematical model of a monofin fish offers insights into the propulsion mechanisms of aquatic creatures and by emulating the swimming patterns and fin movements of fish, this model contributes to the design and control strategies of biomimetic vehicles. It also serves as a valuable reference for understanding the intricate dynamics involved in underwater locomotion.

This chapter outlines the development of a six-degrees-of-freedom non-linear dynamic model for a fish robot, following Fossen's theoretical framework [155]. The model is obtained by transforming into vectorial representation the mathematical model derived from previous works, where the vehicle body was approximated to a cylindrical shape with radius R and length L [157,158]. The decision to represent the equation of motion in vector form aims to leverage the physical characteristics of the model, reducing the required control coefficients. Additionally, vector-based models offer computational advantages and facilitate algebraic manipulations, making them suitable for implementing various control algorithms. This non-linear vector model can be employed in environments like Simulink for simulation purposes, and with tools such as Simulink 3D Animation (incorporating the Virtual Reality Toolbox) that can link Simulink models with MATLAB algorithms to 3D graphical objects in virtual reality scenes [159].

The kinematic and dynamic equations of motion are now briefly presented, followed by the forces and moments generated by a propulsion system of a robotic fish. For further details, the work from Fossen [156] is highly recommended due to its completeness.

Mathematical Model

In order to introduce the analysis to obtain the mathematical model of the system, the hypothesis considered are that the fish robot is a rigid body assumed of cylindrical shape with 6 degrees of freedom (DOF) and the fluid is incompressible and irrotational. The first step is to introduce both the environmental contributions that interact with the robot and the physics principles generated by the vehicle's movements. A linear system modulation of the problem is adopted, along with the Newton-Euler equation of motion on the dynamic aspect.

The equation of motion of a marine vehicle can be written in vector form according to Fossen [155] as:

$$\dot{\eta} = J_{\Theta}(\eta)\, v \tag{3.1}$$

$$M\dot{v} + C(v)\, v + D(v)\, v + g(\eta) = \tau \tag{3.2}$$

The involved matrices and vectors and their properties will be described in the following paragraphs. Before continuing, it is important to state that when analysing the motion of a marine robot in six degrees of freedom it is convenient to define two coordinate frames:

- the moving frame {b} is fixed to the body of the craft and its origin O_b is usually chosen in such a way as to coincide with the vehicle's centre of gravity. The motion of the body-fixed frame is described relative to the Earth-centered one, the North-East-Down (NED) frame
- the NED frame {n}, which can be considered inertial, since the effects of the Earth's motion on the vehicle at low speed is negligible.

The suggestion given by this consideration, is that the position and orientation of the robotic fish should be described relative to the {n}, while the linear and angular velocities should be expressed in {b}. The notation adopted for the vectors in {b} and {n} frames for the marine robot are the following:

- $v^b_{b/n} = \begin{bmatrix} u \\ v \\ w \end{bmatrix}$, linear velocity of the point O_b relative to {n} expressed in {b};
- $w^b_{b/n} = \begin{bmatrix} p \\ q \\ r \end{bmatrix}$, angular velocity of the point O_b relative to {n} expressed in {b};
- $p^n_{b/n} = \begin{bmatrix} x \\ y \\ z \end{bmatrix}$, position of O_b in the {n} frame;
- $\Theta_{nb} = \begin{bmatrix} \phi \\ \theta \\ \psi \end{bmatrix}$, Euler angles between {n} and {b};

Kinematics

The first equation (3.1) describes the relationship between the body-fixed reference frame {b} placed on the center of buoyancy of the robot and the North East Down (NED) coordinate system {n}. This relation is about the position $\eta_1 = p^n_{b/n} = [x,\ y,\ z]^T$ expressed in meters and orientation $\eta_2 = \Theta_{nb} = [\phi,\ \theta,\ \psi]^T$ in radians, in NED frame and linear and angular velocity (m/s and rad/s) in the body frame $v = [v_1, v_2]^T = [v^b_{b/n}, w^b_{b/n}]^T$ by adopting the transformation matrix J_Θ. So, η denotes the position and attitude of the vehicle, in which the position vector $p^n_{b/n}$ is the distance between NED frame and the body-fixed frame expressed in the NED coordinate frame (n), Θ_{nb} is the Euler angles vector and v denotes linear and angular velocity vector.

The Euler parameters representation is used for the attitude of the robot consisting of roll (ϕ), pitch (θ), and yaw (ψ) angles. In particular, the first equation becomes as follows for the position and attitude of the fish robot:

$$\begin{bmatrix} \dot{\eta_1} \\ \dot{\eta_1} \end{bmatrix} = \begin{bmatrix} J_1(\eta_2) & 0_{3\times3} \\ 0_{3\times3} & J_2(\eta_2) \end{bmatrix} = \begin{bmatrix} v_1 \\ v_2 \end{bmatrix} \tag{3.3}$$

where $J_1(\eta_2)$ and $J_2(\eta_2)$ are transformation matrices.

At this point, it has to be said that this representation by Euler angles is very common thanks to their easy physical interpretation and to the fact that they can be measured directly by the sensors (gyroscopes). There are, however, some disadvantages that arise due to the presence of singular points [160] and since marine robots could operate near these singularities, this can be a problem. An alternative to Euler angle representation is the four-parameter method based on unit quaternion (q), which is an extension of complex numbers. A quaternion unit is defined as:

$$q = \begin{bmatrix} q_0 & q_1 & q_2 & q_3 \end{bmatrix}^T \tag{3.4}$$

Through a series of calculations, the kinematics equation expressed by means of the Euler parameters (unit quaternion) can be obtained. Nevertheless, as this discussion exceeds the confines of this thesis, it has been deemed essential to only acknowledge their existence, explaining that the Euler parameters representation can be defined for any valid unit quaternion and singularity is avoided (typical of a three-parameter representation). For more comprehensive insights, kindly consult the reference [161].

Dynamics

In general, when the body-fixed frame's origin (which in this case coincides with the center of buoyancy, O=CB) does not coincide with the center of gravity (CG), the general dynamic equation of motion of a rigid body with six degrees of freedom can be written as follows [155, 162]:

$$M_{RB}\dot{v} + C_{RB}(v)\,v = \tau_{RB} \tag{3.5}$$

where M_{RB} is the constant inertia matrix of the rigid body, it is symmetric, positive definite, C_{RB} is a skew-symmetrical parametrization of the rigid body, corresponding to the Coriolis and centripetal matrix, and τ_{RB} represents the generalized vector of external forces (in N), including control and hydrodynamic forces, and moments (in N m). These forces can be divided in:

- disturbances by the environment (wind, waves, sea current), here considered null, since the simulation can refer, at least at the beginning, to the devices working on an internal pool;
- restoring forces due to gravity and buoyancy forces due to the Archimedes principles;
- forces related to the added mass due to the surrounding fluid inertia and the consequent damping induced by the waves thus generated;
- forces and torques generated by the propellers or other actuators present in the vehicle.

With the forces above described, the equation of motion (3.5) of the marine robot with 6 degrees of freedom in body-fixed frame can be written, in compact form, as:

$$\underbrace{(M_{RB} + M_A)}_{M}\dot{v} + \underbrace{(C_{RB}(v) + C_A(v))}_{C(v)}v + D(v)v + g(\eta) = \tau_E + \tau \tag{3.6}$$

where M is the inertia matrix including M_{RB} as the inertia matrix of the rigid body and M_A for the added mass; $C(v)$ is the Coriolis and centripetal matrix composed of $C_{RB}(v)$ for the rigid body and $C_A(v)$ for the added mass; $D(v)$ is the total hydrodynamic and centripetal matrix, $g(n)$ is the vector of restoring (gravitational and buoyant) forces and moments, τ_E is the vector of environmental forces and moments, and τ is the vector of propulsion forces and moments.

Furthermore, by applying the transformation matrix according to the Euler angles, the restoring forces and moments can be defined in the body-fixed frame as follow:

$$g(\eta) = \begin{bmatrix} (W-B)\sin\theta \\ -(W-B)\cos\theta\sin\phi \\ -(W-B)\cos\theta\cos\phi \\ -y_g W\cos\theta\cos\phi + z_g W\cos\theta\sin\phi \\ z_g W\sin\theta + x_g W\cos\theta\cos\phi \\ -x_g W\cos\theta\sin\phi - y_G W\sin\theta \end{bmatrix} \tag{3.7}$$

where W represents the weight of the vehicle (in N), B is its buoyancy (in N), and x_g, x_g and x_g are the distances (in m) between the center of mass and center of buoyancy in the body-fixed reference frame.

Remark 1 *These mathematical models are very useful to make simulations of the considered systems. For example, within the European project DiveSafe [163], an interesting work has involved the development of a Digital Twin of a Diver Propulsion Vehicle (DPV) [164]. The virtual infrastructure was developed to study and test the buoyancy of the DPV, with and without payloads, prior to the underwater survey. MATLAB/Simulink (for physical and mathematical models) was there used linked to Unity (for robot and environment visualization and navigation) and a user interface was produced to simulate the model, guiding the user in adding payloads to the DPV and in running the code to recalculate the parameters of the model, also based on the Fossen model. A similar work can also be carried out in this context by considering fish robots and making the necessary modifications to the mathematical model.*

3.1.3. Navigation Technologies

Navigation technologies are pivotal for ensuring precise control and maneuverability of marine vehicles. Several sensing systems have to be integrated into the vehicles to enhance their navigation capabilities in the underwater environment and achieve their mission objectives. These technologies provide vehicles with the ability to determine their position and orientation, as well as to track their movement over time. Accurate and reliable navigation is essential for a wide range of maritime applications, that can involve fish robots, AUVs, ROVs and ASVs. In this regard, a good review of the State of The Art for AUV navigation and localization is [165].

The commonly employed technologies are listed as follows.

IMU The IMU, acronym for Inertial Measurement Unit", is a key component in robotics in general and especially in the navigation and control of robotic devices. It is a system that combines several inertial sensors, typically composed of three accelerometers and three gyroscopes, that measure accelerations, angular velocities and orientation of an object. The accelerometers measure the vehicle's acceleration in three axes, while the gyroscopes measure the vehicle's rotation rate in three axes. It therefore provides valuable information on the position, rotation and movement of the object on which it is mounted, without depending on external references such as GPS or fixed landmarks. It is essential for measuring and understanding how an object moves and is oriented in space, both in terrestrial and underwater environments. IMUs are widely used in navigation systems because they are relatively inexpensive, compact, and reliable. However, IMUs are susceptible to drift, which can accumulate over time and lead to significant errors in position and orientation.

AHRS An Attitude and Heading Reference System (AHRS) is a navigation device that combines IMU data with additional sensor data to provide a more accurate estimate of the vehicle's attitude and heading. An AHRS typically incorporates data from magnetometers, which measure the Earth's magnetic field, and GPS receivers, which provide position information. AHRSs are more expensive than IMUs, but they offer improved accuracy and reliability.

DVL A Doppler Velocity Log (DVL) is a navigation device that measures the vehicle's velocity relative to the water. A DVL works by emitting sound waves and measuring the Doppler shift of the reflected waves. DVLs are particularly useful for underwater vehicles because they provide a direct measure of velocity, even in the absence of external references. A recent work that evaluates the performance of IMU and DVL integration in marine navigation is [166].

FOG A Fiber Optic Gyro (FOG) is a type of gyroscope that uses fiber optics to measure the vehicle's angular rate. FOGs are more expensive than traditional gyroscopes, but they offer improved accuracy and reliability. FOGs are becoming increasingly popular for use in high-performance navigation systems.

Vision Underwater vehicles equipped with visual sensors, such as cameras or video cameras, are essential to inspect the underwater environment, being able to capture photos and videos. This capability enables scientists and operators to extract valuable information and data in this regard. Furthermore, the sequential images or video frames obtained from these cameras can be used for the generation of accurate 3D reconstructions. These reconstructions contribute significantly to the creation of detailed models depicting submerged objects, seabeds, and underwater structures. Vision-based navigation systems leverage cameras to capture images of the vehicle's surroundings, processing them to extract features. These features, ranging from landmarks to distinctive patterns, are also used to determine the vehicle's position and orientation. The popularity of vision-based navigation systems is driven by their capacity to provide rich and detailed environmental information. The integration of underwater vision systems with IMUs, for example, is paramount for robots navigating and exploring the marine environment. Together, these tools empower robots to comprehend their surroundings and interact with them effectively. The synergistic combination of data from IMUs and underwater vision broadens the scope of applications, spanning scientific research to environmental protection.

USBL Communication in marine environment is a crucial aspect for underwater robots and successful underwater missions. Since radio waves propagate only to a very limited extent in water, due to water absorption, other communication modes and technologies are required to transmit data underwater. Acoustic systems, such as USBL (Ultra Short BaseLine), allow the position of one or more underwater robots to be calculated based on the arrival times of acoustic signals sent and received. USBL is a key technology for the accurate communication and positioning of such robots, e.g. for search or recovery work. It plays a vital role in the navigation and control of marine vehicles, contributing to their efficiency during the explorations. It offers high-precision underwater localization and its integration with other navigation technologies forms a synergistic approach to address the complexities related to the marine environment. The USBL positioning system consists of a transceiver mounted on a vessel, which utilizes acoustic signals to determine distances and bearings to tracking targets like AUVs or ROVs. Each target is equipped with a transponder that responds to the transceiver's signals with acoustic pulses, allowing precise calculation of the targets' positions. An USBL operating scheme, taken from the EvoLogics website, is shown in Fig. 3.2. This system measures the time between signal transmission and transponder reply, converting it into distance using a phase-difference method. Optional instruments, such as an AHRS and/or a Global Navigation Satellite System (GNSS) receiver, can be used to provide additional vessel information, such as orientation and coordinates. The computer, on the vessel, interfaces with the USBL transceiver and other instruments, connected to the local network and a dedicated software on it controls the positioning system to monitor the mission in real-time and exchange data. This acoustic positioning system offers several advantages, including high accuracy, real-time tracking, and suitability for both shallow and deep-water environments. Its ability to provide precise position information makes it valuable for various underwater applications, such as subsea exploration, pipeline inspection, and AUV missions. In summary, an USBL system combines acoustic signals, transponders, and optional instruments to deliver accurate and real-time information on underwater target positions, with the navigation computer facilitating centralized control.

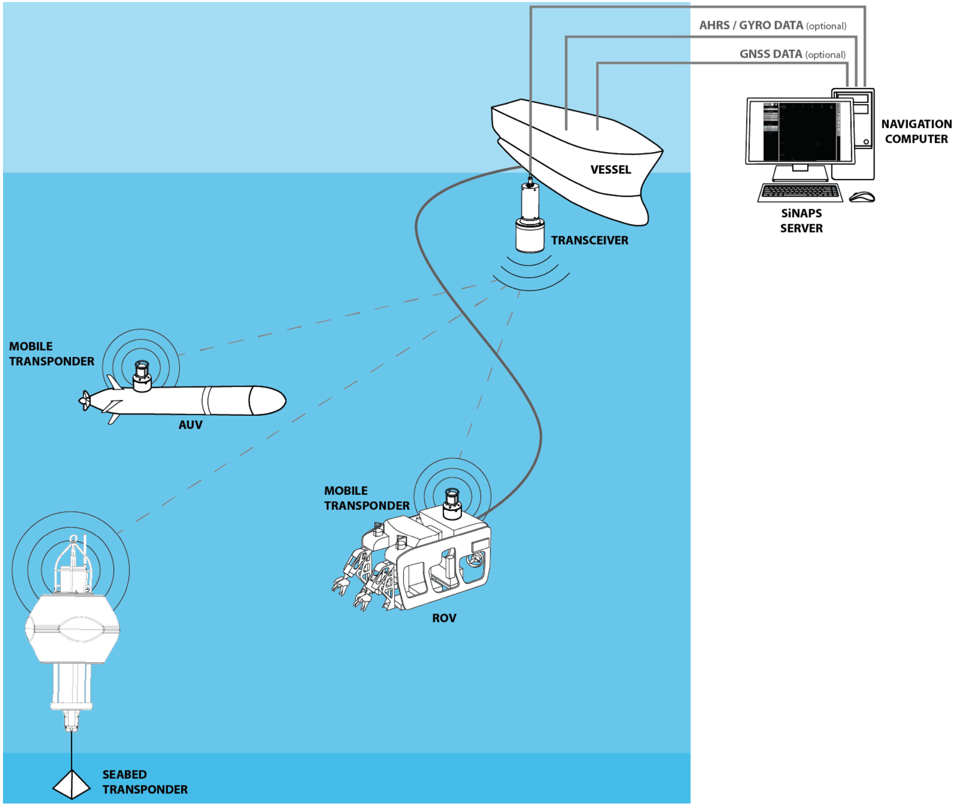

Figure 3.2.: USBL operating scheme, *www.evologics.de/usbl*

3.2. Max-Plus Algebra Mathematical Framework

Following the state of the art of section 2.3 related to max-plus algebra, its applications and the concepts of controlled invariance and Model Matching Problem, it is now possible to explain in detail the theory behind this discrete algebraic system.

Most of the contributions of this chapter are taken from the paper [1], produced during the doctoral period spent at the *Laboratoire des Sciences du Numérique de Nantes*, which led to the discussion of new sufficient conditions for causal controlled invariance and to the development of an algorithm to verify this property.

The max-plus algebra framework was chosen to develop this work as it has proven effective in modelling real-world situations. Consequently, it has also demonstrated to be a valid tool for modelling the context here examined, in which repetitive patrolling by cooperating underwater devices is considered, especially for marine areas characterized by predefined Points of Interest (POIs).

Before moving on to the more advanced theory, a small premise is needed about the elementary operations that can be modelled for Discrete Event Systems (DESs).

Elementary Operations Within a DES, elementary operations include:

- Concatenation: an operation P1 must complete before operation P2 can start. This applies, for example, to successive production stages along an assembly line and the operation considered is the $\otimes$, that represents a sum, e.g. between the completion time of P1 and the time required by P2, to obtain the time at which the whole process is completed.
- Synchronization: both tasks can proceed independently, but the entire process is not considered complete until both P1 and P2 have concluded. In this case, an example is the production of two components that must be assembled before leaving a factory and the maximum between the conclusion time of P1 and that of P2, represents the global completion time. The operation is here $\oplus$.

Dater Representation Another concept related to DES is the so called *dater* representation, that represents the predominant approach for modelling a sequence of events in the max-plus algebra. In the DES that are here considered, events of different types occur with a precise timeline and in modelling a situation in which events of n different types can occur, an n-dimensional dater function $d(.) : \mathbb{N} \rightarrow \mathbb{R}^n_{max}$, can be considered, whose value at $k \in \mathbb{N}$ is a vector $d(k) = (d_1(k), ..., d_n(k))^\top$. The i-th component $d_i(k)$ indicates the time instant at which an event of the i-th type occurs for the k-th time. Of course, dater functions must be non-decreasing in order to have physical meaning, that means $d(k+1) \geq d(k)$ for each $k \in \mathbb{N}$.

3.2.1. Theoretical Background

By denoting the extended real line as $\mathbb{R}$, the max-plus semiring is defined as the set $\mathbb{R}_{\max} = \mathbb{R} \cup \{-\infty\}$. Therefore, $\mathbb{R}_{\max}$ represents the set of real numbers extended by $-\infty$, and the operations *max* and *plus*, with which it is equipped, are denoted as $\oplus$ and $\otimes$, respectively. For any $x, y \in \mathbb{R}_{\max}$, the two operations for addition and multiplication are defined as follows:

$$x \oplus y = \max(x, y) \quad \text{if } x, y \in \mathbb{R}_{\max} \tag{3.8}$$

$$\begin{cases} x \otimes y = x + y & \text{if } x, y \in \mathbb{R}_{\max} \\ x \otimes -\infty = -\infty \otimes x = -\infty & \text{if } x \in \mathbb{R}_{\max} \end{cases} \tag{3.9}$$

The neutral element for the operation $\oplus$ is $\epsilon = -\infty$, and the neutral element for the operation $\otimes$ is $e = 0 \in \mathbb{R}$. In this structure, the ϵ element is absorbent for multiplication, i.e. $x \otimes \epsilon = \epsilon \otimes x = \epsilon$ for all $x \in \mathbb{R}_{\max}$. Since $x \oplus \epsilon = \epsilon \oplus x = x$ and $x \otimes e = e \otimes x = x$ hold for any $x \in \mathbb{R}_{\max}$, we can understand that ϵ and e play the role of 0 and 1 in conventional algebra.

The operations $\oplus$ and $\otimes$ are associative, and multiplication is distributive over finite sums, meaning that for any $a, b, c \in \mathbb{R}_{\max}$, $(a \oplus b) \otimes c = (a \otimes c) \oplus (b \otimes c)$ and $c \otimes (a \oplus b) = (c \otimes a) \oplus (c \otimes b)$.

Therefore, $\mathbb{R}_{\max}$ possesses a semi-ring structure. Furthermore, it is important to note that the operation $\oplus$ is commutative, and that addition $\oplus$ is idempotent, which means that for any $a \in \mathbb{R}_{\max}$, we have $a \oplus a = a$. With these properties, $\mathbb{R}_{\max}$ is referred to as a dioid [62]. Moreover, as in $\mathbb{R}_{\max}$ the operation $\otimes$ is also commutative (whereas in general only $\oplus$ is like this), in this case, thanks to this additional property, it is referred to as a commutative dioid.

Another dioid is the min-plus semi-ring, defined as the set $\mathbb{R}_{\min} = \mathbb{R} \cup \{+\infty\}$ equipped with the addition $\min(a, b) = a \oplus' b$ and multiplication $a + b = a \otimes' b$. The identity element is $+\infty$, and the unit is 0. The dioids $\overline{\mathbb{R}}_{\max}$ and $\overline{\mathbb{R}}_{\min}$ are understood as the set $\mathbb{R} \cup \{-\infty, +\infty\}$, equipped with the operations $\oplus, \otimes$, or $\oplus', \otimes'$. These two dioids are complete in the sense that the sums $\oplus$ and $\oplus'$, even of an infinite number of elements, are always well-defined in these sets. Note that the multiplications $\otimes'$ and $\otimes$ are different because by convention, we have $-\infty \otimes +\infty = -\infty$, while $-\infty \otimes' +\infty = +\infty$. Both operations coincide with the usual addition when applied to real numbers.

The notations $\oplus$ and $\otimes$ are extended to vectors and matrices. In fact, $\mathbb{R}_{\max}^{p \times q}$ represents the set of $p \times q$ matrices with coefficients in $\mathbb{R}_{\max}$, where $p, q \in \mathbb{N}$. For two matrices $A, B \in \mathbb{R}_{\max}^{m \times n}$, the sum $A \oplus B$ is defined as $(A \oplus B)_{ij} = A_{ij} \oplus B_{ij}$. If $A \in \mathbb{R}_{\max}^{p \times n}$ and $B \in \mathbb{R}_{\max}^{n \times m}$, the product $A \otimes B$ is defined as $(A \otimes B)_{ij} = \bigoplus_{k=1}^{n} A_{ik} \otimes B_{kj}$. This product is often denoted as AB.

The null matrix is symbolized by ϵ, and the identity matrix I_n is an $n \times n$ matrix with diagonal elements as $e = 0$ and off-diagonal elements as ϵ. Instead, the vector in which all components are equal to $e = 0$ is denoted as 0. The notation $\otimes$ is also used to represent the external product of a scalar $\lambda \in \mathbb{R}_{\max}$ and a matrix $A \in \mathbb{R}_{\max}^{p \times n}$, defined as $(\lambda \otimes A)_{ij} = \lambda \oplus A_{ij}$, for $i = 1$ to p and $j = 1$ to n.

By replacing, in the notions of vector space or module, the field or ring of scalars with a semi-ring, one obtains what is called in the literature a semi-module, a moduloid [62], or simply a module[1].

We are particularly interested in the sub-semi-modules of the Cartesian product $\mathbb{R}^n_{\max}$ and finite-type modules generated by a finite family of vectors in $\mathbb{R}^n_{\max}$.

If $M \in \mathbb{R}^{n\times m}_{\max}$, we can define $\operatorname{Im} M = \{x \in \mathbb{R}^n_{\max} \mid \exists v \in \mathbb{R}^m_{\max},\ x = Mv\}$. In other words, $\operatorname{Im} M$ is generated by the columns of M. In this regard, an important and widely discussed result in the literature is due to Butkovič and Hegedüs [167], who established that the family of finite-type sub-semi-modules of $\mathbb{R}^n_{\max}$ coincides with the family of finite-type cones $\operatorname{Cone}(C, D) = \{x \in \mathbb{R}^n_{\max} \mid Cx = Dx\}$, where C and D are $p \times n$ matrices, for an integer p. This remark is formalized in the following statement.

Theorem 1 *Given a semi-module $\mathscr{M} \subset \mathbb{R}^n_{\max}$, the following statements are equivalent.*
(i) There exists an integer q and a matrix $M \in \mathbb{R}^{n\times q}_{\max}$ such that $\mathscr{M} = \operatorname{Im} M$.
(ii) There exists an integer p and matrices $C, D \in \mathbb{R}^{p\times n}_{\max}$ such that $\mathscr{M} = \operatorname{Cone}(C, D)$.

Algorithms for converting between the two representations are introduced in [167], and they have been refined by Allamigeon *et al.* [139]. These algorithms were implemented using the max-plus toolbox included in Scicoslab [168], to handle the examples and simulations presented with this thesis.

Allamigeon *et al.* [139] also described algorithms for computing generators of max-plus polyhedra to characterize the set of all vectors x satisfying inequalities of the form $Ax \oplus c \leq Bx \oplus d$. In the following, we will only need the following well-known result, which characterizes the existence of at least one solution to a monolateral equation from its greatest sub-solution [62].

[1] A few years ago, Christophe Reutenauer pointed out to Édouard Wagneur that the term "module" is preferable, as the definitions of a module and a semi-module are identical, except for the fact that the reference set is a ring or a semi-ring. They were discussing the notion of dimension for these objects and indeed, rings or semi-rings pose the same questions for this type of property. For this reason, this advice is followed and the terms module or semi-module are used interchangeably in this thesis.

Theorem 2 *Given integers q and n, along with a matrix $A \in \mathbb{R}_{\max}^{q\times n}$ and a vector $y \in \mathbb{R}_{\max}^{q}$, the following statements are equivalent.*
(i) There exists a vector $x \in \mathbb{R}_{\max}^{n}$ such that $Ax = y$,
(ii) The equality $A \otimes (A^{-T} \otimes' y) = y$ is satisfied.

3.2.2. Max-Plus Linear Systems

Another important basic concept is that of max-plus linear system, which is a dynamical system whose evolution is guided by the following first recurrence law:

$$\Sigma \equiv \begin{cases} x(k+1) = A \otimes x(k) \oplus B \otimes u(k+1) \\ y(k) = Cx(k) \\ x(0) = \epsilon \end{cases} \tag{3.10}$$

where $A \in \mathbb{R}_{\max}^{n\times n}$, $B \in \mathbb{R}_{\max}^{n\times m}$ and $C \in \mathbb{R}_{max}^{p\times n}$. In this system, $k \in \mathbb{N}$ represents the event instance index and the elements $x(k): \mathbb{N} \to \mathbb{R}_{max}^{n}$, $u(k): \mathbb{N} \to \mathbb{R}_{max}^{m}$ and $y(k): \mathbb{N} \to \mathbb{R}_{max}^{p}$ respectively represent the dater of internal events (state vector), the dater of input events (control input), and the dater of output data of the system, for integers $k > 0$.
The solution of the system (3.10) is uniquely determined by the control input u and the initial condition $x(0) \in \mathbb{R}_{max}^{n}$. The components of $x(k)$ and $u(k)$ here represent event daters, such as resource activation or deactivation.

3.2.3. Controlled Invariance

Among the various theoretical concepts behind max-plus linear systems, there are the notions of invariance, controlled invariance or (A,B)-invariance, and causal controlled invariance. A large amount of theory is available in the literature on these concepts, as presented in section 2.3.2, and the main definitions are now reported.

Before discussing controlled invariance, it is considered necessary to also mention the notion of invariance. An invariant semi-module of a system is a semi-module of the state module such that, if the initial state is contained in that set, then the free evolution of the system, that is the evolution of the state with a zero input ($u(k) = \epsilon$ for all $k \in \mathbb{N}$), is entirely within it.

Definition 1 *(Invariance) Given a max-plus linear system of the form (3.10) we say that a semi-module $\mathcal{V} \subseteq \mathcal{X}$ is* invariant*, or A-invariant, if, for all $x \in \mathcal{V}$, $Ax \in \mathcal{V}$.*

The concept of invariant semi-module can be extended to an arbitrary controllable input for the system with the notion of controlled invariant semi-module.

Therefore, in this section, some results concerning controlled invariance in $\mathbb{R}_{\max}$ are presented: specifically, properties (i) and (ii) of Theorem 3 below were stated by Katz [103], while property (iii) was expressed in [136].

Definition 2 *(Controlled Invariance) Given matrices $A \in \mathbb{R}_{\max}^{n\times n}$ and $B \in \mathbb{R}_{\max}^{n\times m}$, a semi-module $\mathscr{M} \in \mathbb{R}_{\max}^{n}$ is (A, B)-invariant, or controlled invariant, if $\forall x_0 \in \mathscr{M}$, there exists a control input u such that the unique solution of the system (3.10), initialized at x_0, satisfies $x(k) \in \mathscr{M}$ for $k > 0$.*

Theorem 3 *The following properties are satisfied.*
(i) A semi-module $\mathscr{M} \subset \mathbb{R}_{\max}^{n}$ is (A, B)-invariant [103] if and only if:

$$A\mathscr{M} \subset \mathscr{M} \ominus \operatorname{Im} B \ ,$$

where $\mathscr{M} \ominus \operatorname{Im} B$ is the set $\{x \in \mathbb{R}_{\max}^{n} \,|\, \exists b \in \operatorname{Im} B,\ x \oplus b \in \mathscr{M}\}$.
(ii) A semi-module $\mathscr{M} \subset \mathbb{R}_{\max}^{n}$ generated by a matrix $M \in \mathbb{R}_{\max}^{n\times q}$ is (A, B)-invariant [103] if and only if there exist matrices $U \in \mathbb{R}_{\max}^{m\times q}$ and $V \in \mathbb{R}_{\max}^{q\times q}$ such that:

$$A \otimes M \oplus B \otimes U = M \otimes V.$$

(iii) A semi-module $\mathscr{M} \subset \mathbb{R}_{\max}^{n}$ such that $\mathscr{M} = \operatorname{Im} M = \operatorname{Cone}(C, D)$, where $M \in \mathbb{R}_{\max}^{n\times q}$ and $C, D \in \mathbb{R}_{\max}^{p\times n}$ is (A, B)-invariant if and only if there exists a matrix $U \in \mathbb{R}_{\max}^{m\times q}$ such that the following equality holds:

$$C(AM \oplus BU) = D(AM \oplus BU) \ .$$

Property (i) forms the basis of the geometric approach to control, while (ii) and (iii) form the basis of its algebraic approach. They are established in the same way as in the case of systems over a field, by constructing the columns of matrices U and V with initial conditions equal to the columns of M.

In summary, we have seen that the module $\mathscr{M} = \operatorname{Im} M$ is controlled invariant when there exist matrices U and V of appropriate dimensions such that $AM \oplus BU = MV$.

Under these conditions, any control law satisfying:

$$\begin{cases} u(k) &= Uv(k), \\ x(k) &= Mv(k), \end{cases}$$

for a sequence $v(k) \in \mathbb{R}^q_{\max}$, leads to the equalities:

$$x(k+1) = AMv(k) \oplus BUv(k) = (AM \oplus BU)v(k) = MVv(k) \tag{3.11}$$

which means that $x(k) \in \mathscr{M}$ for $k \geq 1$, if $x(1) \in \mathscr{M}$. In this case, there exists a vector $v(1) \in \mathbb{R}^q_{\max}$ such that $x(1) = Mv(1)$, and the sequences defined by $v(k+1) = Vv(k)$ for $k \geq 2$, and $u(k) = Uv(k)$ for $k \geq 1$, define a control law that makes the module $\mathscr{M}$ invariant for the closed-loop system.

Definition 3 *The module $\mathscr{M}$ is static state feedback invariant if there exists a control law $u(k) = f(x(k))$ such that the trajectory of the closed-loop system remains in $\mathscr{M}$ during its evolution if $x(1)$ is itself an element of $\mathscr{M}$. In this case, such a function f is called admissible for $\mathscr{M}$.*

Theorem 4 *Given a finite type sub-semi module of $\mathbb{R}^n_{\max}$, denoted as $\mathscr{M} = Im\, M$, with $M \in \mathbb{R}^{n\times q}_{\max}$, the following two statements are equivalent* [136].

(i) $\mathscr{M}$ is controlled invariant.

(ii) $\mathscr{M}$ is invariant under static state feedback, or static state feedback invariant.

Under these conditions, a maximal admissible state feedback exists and it can be written as:

$$u(k) = U \otimes M^\sharp(x(k)) = U \otimes (M^{-T} \otimes' x(k)) \,,$$

where U is the matrix of properties (ii) and (iii) of the Theorem 3, and $M^\sharp(x(k))$ is defined by:

$$(M^\sharp(x(k)))_i = (M^{-T} \otimes' x)_i = -\bigoplus_{j=1}^{n}\{M_{ji} - x_j(k)\}, \quad \text{for } i = 1 \text{ to } q.$$

3.2.4. Model Matching Problem

In this section, the theoretical background of the geometric approach to the Model Matching Problem (MMP) for max-plus linear systems, as presented in [90], will be briefly reported. Further details and remarks can be found in the cited work, where sufficient conditions for checking the problem's solvability and algorithms for computing solutions, if they exist, have been developed for stationary [70], switching [91], and periodic [154] max-plus linear systems. This work will only consider the case of stationary max-plus systems, since the model developed below is of this type.

This section leads to the solution of a MMP formulated as a problem in which the applied control forces a max-plus linear plant to generate an output exactly equal to that of a given model of the same kind. The main definitions are reported below.

Problem 1 (Model Matching Problem [70]) *Given a linear max-plus system*

$$\Sigma_P \equiv \begin{cases} x_P(k) = A_P x_P(k-1) \oplus B_P u_P(k) \\ y_P(k) = C_P x_P(k) \\ x_P(0) = \epsilon \end{cases} \tag{3.12}$$

called the plant, and a linear max-plus system

$$\Sigma_M \equiv \begin{cases} x_M(k) = A_M x_M(k-1) \oplus B_M u_M(k) \\ y_M(k) = C_M x_M(k) \\ x_M(0) = \epsilon \end{cases} \tag{3.13}$$

called the model, with $x_P : \mathbb{N} \to \mathbb{R}^{n_P}_{max}$, $x_M : \mathbb{N} \to \mathbb{R}^{n_M}_{max}$, $u_P : \mathbb{N} \to \mathbb{R}^{m_P}_{max}$, $u_M : \mathbb{N} \to \mathbb{R}^{m_M}_{max}$ and y_P, $y_M : \mathbb{N} \to \mathbb{R}^{p}_{max}$, the MMP consists in finding, for all possible non-

decreasing input sequences $\{u_M(k)\}_{k\in\mathbb{N}}$ *of the model, an appropriate non-decreasing control input sequence* $\{u_P(k)\}_{k\in\mathbb{N}}$ *for the plant, such that the output* $\{y_P(k)\}_{k\in\mathbb{N}}$ *of this latter equals the output* $\{y_M(k)\}_{k\in\mathbb{N}}$ *of the model, i.e.* $y_P(k) = y_M(k)$ *for all* $k \in \mathbb{N}$.

In addition to the formulation presented above, a more restrictive MMP is also introduced, requiring the control signal to be a linear function of the state of the plant, the state of the model, and the input of the model. In this case, the control signal can be viewed as a feedback map.

Problem 2 (Feedback Model Matching Problem [70]) *Given a plant of the form (3.12) and a model of the form (3.13), the Feedback Model Matching Problem (FMMP) consists in finding, for all possible non-decreasing input sequences* $\{u_M(k)\}_{k\in\mathbb{N}}$ *of the model, two appropriate matrices* $F \in \mathbb{R}_{max}^{m_P\times(n_P+n_M)}$ *and* $G \in \mathbb{R}_{max}^{m_P\times m_M}$ *such that the control input sequence* $\{u_P(k)\}_{k\in\mathbb{N}}$ *defined by*

$$u_P(k) = F \begin{pmatrix} x_P(k-1) \\ x_M(k-1) \end{pmatrix} \oplus G u_M(k) \text{ for } k \geq 1 \tag{3.14}$$

is a solution for the corresponding MMP.

Remark 2 *If* $x_P(k)$, $x_M(k)$ *and* $u_M(k)$ *are all non-decreasing daters, then the control input sequence* $u_P(k)$ *defined by (3.14) is also non-decreasing, since in the max-plus algebra every linear function is monotone, and both the terms in the right-hand term of equation (3.14) are monotone.*

Solution

Given the plant Σ_P described by (3.12) and the model Σ_M described by (3.13), the joint internal event dater $x_E(.) = \begin{pmatrix} x_P(.) \\ x_M(.) \end{pmatrix} : \mathbb{N} \to \mathbb{R}_{max}^{(n_P+n_M)}$ is considered, together with the related joint dynamics, described by the equation:

$$x_E(k) = A_E x_E(k-1) \oplus B_1 u_P(k) \oplus B_2 u_M(k) \tag{3.15}$$

with $A_E = \begin{pmatrix} A_P & \epsilon \\ \epsilon & A_M \end{pmatrix}$, $B_1 = \begin{pmatrix} B_P \\ \epsilon \end{pmatrix}$, $B_2 = \begin{pmatrix} \epsilon \\ B_M \end{pmatrix}$ and $x_E(0) = \epsilon$.

At this point, the control problem expressed in Problem 1 can be reformulated as that of finding, for any input sequence of the model $\{u_M(k)\}_{k\in\mathbb{N}}$, a control input sequence for the plant $\{u_P(k)\}_{k\in\mathbb{N}}$ that keeps $\{x_E(k)\}_{k\in\mathbb{N}}$ inside the *output equalizer* subsemimodule $\mathcal{K} \subseteq \mathbb{R}_{max}^{(n_p+n_M)}$ defined by

$$\mathcal{K} = \left\{ x_E = \begin{pmatrix} x_P \\ x_M \end{pmatrix} \in \mathbb{R}_{max}^{(n_p+n_M)}, \text{ such that } C_P x_P = C_M x_M \right\} \tag{3.16}$$

Viewing $\{u_M(k)\}_{k\in\mathbb{N}}$ as a disturbance input and $\{u_P(k)\}_{k\in\mathbb{N}}$ as a control input, similarities can be noted with the disturbance decoupling problem over the conventional algebra. In that case the objective is to constrain the state of the joint dynamics inside the null space of the output matrix. Although the parallelism is clear, there are some differences discussed in the Remark 4 of [90].

The formulation of the MMP that consists of keeping $x_E(k)$ inside the output equalizer subsemimodule $\mathcal{K}$ can be tackled with a structural geometric approach, obtaining a necessary and sufficient condition for the existence of a solution for the MMP. Before introducing the theorem, the following definition has to be introduced.

Definition 4 (Non-anticipativeness) *We say that a max-plus linear system of the form 3.10 is non-anticipative if* $A \geq I_n$*.*

Theorem 5 ([70]) *Given a non-anticipative plant* Σ_P *of the form (3.12) and a non-anticipative model* Σ_M *of the form (3.13), the related MMP is solvable if and only if for all* $x \in Im\, B_2 = Im \begin{pmatrix} \epsilon \\ B_M \end{pmatrix}$ *there exists* $z \in Im\, B_1 = Im \begin{pmatrix} B_P \\ \epsilon \end{pmatrix}$ *such that*

$x \oplus z$ belongs to $\mathcal{V}^*(\mathcal{K})$, where $\mathcal{V}^*(\mathcal{K})$ is the maximum (A_E, B_1)-invariant semimodule contained in the output equalizer semimodule $\mathcal{K}$ defined by (3.16).

In this case, the detailed proof is provided [70], since it will be useful for the development of some parts of the work.

Proof *If*. By the (A_E, B_1)-controlled invariance of $\mathcal{V}^*(\mathcal{K})$, it follows that given $x_E(k-1) \in \mathcal{V}^*(\mathcal{K})$, there exists $u_1(k) \in \mathbb{R}_{max}^{m_P}$ such that $A_E x_E(k-1) \oplus B_1 u_1(k)$ belongs to $\mathcal{V}^*(\mathcal{K})$. Moreover, by hypothesis, given $u_M(k) \in \mathbb{R}_{max}^{m_M}$, there exists $u_2(k) \in \mathbb{R}_{max}^{m_P}$ such that $B_1 u_2(k) \oplus B_2 u_M(k)$ belongs to $\mathcal{V}^*(\mathcal{K})$. We can then construct recursively a control input $\{u_P(k)\}_{k\in\mathbb{N}}$ for the dynamics (3.15) as

$$u_P(k) = \begin{cases} u_2(1) \text{ for } k = 1 \\ u_1(k) \oplus u_2(k) \oplus u_P(k-1) \text{ for } k > 1 \end{cases} \tag{3.17}$$

More precisely, we start by taking $u_2(1)$ such that $B_1 u_2(1) \oplus B_2 u_M(1) \in \mathcal{V}^*(\mathcal{K})$ and we set $u_P(1) = u_2(1)$. Then, we compute $x_E(1)$ by means of (3.15), $x_E(0)$, $u_P(1)$ and $u_M(1)$, and we take $u_1(2)$ and $u_2(2)$ such that $A_E x_E(1) \oplus B_1 u_1(2) \in \mathcal{V}^*(\mathcal{K})$ and $B_1 u_2(2) \oplus B_M u_M(2) \in \mathcal{V}^*(\mathcal{K})$. We set $u_P(2) = u_1(2) \oplus u_2(2) \oplus u_P(1)$ and we iterate the same procedure increasing by 1 the index k at each step. Note that the sequence $\{u_P(k)\}_{k\in\mathbb{N}}$, thanks to the presence of the term $u_P(k)$ in the second equation of (3.17), is non decreasing and it gives rise to the following state evolution

$$x_E(k) = \begin{cases} A_E x_E(0) \oplus B_1 u_1(1) \oplus B_2 u_M(1) \quad \text{for } k = 1 \\ A_E x_E(k-1) \oplus B_1 u_1(k) \oplus (B_1 u_2(k) \\ \oplus B_2 u_M(k)) \oplus B_1 u_P(k-1) \quad \text{for } k > 1 \end{cases} . \tag{3.18}$$

In equation (3.18), the term $B_1 u_P(k-1)$ is irrelevant, since, we have $x_E(k-1) \geq B_1 u_P(k-1)$ and hence, thanks to the assumption of non-anticipativity that implies $A_E \geq I$, also $A_E x_E(k-1) \geq B_1 u_P(k-1)$. Then, disregarding this last term, we can show by induction that the state evolution $\{x_E(k)\}_{k\in\mathbb{N}}$ given in (3.18) is contained in $\mathcal{V}^*(\mathcal{K})$. In fact, $x_E(0) = \epsilon$ belongs to $\mathcal{V}^*(\mathcal{K})$. Moreover, by the definition of $u_1(.)$ it follows that the summand $(A_E x_E(k-1) \oplus B_1 u_1(k))$ in the right-hand term of (3.18) is contained in $\mathcal{V}^*(\mathcal{K})$ if $x_E(k-1)$ is contained in $\mathcal{V}^*(\mathcal{K})$. Finally, the second summand $(B_1 u_2(k) \oplus B_2 u_M(k))$ in the right-hand term of (3.18) is contained in $\mathcal{V}^*(\mathcal{K})$ by the definition of $u_2(k)$. Since $\mathcal{V}^*(\mathcal{K}) \subseteq \mathcal{K}$, by the definition of $\mathcal{K}$ given in (3.16), it follows that the output $\{y_P(k)\}_{k\in\mathbb{N}}$ of the plant generated by the input $\{u_P(k)\}_{k\in\mathbb{N}}$ defined by (3.17) is equal to the output $\{y_M(k)\}_{k\in\mathbb{N}}$ of the model generated by the input $\{u_M(k)\}_{k\in\mathbb{N}}$ and the MMP is solved.

Only if. If the condition of the theorem does not hold, there exists an input vector $\bar{u}_M$ such that $B_2\bar{u}_M \oplus B_1u_P \notin \mathcal{V}^*(\mathcal{K})$ for any $u_P \in \mathbb{R}^{m_P}_{max}$. Then, for the constant input $u_M(k) = \bar{u}_M$ for $k \in \mathbb{N}$, we have, from (3.15), that $x_E(1) = A_Ex_E(0)\oplus B_1u_P(1)\oplus B_2u_M(1) = A_E\epsilon \oplus B_1u_P(1) \oplus B_2\bar{u}_M = B_1u_P(1) \oplus B_2\bar{u}_M$ does not belong to $\mathcal{V}^*(\mathcal{K})$ for any value $u_P(1) \in \mathbb{R}^{m_P}_{max}$ and also $x_E(1) \geq B_2\bar{u}_M$. The latter inequality, thank to the fact that $A_E \geq I$, implies recursively $x_E(k) = A_Ex_E(k-1)\oplus B_1u_P(k)\oplus B_2u_M(k) = A_Ex_E(k-1)\oplus B_1u_P(k)\oplus B_2\bar{u}_M = A_Ex_E(k-1) \oplus B_1u_P(k)$, while the fact that $x_E(1)$ does not belong to $\mathcal{V}^*(\mathcal{K})$ implies that for any input $\{u_P(k)\}_{k\in\mathbb{N}}$ there exists $\bar{k} \in \mathbb{Z}$ such that $x_E(\bar{k}) = A_Ex_E(\bar{k}-1) \oplus B_1u_P(\bar{k}) \notin \mathcal{K}$. In other words, $x_E(k)$ cannot be kept indefinitely inside the subsemimodule $\mathcal{K}$ and the MMP cannot be solved. □

Remark 3 *By analysing the proof of the Theorem 5, it can be realised that the hypothesis of non-anticipativeness can actually be suppressed, since this condition is not actually used in the first part of the proof of Theorem 5 [70], where the equalities 3.17 and 3.18 are enough to get $A_Ex_E(k) \geq B_1u_p(k)$, without using the hypothesis $A_E \geq I_{n+1}$. The second part of the proof cannot be simplified in the same way, but it is possible to say that the condition of the theorem is at least sufficient to provide a solution of the MMP, without this hypothesis. The proof was deeply analysed during the simulations of the MMP of Section 4.2 since the matrix A obtained for the plant in Section 4.1.3 is non-anticipative, at least in the sense explained in [90]. As a consequence, the need to obtain an alternative proof for this theorem has emerged to avoids the condition $A_E \geq I_{n+1}$ and it is provided in Appendix B.*

For the feedback version stated in Problem 2, a specialized, more restrictive condition is derived in [70], with the following result.

Theorem 6 ([70]) *Given a plant Σ_P of the form (3.12) and a model Σ_M of the form (3.13) as in Theorem 5, the related FMMP is solvable if and only if there exists an (A_E, B_1)-invariant subsemimodule $\mathcal{V}$ of feedback type contained in the output equalizer subsemimodule $\mathcal{K}$ such that for all $x \in Im B_2 = Im \begin{pmatrix} \epsilon \\ B_M \end{pmatrix}$ there exists $z \in Im B_1 = Im \begin{pmatrix} B_P \\ \epsilon \end{pmatrix}$ with $x \oplus z \in \mathcal{V}$.*

Remark 4 ([90]) *The solvability condition for the FMMP given in Theorem 6 is strictly stronger than the solvability condition for the MMP given in Theorem 5, since any (A, B)-invariant of feedback type $\mathcal{V}$ contained in $\mathcal{K}$ is also contained in $\mathcal{V}^*(\mathcal{K})$ due to the maximality of the latter, and $\mathcal{V}^*(\mathcal{K})$ is not necessarily of feedback type. Therefore, the solvability of the FMMP implies the solvability of the MMP and any solution for the first is a solution also for the second.*

Remark 5 *In practice, the condition of Theorem 5 can be checked and the elements $u_1(k)$, $u_2(k)$ that are needed in (3.17) to construct the control input $\{u_P(k)\}_{k\in\mathbb{N}}$ can be found by solving systems of linear equations that involve the matrices A_E, B_1, B_2 and the generators of $\mathcal{V}^*(\mathcal{K})$. The same holds for the condition of Theorem 6 with the matrices F and G. An example with the computations involved in solving the FMMP is given in [90].*

3.2.5. Causality and Causal Controlled Invariance

In this section, the concept of causal controlled invariance, in the framework of max-plus linear systems, is explored in depth. This concept is very useful and applicable to various control problems for such systems, and although it has already been presented in the literature, it is currently represented, and defined only through sufficient conditions that allow to verify if a module has this property. In order to design appropriate control laws for these systems, in which specifications and constraints are given in terms of vector space, it is indeed necessary to consider the concepts of controlled invariance and causal controlled invariance. However, for the latter no algorithm has so far been designed to test the sufficient conditions already defined or other equivalent conditions. It is for this reason that, in addition to various considerations on this topic, a preliminary version of an algorithm is presented within this work. In this way, it makes possible to check more easily whether a module is causally controlled invariant or not. We introduce the concept of causal projection relative to a matrix, which plays a central role in the development of the concepts that are presented. The described algorithm has been implemented on ScicosLab software package. It consists in a procedure that is applied recursively to each row of the matrix under consideration, until convergence is achieved, which is ensured within a defined number of steps. Some examples are then provided in Appendix A, to illustrate how the algorithm permits to confirm whether or not a given module is causally controlled invariant.

Causality and Related Operators

The concept of causality, deeply studied by Bousch [137], stems from the fact that functions modelling the evolution of discrete event systems not only possess the classical properties of monotonicity and additive homogeneity, but also generally have a third property that expresses the causal (i.e., non-anticipative) character of the transformation.

Max-plus linear operators belong to the class of topical operators, which are formulated using the *min*, *max*, and *plus* operations. A topical function $u = \phi(x) : \mathbb{R}^n_{\max} \to \mathbb{R}_{\max}$ is represented by the infimum (symbol $\bigwedge$) of max-plus linear functions or the supremum (symbol $\bigvee$) of min-plus linear functions. This means that for a finitely generated function, there exist integers q, r, and matrices $\alpha \in \mathbb{R}^{q\times n}_{\max}$ and

$\beta \in \mathbb{R}_{\max}^{r\times n}$ such that:

$$\phi(x) = \bigvee_{j=1}^{q} \bigwedge_{k=1}^{n} (\alpha_{jk} + x_k) = \bigwedge_{j=1}^{r} \bigvee_{k=1}^{n} (\beta_{jk} + x_k) \ . \tag{3.19}$$

Our interest in topical operators arises from the fact that the control law expressed in Theorem 4 belongs to this class. Functions of this type are monotonic, i.e., $\forall x$, $x' \in \mathbb{R}_{\max}^{n}$ such that $x \leq x'$, we have $\phi(x) \leq \phi(x')$, and additively homogeneous, i.e., $\forall x \in \mathbb{R}_{\max}^{n}$ and $\lambda \in \mathbb{R}_{\max}$, we have $\phi(\lambda \otimes x) = \lambda \otimes \phi(x)$.

Furthermore, the operator $\phi(x)$ is causal if $\forall x$, $y \in \mathbb{R}_{\max}^{n}$, and for any date $\lambda \in \mathbb{R}_{\max}$, we observe that $\phi(x) = \phi(y) < \lambda$ or $\phi(x), \phi(y) \geq \lambda$, whenever $x_i = y_i < \lambda$ or $x_i, y_i \geq \lambda$, for $i = 1$ to n.

Definition 5 *A function ϕ from $\mathbb{R}_{\max}^{n}$ to $\mathbb{R}_{\max}$ is causal if for all $\lambda \in \mathbb{R}_{\max}$, the equality $\min(x_i, \lambda) = \min(y_i, \lambda)$ for $i = 1$ to n implies that $\min(\phi(x), \lambda) = \min(\phi(y), \lambda)$. A multivariable function is said to be causal if all its components are causal.*

Next, we also recall some other definitions and basic results.

Theorem 7 *A topical function ϕ from $\mathbb{R}_{\max}^{n}$ to $\mathbb{R}_{\max}$ is causal if and only if for all $x \in \mathbb{R}_{\max}^{n}$, the inequality $\phi(x \wedge 0) \geq \phi(x) \wedge 0$ holds.*

Theorem 8 *A max-plus linear form of $\mathbb{R}_{\max}^{n}$, of the form $f(x) = v^T \otimes x$, for $v \in \mathbb{R}_{\max}^{n}$, is causal if and only if the vector v is defined over $\mathbb{R}_{\max}^{+n}$. A topical function $\phi : \mathbb{R}_{\max}^{n} \to \mathbb{R}_{\max}$ is causal if and only if it is equal to the infimum of causal max-plus functions.*

Bousch [137] achieves an explicit characterization of causal topical functions by using the set $\mathbb{R}_{\max}^{+}$ of positive reals extended by $-\infty$. However, the results presented for real topical functions also extend to $\mathbb{R}_{\max}$, considering the following alternative characterization.

Definition 6 *The sub-semi-ring of causal elements in* $\mathbb{R}_{\max}$ *is defined as:*

$$\mathscr{C} = \mathbb{R}^{+}_{\max} = \{x \in \mathbb{R}_{\max} \,|\, x \geq 0 \text{ or } x = \epsilon\} \ .$$

Proposition 1 *A topical function* ϕ *defined on* $\mathbb{R}^n_{\max}$ *and taking values in* $\mathbb{R}_{\max}$ *is causal if, for every vector* $x \in \mathbb{R}^n_{\max}$ *satisfying* $\bigoplus_{i=1}^{n} x_i = 0$*, we have* $\phi(x) \in \mathscr{C}$*.*

Definition and Sufficient Conditions

The concept of causal controlled invariance, although previously presented in the literature [136], is characterized through sufficient conditions to verify if a module possesses this property. These sufficient conditions, in summary, require the existence of a causal matrix U such that $AM \oplus BU$ has its columns in $\operatorname{Im} M$.

Let us first recall some definitions and basic results from [136].

Definition 7 *(Causal Controlled Invariance) We say that the module* $\mathscr{M} \subset \mathbb{R}^n_{\max}$ *is a causal* (A, B)*-invariant, or causal controlled invariant, if there exists a causal admissible control law for* $\mathscr{M}$*.*

Proposition 2 *The state feedback* $u(k) = U(M^{-T} \otimes' x)$ *from Theorem 4 is causal if the coefficients* $U_{ij} - M_{kj}$ *are all causal for* $i = 1$ *to* m*,* $j = 1$ *to* q*, and* $k = 1$ *to* n*, at least when* $M_{kj} \neq \epsilon$*.*

Definition 8 *We say that the matrix* M *is normalized if the maximal element in each of its columns is equal to* 0*.*

Proposition 3 *A finitely generated module* $\mathscr{M}$ *is a causal* (A, B)*-invariant if there exist a matrix* U *over* $\mathcal{C}$ *and a matrix* V *satisfying the conditions of Theorem 3, with the matrix* M *being normalized.*

3.3. The Algorithm for Causal Controlled Invariance

At this stage, it is possible to proceed with further considerations. Despite the existence of sufficient conditions for the causal controlled invariance of a module, there is no current characterization or algorithm designed to test these sufficient conditions or other equivalent conditions. In order to develop such an algorithm, the following results are first introduced, which generalize Theorem 2 to characterize the existence of causal solutions to a max-plus linear monolateral equality.

3.3.1. Causal and R-causal Projections

Theorem 9 *For any matrix $A \in \mathbb{R}_{\max}^{q \times n}$ and any vector $y \in \mathbb{R}_{\max}^{q}$, the following statements are equivalent:*

(i) There exists $x \in \mathcal{C}^n$ such that $Ax = y$.

(ii) $AP_c(A^{-T} \otimes' y) = y$, where P_c is the causal projection defined as:

$$P_c(x) = sup\{z \,|\, z \in \mathcal{C},\ z \leq x\} \ , \tag{3.20}$$

for $x \in \mathcal{C}^n$. In other words, we have:

$$(P_c(x))_i = \begin{cases} -\infty, & \text{if } x_i < 0, \\ x_i, & \text{if } x_i \geq 0 \ . \end{cases}$$

Proof The proof relies on the following chain of inequalities:

$$\begin{aligned} y &= Ax && \text{, if } x \text{ is a solution of } Ax = y \\ &= AP_c(x) && \text{, if } x \text{ is a causal solution} \\ &\leq AP_c(A^{-T} \otimes' y) && \text{, because } x \leq A^{-T} \otimes' y \text{, if } Ax \leq y \\ &\leq A(A^{-T} \otimes' y) && \text{, by the definition of } P_c \\ &\leq y && \text{, because } x \leq A^{-T} \otimes' y \text{ implies } Ax \leq y \text{, so } A(A^{-T} \otimes' y) \leq y. \end{aligned}$$

Since both ends of the chain are equal, we conclude that all its terms are equal, which implies the equality (ii) of the theorem. This shows that statement (ii) implies statement (i). The converse is immediate, as $x = A^{-T} \otimes' y$ is a solution if (ii) is satisfied.

□

This result can be extended to an equation of the form $Ax \oplus b = y$.

Theorem 10 *For any matrix $A \in \mathbb{R}_{\max}^{q\times n}$ and vectors $b, y \in \mathbb{R}_{\max}^{q}$, we have the following equivalences:*
(i) There exists $x \in \mathcal{C}^n$ such that $Ax \oplus b = y$.
(ii) $AP_c(A^{-T} \otimes' y) \oplus b = y$.

Proof The proof is based on the same chain of inequalities:

$$
\begin{aligned}
y &= Ax \oplus b && \text{, if } x \text{ is a solution of } Ax \oplus b = y\\
&= AP_c(x) \oplus b && \text{, if } x \text{ is a causal solution}\\
&\leq AP_c(A^{-T} \otimes' y) \oplus b && \text{, because } x \leq A^{-T} \otimes' y \text{, if } Ax \leq y\\
&\leq A(A^{-T} \otimes' y) \oplus b && \text{, by definition of } P_c\\
&\leq y && \text{, because } A(A^{-T} \otimes' y) \leq y \text{ and } b \leq y \text{, if } Ax \oplus b \leq y.
\end{aligned}
$$

The theorem is deduced as previously. □

The two previous results are inspired by those of Cottenceau [138], which were established for formal series associated with a max-plus linear system. We now introduce the notion of projection relative to a matrix R, or R-projection, in order to formulate a test to verify the existence of a causal solution as mentioned in Proposition 3.

Theorem 11 *Given integers n, m, p, and q, and matrices $H \in \mathbb{R}_{\max}^{n\times p}$, $M \in \mathbb{R}_{\max}^{n\times q}$, and $R \in \mathbb{R}_{\max}^{m\times p}$, there exists a matrix W such that $HW = M$ and RW is causal, in $\mathcal{C}^{n\times q}$, if and only if the following equality holds:*

$$HP_C^R(H^{-T} \otimes' M) = M \ , \tag{3.21}$$

where the causal projection relative to a matrix R, or R-projection, is defined as $P_c^R : \mathbb{R}_{\max}^{q} \to \mathbb{R}_{\max}^{q}$, by:

$$\forall w \in \mathbb{R}_{\max}^{q} \ , \ P_c^R(w) = sup\{z \in \mathbb{R}_{\max}^{q} \mid Rz \in \mathcal{C}^n, z \leq w\} \ . \tag{3.22}$$

Proof This follows the same logic as before. Formally, the matrix $H^{-T} \otimes' M$ is defined on $\overline{\mathbb{R}}_{\max}$, as well as its projection. The projection is defined column by column. If the equality in the theorem is verified, then $W = P_C^R(H^{-T} \otimes' M)$ is a solution to $HW = M$ such that RW is causal, by definition of the projection P_C^R. Conversely, if $M = HW$ with RW causal, we have the following chain of inequalities:

$$
\begin{aligned}
M &= HW && \text{with } RW \text{ causal} \\
&= HP_C^R(W) && \text{since } RW \text{ is causal, so } P_C^R(W) = W \\
&\leq HP_C^R(H^{-T} \otimes' M) && \text{because } HW \leq M \text{ so } W \leq H^{-T} \otimes' M \text{ and } P_C^R \text{ isotone} \\
&\leq H(H^{-T} \otimes' M) && \text{because } \forall z,\ P_C^R(z) \leq z \\
&\leq M && \text{because } z = H^{-T} \otimes' M \text{ satisfies } Hz \leq M.
\end{aligned}
$$

This chain has identical endpoints, which means that all terms are actively equal, and in particular, $HP_C^R(H^{-T} \otimes' M) = M$, which concludes the proof. □

At this point, it is possible to introduce the algorithm for verifying the conditions in Proposition 3.

3.3.2. Development of the Algorithm

Finally, we see that Theorem 11 allows for the effective verification of the sufficient conditions in Proposition 3. This is expressed in the following statement:

Proposition 4 *Given the matrices A, B, and M defined as before, let H, R, and V be the matrices such that:*

$$
\operatorname{Im}\begin{pmatrix} H \\ R \\ V \end{pmatrix} = \operatorname{Cone}\left(\begin{pmatrix} A & B & \epsilon \end{pmatrix}, \begin{pmatrix} \epsilon & \epsilon & M \end{pmatrix}\right),
$$

then the conditions from Proposition 3, which are sufficient for $\operatorname{Im} M$ *to be causal controlled invariant, are satisfied if and only if the conditions from Theorem 11 are also satisfied.*

Proof The condition from Proposition 3 is that there exists a causal matrix U and a matrix X such that $AM \oplus BU = MX$. This leads to considering the module of solutions (Y, U, X) of the identity $AY \oplus BU = MX$. If the matrices H, R, and V are defined as in the statement, then the solutions are parameterized in the form:

$$\begin{pmatrix} Y \\ U \\ X \end{pmatrix} = \begin{pmatrix} H \\ R \\ V \end{pmatrix} W ,$$

where W is a free parameter matrix. Testing the causal controlled invariance of $\operatorname{Im} M$ then amounts to verifying the existence of a matrix W of adequate size such that $HW = M$, and such that RW is causal, which is the object of theorem 11, and completes the demonstration. □

The verification of the sufficient condition in Proposition 3 is performed by testing the equality $HP_C^R(H^{-T} \otimes' M) = M$. In practice, the algorithm involves two main steps, as follows:

- given the matrices A, B and M, compute the matrices H, R, et V,
- finally, check whether there exists a matrix W such that RW is causal and $HW = M$.

The first step of this procedure can be achieved using the algorithm by Allamigeon *et al.* [139]. The computations may have high complexity, but the results are matrices of finite order. The last point is to effectively compute the projection $P_C^R(W)$ of a given matrix $W \in \mathbb{R}_{\max}^{p \times q}$. The R-projection of a matrix is performed column by column using Theorem 11, starting from the columns w of the matrix W for which $P_c^R(w) = \sup\{z \in \mathbb{R}_{\max}^p \mid Rz \in \mathcal{C}^m, z \leq w\}$. To this end, we establish some elementary properties of the R-projection.

Proposition 5 *The following properties are verified:*

(i) A scalar $z \in \mathbb{R}_{max}$ is causal if and only if $z \leq z^2$.

(ii) Using the notation $(v^2)_i = v_i^2$, for a vector v, it is also true that v is causal if and only if $v \leq v^2$.
(iii) If R is a row vector, then

$$P_c^R(w) = \begin{cases} w & \text{if } Rw \text{ is causal,} \\ z & \text{else,} \end{cases} \tag{3.23}$$

where z is defined by:

$$z_i = \begin{cases} w_i & \text{if } R_{1i} = -\infty, \\ -\infty & \text{if } R_{1i} + w_i < 0, \text{ and } R_{1i} \neq -\infty. \end{cases} \tag{3.24}$$

(iv) In the case of a matrix, the R-projection is computed by applying the procedure successively for each row of the matrix R, from the first row to the last one, and then repeating this calculation until the rows are no longer modified.

Proof Properties (i) and (ii) are verified directly. To show (iii), we notice that Hw is not causal, thus $-\infty < \max_{i|R_{1i}\neq\epsilon} (R_{1i} + w_i) < 0$, which means there exist indices i for which $R_{1i} + w_i$ is negative. In the case (iv) of a matrix, we can apply the same procedure successively for each row until convergence. At each step of the procedure, certain coefficients of the vector are set to zero. Since the number of rows and coefficients is finite, and the size of the matrix W is $p \times q$, convergence is guaranteed in a maximum of $p \times q$ steps. □

These remarks lead to an effective calculation procedure. The resulting algorithm is given in the table named Algorithm 1. Moreover, in the paper [1], three simple examples of application of the algorithm for verifying the sufficient conditions of causal controlled invariance of different modules are presented. These examples are reported in Appendix A.

Algorithm 1 The algorithm for calculating the R-projection of a matrix W

function PCR(W, R)
  $[nlin, ncol] \leftarrow \text{size}(R)$
  $pout \leftarrow ((W, R(1, :)))$
  for $i = 2$ to $nlin$ **do**
    $z \leftarrow (W, R(i, :))$
    $pout \leftarrow pout + (z)$
  $pout \leftarrow (pout)$
  return $pout$

function SINGLPCR(W, R)
  $[nlin, ncol] \leftarrow \text{size}(W)$
  $pout \leftarrow \text{zeros}(nlin, ncol)$
  $i \leftarrow 1$
  for $j = 1$ to $nlin$ **do**
    if $\text{full}(R(i, j) \cdot W(j, i)) \leq \text{full}((R(i, j) \cdot W(j, i)) \cdot (R(i, j) \cdot W(j, i)))$ **then**
      $pout(j, i) \leftarrow W(j, i)$
  return $pout$

function TWIN(M)
  $N \leftarrow \text{maxplus}(-\text{plustimes}(\text{full}(M)))$
  return N

In conclusion of this section, it has to be remarked that a module $\mathscr{M}$ is controlled invariant if the control law makes it invariant for the closed-loop system and that, in the context of max-plus algebra, this law has also to be causal, that means that has to express the non-anticipative character of the transformation.

With the theoretical foundation in place, the subsequent sections delve into the methodology developed to model cooperating underwater devices used in repetitive patrolling. Additionally, it will be explored how the patrolling problem can be formulated and solved through a "Model Matching Problem (MMP)" to manage the synchronization of the devices and their coordinated behaviour, including the verification of the causal controlled invariance of the found module.

Chapter 4.

The Problem of Patrolling

This analysis concerns the modelling of the situation presented in Fig. 4.1, where a shoal of three fish-like robots have to explore many areas through predefined paths. In this way, fish robots are considered as units performing work in a pre-established sequence [2]. This phase is carried out using the Max-Plus Algebra Toolbox for MATLAB [169] and for Scilab [168], the latter now integrated into ScicosLab [170].

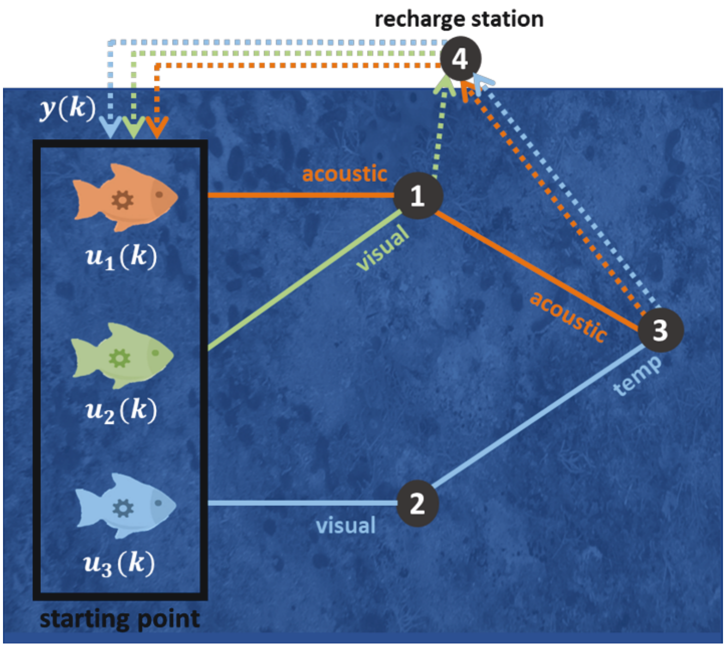

Figure 4.1.: General scheme for the patrolling

4.1. The Modelling Process

The modelling process begins with a detailed definition of the considered system. To that end, it has to be specified that each fish robot within the shoal is characterized by distinct sensor equipment and mobility features. These robots have to repeatedly patrol an area containing predefined Points of Interest (POIs). Each POI can have different characteristics such as extension, topology, and depth and has to be surveyed by some robots of the shoal, that have the most suitable capabilities (sensors) for those points. There may be POIs that need to be explored in a visual way, others in an acoustic way, or with environmental sensors (e.g., temperature).

In the diagram in Fig. 4.1, when a robot has moved to the end of a "segment", it means that it has reached and explored that point. Moreover, when a robot reaches the end of its path, that is the POI n.4 containing the recharge station, it must be recharged to then be positioned at its starting point for a new patrolling round.

The modelling of this control problem can be faced with the max-plus algebra and therefore, the primary challenge of this work concerns the study of the problem through this theoretical framework.

4.1.1. Constraints and Operational Procedures

In formulating the model for the fish robot exploration scenario depicted in Fig. 4.1, it was chosen to directly outline the constraints and specifications governing the behavior of the fish robots within the system. While an intermediate event graph is not used in this process, the constraints are explicitly formulated and integrated into the modelling method for clarity and coherence. These constraints encompass priority management among fish robots, task sequencing for each robot, conflict avoidance given by exclusive exploration, and other pertinent considerations.

The subsequent list delineates the key constraints and their corresponding handling mechanisms within the model:

- Exclusive exploration: only one fish at a time can explore every point.
- Priority assignment: fish robot 1 has priority over the others in exploring points in common with them. This choice may be dictated by knowing that that robot is slower and/or has to take a longer route [1].
- Sequential task execution: each fish starts a new round only after recharging, returning to its starting point, and after receiving the start command.
- Availability of charging basis: there are three charging basins, one for each fish
- Exclusion of final POI: POI n.4 does not have to be explored as it corresponds to the final point where recharge stations are located out of the water.
- Operator intervention exclusion: the human intervention for device retrieval and charging is not considered during the survey, assuming that, when the survey is performed, there is always someone to charge the devices and, once charging is complete, to return the fish robots to their starting point.

4.1.2. Definition of the Model

In the Table 4.1, the involved variables are presented, where the index k is related to the number of the survey (k-th round). Three input events, $u_1(k)$, $u_2(k)$ and $u_3(k)$, are triggered from outside of the system and they represents the "time when fishes of type 1, 2 and 3 are commanded to start": these values needs to be provided by some external source, while other values can be computed with appropriate rules. Then, internal events are the ones of type "exploration start time of a fish in one POI" and "exploration completion time by a fish in one POI": events of this type can only occur after the fish has arrived at the POI and, if the point is in common with a higher priority fish, once the previous exploration in the same POI has been completed by the high priority fish involved there. Finally, the "global end of charge" is an output event, triggered internally by the system and visible from outside.

[1]In general, the prioritization of certain robot actions over other robots can be influenced by several factors, including mission objectives, available resources, environmental constraints, and complexity of actions. These design choices aim to optimize the overall performance and success of the robotic system in accomplishing its mission.

Table 4.1.: Involved Variables

Variable name	**Meaning**
$u_i(k)$	Time when the fish i is commanded to start, for the k-th round
$x_{aij}(k)$	Exploration start time, after the travel, by fish i, in the POI j, for the k-th round
$x_{eij}(k)$	Exploration completion time, after the data survey, by fish i, in the POI j, for the k-th round
$x_{ri}(k)$	Time when the fish i has completed its recharge and it is ready for a new round
$x_{r4}(k) = y(k)$	Global end of charge, for the k-round, in correspondence with the recharge completion after the patrolling by the three robots and their positioning at the starting point

The variables' indexes, starting from x_{aij} and x_{eij}, have been defined as follows:

- the first index can be "a" if it refers to the exploration start time by a fish; "e" represents instead the exploration completion time, after the data survey,
- i is related to the specific fish and can be 1, 2 or 3,
- j is related to the considered POI and can be 1, 2, 3 or 4 (final point).

However, for POI n.4, there is only x_{ai4} and not x_{ei4}, since that POI does not have to be explored, as it represents the end of each robot's path where the recharge bases are located. So, actually, x_{ai4} does not represent an exploration start time, but the recharge start time for the fish i. Moreover, because of the robots' return-to-start, represented by their readiness for a new round after the recharge, other variables, x_{r1}, x_{r2} and x_{r3} has to be added, to represent the time when each fish type (indicated by the subscript) has completed its recharge and is ready again at the starting point[2]. Finally, one last variable, that is $x_{r4}(k)$, represents the output of the system, and it is related to the global end of charge, that considers the end of the charging of all three robots and their readiness at the starting point.

[2] Actually, these variables could have been called x_{ei4}, but it was preferred to distinguish exploration actions from charging actions, for better readability and understanding by the reader. Moreover, knowing the devices, the (maximum) recharging times can be known and fixed a priori, while exploration times may vary if the system configuration changes.

In this situation, the contributions of the three robots and the four POIs, for the k-th round (Fig. 4.6), are as follows:

- $x_{a11}(k)$ as the exploration start time of the fish 1 in POI n.1
- $x_{a21}(k)$ as the exploration start time of the fish 2 in POI n.1
- $x_{a32}(k)$ as the exploration start time of the fish 3 in POI n.2
- $x_{e11}(k)$ as the exploration completion time of the fish 1 in POI n.1
- $x_{e21}(k)$ as the exploration completion time of the fish 2 in POI n.1
- $x_{e32}(k)$ as the exploration completion time of the fish 3 in POI n.2
- $x_{a13}(k)$ as the exploration start time of the fish 1 in POI n.3
- $x_{a33}(k)$ as the exploration start time of the fish 3 in POI n.3
- $x_{e13}(k)$ as the exploration completion time of the fish 1 in POI n.3
- $x_{e33}(k)$ as the exploration completion time of the fish 3 in POI n.3.
- $x_{a14}(k)$ as the arrival time of the fish 1 in POI n.4 (recharge station).
- $x_{a24}(k)$ as the arrival time of the fish 2 in POI n.4 (recharge station).
- $x_{a34}(k)$ as the arrival time of the fish 3 in POI n.4 (recharge station).
- $x_{r1}(k)$ as the time when the fish 1 is ready for a new round after the recharge.
- $x_{r2}(k)$ as the time when the fish 2 is ready for a new round after the recharge.
- $x_{r3}(k)$ as the time when the fish 3 is ready for a new round after the recharge.

In a similar way as before, some constants have been defined with T_{ijm}, where:

- i is related to the fish type and can be 1, 2 or 3,
- j is related to the POI to be reached or explored and can be 1, 2 or 3 or 4,
- m is denoted by "P" if it is a travel time to reach the POI from a previous POI (or the start) or "E" if it represents the exploration time of the same.

Then, there are three T_{iC}, denoting the time for the fish type i to reach the charging base, representing a "flyback" time, and three T_{iR} corresponding to the time of the recharge of the device i and its returning to the start. Let's remember that only 1 fish at a time can explore a POI and that the fish 1 has priority over the other two on common points: therefore, it has to visit POI n.1 and POI n.3 first. Moreover, each fish starts a new round after that it has recharged, has returned to the start at time $x_{ri}(k)$, and once received the start command at time $u_i(k+1)$: the contributions in the parenthesis of the first three equations of the model guarantee this concept.

At this point, the model can be shown as follows:

$$\begin{aligned}
x_{a11}(k+1) &= T_{11P} \otimes (u_1(k+1) \oplus x_{r1}(k)) \\
x_{a21}(k+1) &= T_{21P} \otimes (u_2(k+1) \oplus x_{r2}(k)) \\
x_{a32}(k+1) &= T_{32P} \otimes (u_3(k+1) \oplus x_{r3}(k)) \\
x_{e11}(k+1) &= T_{11E} \otimes x_{a11}(k+1) \\
x_{e21}(k+1) &= T_{21E} \otimes (x_{a21}(k+1) \oplus x_{e11}(k+1)) \\
x_{e32}(k+1) &= T_{32E} \otimes x_{a32}(k+1) \\
x_{a13}(k+1) &= T_{13P} \otimes x_{e11}(k+1) \\
x_{a33}(k+1) &= T_{33P} \otimes x_{e32}(k+1) \\
x_{e13}(k+1) &= T_{13E} \otimes x_{a13}(k+1) \\
x_{e33}(k+1) &= T_{33E} \otimes (x_{a33}(k+1) \oplus x_{e13}(k+1)) \\
x_{a14}(k+1) &= T_{1C} \otimes x_{e13}(k+1) \\
x_{a24}(k+1) &= T_{2C} \otimes x_{e21}(k+1) \\
x_{a34}(k+1) &= T_{3C} \otimes x_{e33}(k+1) \\
x_{r1}(k+1) &= T_{1R} \otimes x_{a14}(k+1) \\
x_{r2}(k+1) &= T_{2R} \otimes x_{a24}(k+1) \\
x_{r3}(k+1) &= T_{3R} \otimes x_{a34}(k+1) \\
x_{r4}(k) = y(k) &= x_{r1}(k) \oplus x_{r2}(k) \oplus x_{r3}(k)
\end{aligned}$$

Using a matrix notation, the equations can be written as:

$$\begin{cases} x(k+1) = A_0 x(k+1) \oplus A_1 x(k) \oplus B' u(k+1) \\ \quad y(k) = Cx(k) \end{cases} \tag{4.1}$$

with:

$$A_0 = \begin{pmatrix}
\epsilon & \epsilon & \epsilon & \epsilon & \epsilon & \epsilon & \epsilon & \epsilon & \epsilon & \epsilon & \epsilon & \epsilon & \epsilon\epsilon & \epsilon & \epsilon \\
\epsilon & \epsilon & \epsilon & \epsilon & \epsilon & \epsilon & \epsilon & \epsilon & \epsilon & \epsilon & \epsilon & \epsilon & \epsilon\epsilon & \epsilon & \epsilon \\
\epsilon & \epsilon & \epsilon & \epsilon & \epsilon & \epsilon & \epsilon & \epsilon & \epsilon & \epsilon & \epsilon & \epsilon & \epsilon\epsilon & \epsilon & \epsilon \\
T_{11E} & \epsilon & \epsilon & \epsilon & \epsilon & \epsilon & \epsilon & \epsilon & \epsilon & \epsilon & \epsilon & \epsilon & \epsilon & \epsilon & \epsilon & \epsilon \\
\epsilon & T_{21E} & \epsilon & T_{21E} & \epsilon & \epsilon & \epsilon & \epsilon & \epsilon & \epsilon & \epsilon & \epsilon & \epsilon & \epsilon & \epsilon & \epsilon \\
\epsilon & \epsilon & T_{32E} & \epsilon & \epsilon & \epsilon & \epsilon & \epsilon & \epsilon & \epsilon & \epsilon & \epsilon & \epsilon & \epsilon & \epsilon & \epsilon \\
\epsilon & \epsilon & \epsilon & T_{13P} & \epsilon & \epsilon & \epsilon & \epsilon & \epsilon & \epsilon & \epsilon & \epsilon & \epsilon & \epsilon & \epsilon & \epsilon \\
\epsilon & \epsilon & \epsilon & \epsilon & \epsilon & T_{33P} & \epsilon & \epsilon & \epsilon & \epsilon & \epsilon & \epsilon & \epsilon & \epsilon & \epsilon & \epsilon \\
\epsilon & \epsilon & \epsilon & \epsilon & \epsilon & \epsilon & T_{13E} & \epsilon & \epsilon & \epsilon & \epsilon & \epsilon & \epsilon & \epsilon & \epsilon & \epsilon \\
\epsilon & \epsilon & \epsilon & \epsilon & \epsilon & \epsilon & \epsilon & T_{33E} & T_{33E} & \epsilon & \epsilon & \epsilon & \epsilon & \epsilon & \epsilon & \epsilon \\
\epsilon & \epsilon & \epsilon & \epsilon & \epsilon & \epsilon & \epsilon & \epsilon & T_{1C} & \epsilon & \epsilon & \epsilon & \epsilon & \epsilon & \epsilon & \epsilon \\
\epsilon & \epsilon & \epsilon & \epsilon & T_{2C} & \epsilon & \epsilon & \epsilon & \epsilon & \epsilon & \epsilon & \epsilon & \epsilon & \epsilon & \epsilon & \epsilon \\
\epsilon & \epsilon & \epsilon & \epsilon & \epsilon & \epsilon & \epsilon & \epsilon & \epsilon & T_{3C} & \epsilon & \epsilon & \epsilon & \epsilon & \epsilon & \epsilon \\
\epsilon & \epsilon & \epsilon & \epsilon & \epsilon & \epsilon & \epsilon & \epsilon & \epsilon & \epsilon & T_{1R} & \epsilon & \epsilon & \epsilon & \epsilon & \epsilon \\
\epsilon & \epsilon & \epsilon & \epsilon & \epsilon & \epsilon & \epsilon & \epsilon & \epsilon & \epsilon & \epsilon & T_{2R} & \epsilon & \epsilon & \epsilon & \epsilon \\
\epsilon & \epsilon & \epsilon & \epsilon & \epsilon & \epsilon & \epsilon & \epsilon & \epsilon & \epsilon & \epsilon & \epsilon & T_{3R} & \epsilon & \epsilon & \epsilon
\end{pmatrix}$$

$$A_1 = \begin{pmatrix}
\epsilon & \epsilon & \epsilon & \epsilon & \epsilon & \epsilon & \epsilon & \epsilon & \epsilon & \epsilon & \epsilon & \epsilon & \epsilon & T_{11P} & \epsilon & \epsilon \\
\epsilon & \epsilon & \epsilon & \epsilon & \epsilon & \epsilon & \epsilon & \epsilon & \epsilon & \epsilon & \epsilon & \epsilon & \epsilon & \epsilon & T_{21P} & \epsilon \\
\epsilon & \epsilon & \epsilon & \epsilon & \epsilon & \epsilon & \epsilon & \epsilon & \epsilon & \epsilon & \epsilon & \epsilon & \epsilon & \epsilon & \epsilon & T_{32P} \\
\epsilon & \epsilon & \epsilon & \epsilon & \epsilon & \epsilon & \epsilon & \epsilon & \epsilon & \epsilon & \epsilon & \epsilon & \epsilon & \epsilon & \epsilon & \epsilon \\
\epsilon & \epsilon & \epsilon & \epsilon & \epsilon & \epsilon & \epsilon & \epsilon & \epsilon & \epsilon & \epsilon & \epsilon & \epsilon & \epsilon & \epsilon & \epsilon \\
\epsilon & \epsilon & \epsilon & \epsilon & \epsilon & \epsilon & \epsilon & \epsilon & \epsilon & \epsilon & \epsilon & \epsilon & \epsilon & \epsilon & \epsilon & \epsilon \\
\epsilon & \epsilon & \epsilon & \epsilon & \epsilon & \epsilon & \epsilon & \epsilon & \epsilon & \epsilon & \epsilon & \epsilon & \epsilon & \epsilon & \epsilon & \epsilon \\
\epsilon & \epsilon & \epsilon & \epsilon & \epsilon & \epsilon & \epsilon & \epsilon & \epsilon & \epsilon & \epsilon & \epsilon & \epsilon & \epsilon & \epsilon & \epsilon \\
\epsilon & \epsilon & \epsilon & \epsilon & \epsilon & \epsilon & \epsilon & \epsilon & \epsilon & \epsilon & \epsilon & \epsilon & \epsilon & \epsilon & \epsilon & \epsilon \\
\epsilon & \epsilon & \epsilon & \epsilon & \epsilon & \epsilon & \epsilon & \epsilon & \epsilon & \epsilon & \epsilon & \epsilon & \epsilon & \epsilon & \epsilon & \epsilon \\
\epsilon & \epsilon & \epsilon & \epsilon & \epsilon & \epsilon & \epsilon & \epsilon & \epsilon & \epsilon & \epsilon & \epsilon & \epsilon & \epsilon & \epsilon & \epsilon \\
\epsilon & \epsilon & \epsilon & \epsilon & \epsilon & \epsilon & \epsilon & \epsilon & \epsilon & \epsilon & \epsilon & \epsilon & \epsilon & \epsilon & \epsilon & \epsilon \\
\epsilon & \epsilon & \epsilon & \epsilon & \epsilon & \epsilon & \epsilon & \epsilon & \epsilon & \epsilon & \epsilon & \epsilon & \epsilon & \epsilon & \epsilon & \epsilon \\
\epsilon & \epsilon & \epsilon & \epsilon & \epsilon & \epsilon & \epsilon & \epsilon & \epsilon & \epsilon & \epsilon & \epsilon & \epsilon & \epsilon & \epsilon & \epsilon \\
\epsilon & \epsilon & \epsilon & \epsilon & \epsilon & \epsilon & \epsilon & \epsilon & \epsilon & \epsilon & \epsilon & \epsilon & \epsilon & \epsilon & \epsilon & \epsilon \\
\epsilon & \epsilon & \epsilon & \epsilon & \epsilon & \epsilon & \epsilon & \epsilon & \epsilon & \epsilon & \epsilon & \epsilon & \epsilon & \epsilon & \epsilon & \epsilon
\end{pmatrix}$$

$$
B' = \begin{pmatrix}
T_{11P} & \epsilon & \epsilon \\
\epsilon & T_{21P} & \epsilon \\
\epsilon & \epsilon & T_{32P} \\
\epsilon & \epsilon & \epsilon \\
\epsilon & \epsilon & \epsilon \\
\epsilon & \epsilon & \epsilon \\
\epsilon & \epsilon & \epsilon \\
\epsilon & \epsilon & \epsilon \\
\epsilon & \epsilon & \epsilon \\
\epsilon & \epsilon & \epsilon \\
\epsilon & \epsilon & \epsilon \\
\epsilon & \epsilon & \epsilon \\
\epsilon & \epsilon & \epsilon \\
\epsilon & \epsilon & \epsilon \\
\epsilon & \epsilon & \epsilon \\
\epsilon & \epsilon & \epsilon
\end{pmatrix}
$$

$$
C = \begin{pmatrix} \epsilon & \epsilon & \epsilon & \epsilon & \epsilon & \epsilon & \epsilon & \epsilon & \epsilon & \epsilon & \epsilon & \epsilon & \epsilon & e & e & e \end{pmatrix}
$$

The equation, due to the presence of the term $A_0 x\,(k+1)$, describes an implicit relation that has to be made explicit to obtain an expression of the form:

$$
\begin{cases} x\,(k+1) = Ax\,(k) \oplus Bu\,(k+1) \\ \quad y(k) = Cx(k) \\ \quad x(0) = \epsilon \end{cases} \tag{4.2}
$$

At this point, it has to be considered that the least solution of an implicit equation $x = Ax \oplus b$ can be expressed, in the max-plus algebra, by means of the Kleene star $A^* = \bigoplus_{n\in\mathbb{N}} A^n$, as $x = A^* b$. In this case, A_0 is lower triangular and therefore $A_0^i = \epsilon$ $\forall i \geq \dim A_0$. In this way, A_0^* can be calculated, obtaining $A_0^* = \bigoplus_{n\in\mathbb{N}} A_0^n$ with $A_0^i = \epsilon$ $\forall i \geq 16$. Once calculated A_0^*, it is possible to finally obtain the representation of the plant as in (4.2) where the final matrices are $A = A_0^* A_1$, $B = A_0^* B'$ and C:

$$
\begin{cases} x\,(k+1) = A_0^*\left(A_1 x(k) \oplus B' u\,(k+1)\right) = A_0^* A_1 x(k) \oplus A_0^* B' u\,(k+1) \\ \quad y(k) = Cx(k) \\ \quad x(0) = \epsilon \end{cases} \tag{4.3}
$$

Using the Symbolic Math Toolbox of MATLAB, combined with the Max-Plus Algebra Toolbox for the same environment, it has been possible to show the matrices A_0^*, A, B and C leaving the various T_{ijm} in a symbolic way, as shown in the following 4.2. The choice of using MATLAB just in this case, derived from the fact that there is no symbolic calculation on ScicosLab, that was instead used for all the rest of calculations and simulations.

Remark 6 *It is possible to simplify the system for better readability, considering the use of a reduced version of the previous model while maintaining its equivalence. In fact, it is worth noting that some components within the model are exclusively represented as additions, allowing specific variables to be incorporated into others. For example, it is possible to substitute the contribution of* x_{e11}*,* x_{e21}*,* x_{e32}*,* x_{e13}*,* x_{e33} *into the other variable, to delete five equations. In this way, the core nature of the system remains unchanged and only a reduction in the number of variables used for representation has been applied. It is important to highlight that also in this scenario, the introduction of numerical values would yield equal results for the outputs, but less variables can be monitored. For this reason, it was preferred to avoid reducing the system, leaving the reader the evaluation and the selection of which variables to monitor depending on specific requirements.*

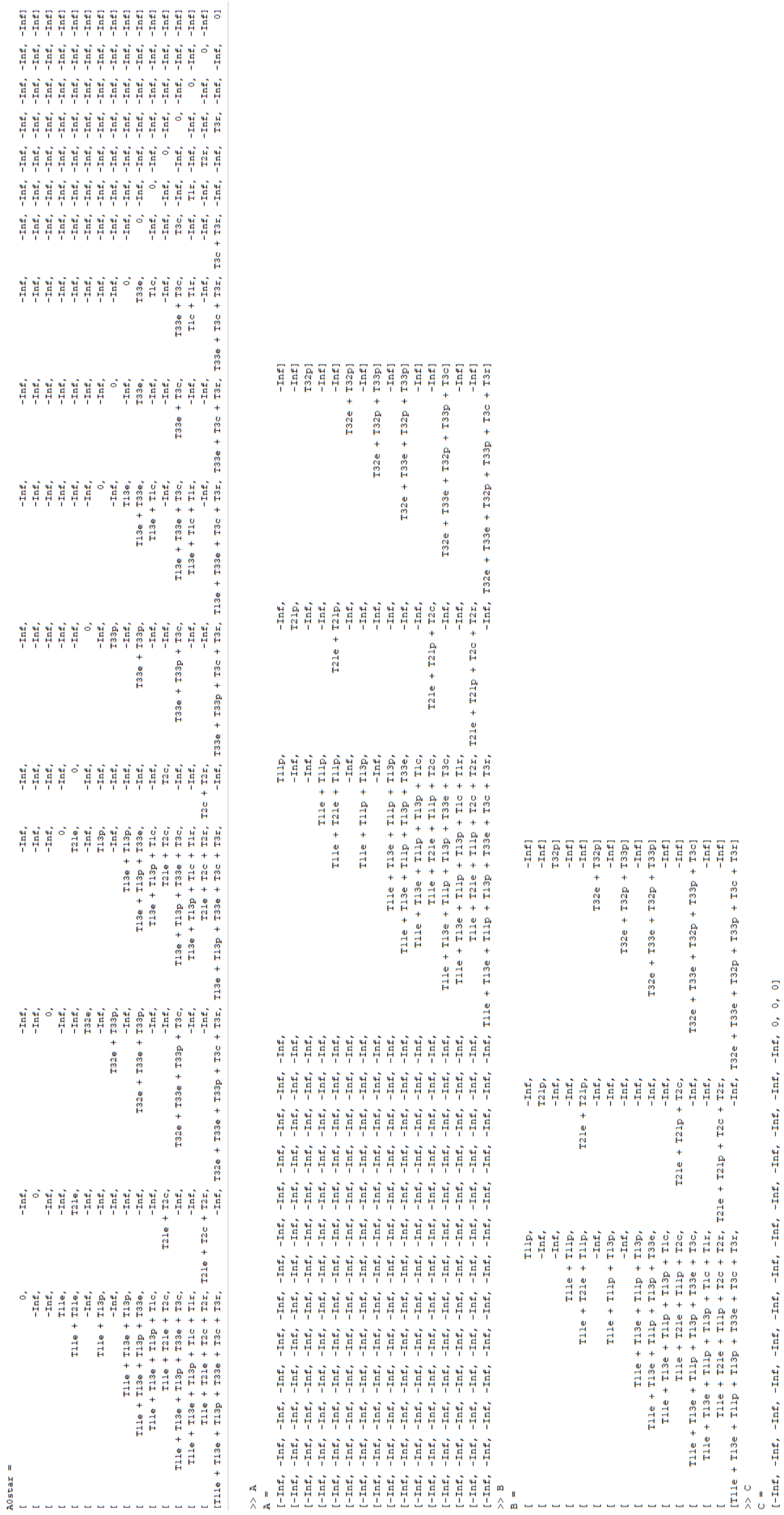

Figure 4.2.: Matrices A_0^*, A, B, and C

4.1.3. Simulations

Once obtained the matrices in parametric form, a numerical example is provided, with the following time units:

- In POI n.1: $T_{11P} = 4, T_{21P} = 6, T_{11E} = 4, T_{21E} = 5$
- In POI n.2: $T_{32P} = 6, T_{32E} = 5$
- In POI n.3: $T_{13P} = 8, T_{33P} = 4, T_{13E} = 4, T_{33E} = 2$
- In POI n.4: $T_{1C} = 35, T_{2C} = 30, T_{3C} = 40$
- At the starting point, after recharging: $T_{1R} = 5, T_{2R} = 10, T_{3R} = 20$.

For this modelling option, with the time units provided, the A, B and C matrices are now as follows, considering that the results are now plotted on ScicosLab where $\epsilon = -\infty$ is represented by a point.

```
A  =

!.  .  .  .  .  .  .  .  .  .  .  .  .  4   .   .   !
!                                                   !
!.  .  .  .  .  .  .  .  .  .  .  .  .  .   6   .   !
!                                                   !
!.  .  .  .  .  .  .  .  .  .  .  .  .  .   .   6   !
!                                                   !
!.  .  .  .  .  .  .  .  .  .  .  .  .  8   .   .   !
!                                                   !
!.  .  .  .  .  .  .  .  .  .  .  .  .  13  11  .   !
!                                                   !
!.  .  .  .  .  .  .  .  .  .  .  .  .  .   .   11  !
!                                                   !
!.  .  .  .  .  .  .  .  .  .  .  .  .  16  .   .   !
!                                                   !
!.  .  .  .  .  .  .  .  .  .  .  .  .  .   .   15  !
!                                                   !
!.  .  .  .  .  .  .  .  .  .  .  .  .  20  .   .   !
!                                                   !
!.  .  .  .  .  .  .  .  .  .  .  .  .  22  .   17  !
!                                                   !
!.  .  .  .  .  .  .  .  .  .  .  .  .  55  .   .   !
!                                                   !
!.  .  .  .  .  .  .  .  .  .  .  .  .  43  41  .   !
!                                                   !
!.  .  .  .  .  .  .  .  .  .  .  .  .  62  .   57  !
!                                                   !
!.  .  .  .  .  .  .  .  .  .  .  .  .  60  .   .   !
!                                                   !
!.  .  .  .  .  .  .  .  .  .  .  .  .  53  51  .   !
!                                                   !
!.  .  .  .  .  .  .  .  .  .  .  .  .  82  .   77  !

B  =

!4   .   .   !
!            !
!.   6   .   !
!            !
!.   .   6   !
!            !
!8   .   .   !
!            !
!13  11  .   !
!            !
!.   .   11  !
!            !
!16  .   .   !
!            !
!.   .   15  !
!            !
!20  .   .   !
!            !
!22  .   17  !
!            !
!55  .   .   !
!            !
!43  41  .   !
!            !
!62  .   57  !
!            !
!60  .   .   !
!            !
!53  51  .   !
!            !
!82  .   77  !

C  =

!.  .  .  .  .  .  .  .  .  .  .  .  .  0  0  0  !
```

Figure 4.3.: Matrices A, B and C with numerical values

Assuming that all fish types are commanded to start at the same time instant 0 and again at the instant 30, from the simulation of the system, it emerges that the first-round ends after 82 time-units and the second one at 159 time-units, i.e. after further 77 time-units, as indicated in the next lines:

$$u(1) = \begin{pmatrix} 0 \\ 0 \\ 0 \end{pmatrix} \rightarrow x(1) = Ax(0) \bigoplus Bu(1) = \begin{pmatrix} 4 & 6 & 6 & 8 & 13 & 11 & 16 & 15 & 20 & 22 & 55 & 43 & 62 & 60 & 53 & 82 \end{pmatrix}^T$$

$$y(1) = Cx(1) = 82$$

$$u(2) = \begin{pmatrix} 30 \\ 30 \\ 30 \end{pmatrix} \rightarrow x(2) = Ax(1) \bigoplus Bu(2) = \begin{pmatrix} 64 & 59 & 88 & 68 & 73 & 93 & 76 & 97 & 80 & 99 & 115 & 103 & 139 & 120 & 113 & 159 \end{pmatrix}^T$$

$$y(2) = Cx(2) = 159$$

This means that after 82 time-units all three robots have finished their first exploration, have recharged and are ready for a new round. In this case, to obtain $x(1)$, only the contribution of $Bu(1)$ was involved since $x(0) = \epsilon$ by hypothesis. As regards the result $x(2)$, instead, start commands u_i are sent before the global return-to-start time x_{r4} (instant 82), and this leads to a state vector $x(2)$ that, for the second round, only depends on the contribution of $Ax(1)$. If, on the other hand, it was assumed that the start commands received by the fishes would have been at the instant 160, i.e., after the global return-to-start time of x_{r4} (instant 82), the following state vector $x(2)$ would have been obtained, only depending on $Bu(2)$:

$$u(2) = \begin{pmatrix} 160 \\ 160 \\ 160 \end{pmatrix} \rightarrow x(2) = \begin{pmatrix} 164 & 166 & 166 & 168 & 173 & 171 & 176 & 175 & 180 & 182 & 215 & 203 & 222 & 220 & 213 & 242 \end{pmatrix}^T$$

$$y(2) = Cx(2) = 242$$

In these two latter results, only one of the two contributions of the expression $x(2) = Ax(1) \oplus Bu(2)$ predominates. However, if the start command times could also be different for each fish, the obtained result would depend for some components on $Ax(1)$ and for others on $Bu(2)$:

$$u(2) = \begin{pmatrix} 30 \\ 30 \\ 160 \end{pmatrix} \to x(2) = \begin{pmatrix} 64 & 59 & 166 & 68 & 73 & 171 & 76 & 175 & 80 & 177 & 115 & 103 & 217 & 120 & 113 & 237 \end{pmatrix}^T$$

$y(2) = Cx(2) = 237$

4.2. The Model Matching Problem

The main steps to solve a MMP for the linear max-plus system are now recalled, as presented in section 3.2.4. In this case, the plant has matrices A_P, B_P and C_P, previously denoted as A, B and C in section 4.1.3. The model was here chosen with the objective that each round should end exactly 120 $(40 + 80)$ time units after the reception of start commands or, alternatively, 180 $(100 + 80)$ time units after the completion of the previous round. This requirement aims to match the output of the plant with the output of the max-plus stationary linear model described by:

$$\begin{cases} x_M(k+1) = 100\ x_M(k) \oplus 40\ u_M(k+1) \\ y_M(k) = 80\ x_M(k) \\ x_M(0) = \epsilon \end{cases} \tag{4.4}$$

with $x_M : \mathbb{N} \to \mathbb{R}_{max}$ as the state vector, $u_M : \mathbb{N} \to \mathbb{R}_{max}$ as the control input and $y_M : \mathbb{N} \to \mathbb{R}_{max}$ as the dater of output data, for integers $k > 0$.

Such MMP consists in finding a suitable control law that forces the given plant to behave accordingly to the given model. Therefore, the MMP consists in finding, for all possible non-decreasing input sequences $\{u_M(k)\}_{k\in\mathbb{N}}$ of the model, a non-decreasing control input sequence $\{u_P(k)\}_{k\in\mathbb{N}}$ for the plant, such that its output $\{y_P(k)\}_{k\in\mathbb{N}}$ equals the $\{y_M(k)\}_{k\in\mathbb{N}}$ of the model, i.e. $y_P(k) = y_M(k)\ \forall k \in \mathbb{N}$.

Considering now the joint internal event dater $x_E = \begin{pmatrix} x_P & x_M \end{pmatrix}^T$ it is possible to describe the related joint dynamics through the equation:

$$x_E(k+1) = A_E x_E(k) \oplus B_1 u_P(k+1) \oplus B_2 u_M(k+1) \tag{4.5}$$

with $A_E = \begin{pmatrix} A_P & \epsilon \\ \epsilon & A_M \end{pmatrix}$, $B_1 = \begin{pmatrix} B_P \\ \epsilon \end{pmatrix}$, $B_2 = \begin{pmatrix} \epsilon \\ B_M \end{pmatrix}$ and $x_E(0) = \epsilon$.

This control problem can now be reformulated as that of finding, for any input $\{u_M(k)\}_{k\in\mathbb{N}}$, a control input $\{u_P(k)\}_{k\in\mathbb{N}}$ that keeps $x_E(k)$ inside the output equalizer semi-module $K = \left\{ x_E = \begin{pmatrix} x_P \\ x_M \end{pmatrix} \in R_{max}^{n_p+n_M} \quad , s.\ t. C_P x_P = C_M x_M \right\}$.

Given a non-anticipative plant Σ_P and a non-anticipative model Σ_M, the related MMP is solvable if for all $x \in ImB_2 = Im \begin{pmatrix} \epsilon \\ B_M \end{pmatrix}$, there exists $y \in ImB_1 = Im \begin{pmatrix} B_P \\ \epsilon \end{pmatrix}$, such that $x \oplus y$ belongs to $V^*(K)$, where $V^*(K)$ is the maximum $(A_E$, $B_1)$-invariant semi module contained in the output equalizer semi-module K.

Remark 7 *At this point, one doubt may arise related to the condition of non-anticipativeness presented in Definition 4, especially for $A_P \geq I_{n_P}$, where A_P is the so-called matrix A of the plant presented in Chapter 4.1.3. Indeed, for the considered plant this hypothesis is not respected, since many components of the diagonal of A_P are ϵ. However, it has to be remarked that the non-anticipativeness condition is not used actually in the first part of the proof of Theorem 5 [70], where the equalities 3.17 and 3.18 are enough to get $A_E x_E(k) \geq B_1 u_p(k)$, without using the hypothesis $A_E \geq I_{n+1}$. The second part of the proof cannot be simplified in the same way, but it is possible to say that the condition of the theorem is at least sufficient to provide a solution of the MMP, without this hypothesis, and this allows to keep on with the example. An alternative proof that avoids the condition $A_E \geq I_{n+1}$, or just the hypothesis $A_P \geq I_{n_P}$, for the Theorem 5 is provided in Appendix B.*

Coming back to the example, matrices A_E, B_1 and B_2 will be:

```
-->full(AE)
 ans  =

!.  .  .  .  .  .  .  .  .  .  .  .  .  4   .   .   .    !
!.  .  .  .  .  .  .  .  .  .  .  .  .  .   6   .   .    !
!.  .  .  .  .  .  .  .  .  .  .  .  .  .   .   6   .    !
!.  .  .  .  .  .  .  .  .  .  .  .  .  8   .   .   .    !
!.  .  .  .  .  .  .  .  .  .  .  .  .  13  11  .   .    !
!.  .  .  .  .  .  .  .  .  .  .  .  .  .   .   11  .    !
!.  .  .  .  .  .  .  .  .  .  .  .  .  16  .   .   .    !
!.  .  .  .  .  .  .  .  .  .  .  .  .  .   .   15  .    !
!.  .  .  .  .  .  .  .  .  .  .  .  .  20  .   .   .    !
!.  .  .  .  .  .  .  .  .  .  .  .  .  22  .   17  .    !
!.  .  .  .  .  .  .  .  .  .  .  .  .  55  .   .   .    !
!.  .  .  .  .  .  .  .  .  .  .  .  .  43  41  .   .    !
!.  .  .  .  .  .  .  .  .  .  .  .  .  62  .   57  .    !
!.  .  .  .  .  .  .  .  .  .  .  .  .  60  .   .   .    !
!.  .  .  .  .  .  .  .  .  .  .  .  .  53  51  .   .    !
!.  .  .  .  .  .  .  .  .  .  .  .  .  82  .   77  .    !
!.  .  .  .  .  .  .  .  .  .  .  .  .  .   .   .   100  !
```

```
-->full(B1)
 ans  =

!4   .   .    !
!.   6   .    !
!.   .   6    !
!8   .   .    !
!13  11  .    !
!.   .   11   !
!16  .   .    !
!.   .   15   !
!20  .   .    !
!22  .   17   !
!55  .   .    !
!43  41  .    !
!62  .   57   !
!60  .   .    !
!53  51  .    !
!82  .   77   !
!.   .   .    !
```

```
-->full(B2)
 ans  =

!.   !
!.   !
!.   !
!.   !
!.   !
!.   !
!.   !
!.   !
!.   !
!.   !
!.   !
!.   !
!.   !
!.   !
!.   !
!.   !
!40  !
```

Figure 4.4.: Matrices A_E, $B1$ and $B2$ with numerical values

In this way, K and V^* can be obtained through a dedicated code written in ScicosLab that provides the following results:

```
Vstar_Found = T

Solvable = T
```

```
-->K
 K  =

!0  .   .  .  .  .  .  .  .  .  .  .  .  .  .   .   !
!.  .   .  .  .  .  .  .  .  .  .  .  .  0  .   .   !
!.  .   .  .  .  .  .  .  .  .  .  .  0  .  .   .   !
!.  .   .  .  .  .  .  .  .  .  .  0  .  .  .   .   !
!.  .   .  .  .  .  .  .  .  .  0  .  .  .  .   .   !
!.  .   .  .  .  .  .  .  .  0  .  .  .  .  .   .   !
!.  .   .  .  .  .  .  .  0  .  .  .  .  .  .   .   !
!.  .   .  .  .  .  .  0  .  .  .  .  .  .  .   .   !
!.  .   .  .  .  .  0  .  .  .  .  .  .  .  .   .   !
!.  .   .  .  .  0  .  .  .  .  .  .  .  .  .   .   !
!.  .   .  .  0  .  .  .  .  .  .  .  .  .  .   .   !
!.  .   .  0  .  .  .  .  .  .  .  .  .  .  .   .   !
!.  .   0  .  .  .  .  .  .  .  .  .  .  .  .   .   !
!.  .   .  .  .  .  .  .  .  .  .  .  .  .  .   80  !
!.  .   .  .  .  .  .  .  .  .  .  .  .  .  80  .   !
!.  80  .  .  .  .  .  .  .  .  .  .  .  .  .   .   !
!.  0   .  .  .  .  .  .  .  .  .  .  .  .  0   0   !
```

```
-->Vstar
 Vstar  =

!.    .   .   .   .    .   .    .   .   .   .   .    .   .   .   59  !
!.    .   .   .   .    .   .    .   .   61  .   .    .   .   .   .   !
!.    .   .   .   .    .   .    .   .   .   .   .    .   32  .   .   !
!.    .   .   .   .    .   .    .   .   .   .   139  .   .   .   .   !
!.    .   .   .   .    .   .    .   .   .   -2  .    .   .   .   .   !
!.    .   .   .   .    59  .    .   .   .   .   .    .   .   .   .   !
!.    .   29  .   .    .   .    .   .   .   .   .    .   .   .   .   !
!.    .   .   .   .    .   .    .   -2  .   .   .    .   .   .   .   !
!.    29  .   .   .    .   .    .   .   .   .   .    .   .   .   .   !
!.    .   .   .   .    .   .    .   .   .   .   .    -2  .   .   .   !
!.    .   .   .   .    .   .    .   .   .   .   .    .   .   27  .   !
!.    .   .   32  .    .   .    .   .   .   .   .    .   .   .   .   !
!.    .   .   .   .    .   .    30  .   .   .   .    .   .   .   .   !
!9    .   .   .   .    .   .    .   .   .   .   .    .   .   .   .   !
!.    .   .   .   9    .   .    .   .   .   .   .    .   .   .   .   !
!.    .   .   .   .    .   9    .   .   .   .   .    .   .   .   .   !
!-71  .   .   .   -71  .   -71  .   .   .   .   .    .   .   .   .   !
```

Figure 4.5.: Matrices K and V^* with numerical values

These results means that the MMP for these two systems is solvable, making it possible the synchronization of the system to the provided model. With the resolution of this synchronization in terms of MMP, future steps are the verification and validation of this solution, either in simulated scenarios with Digital Twins development, and in real marine environments.

Remark 8 *Depending on the defined working model, the objective is to find out whether the system under consideration, with the given modelling, can synchronise on this model or sub-synchronise. Synchronization refers to the phenomenon where the components of a system adjust their states to operate in a coordinated manner. Sub-synchronization, on the other hand, implies a partial alignment or coordination among the system components, which may not achieve full synchronization but still exhibit some degree of coordination. There are different "levels" of synchronisation or sub-synchronisation through Model Matching to achieve the objective fully or partially but satisfactorily if the optimal situation cannot be achieved due to structural issues in the modelled system. If the problem could not be solved, it would have been necessary, for example, to consider weakening certain constraints.*

4.3. Causal Controlled Invariance

At this point, it is possible to consider the contribution of the paper [1], to verify if the V^* found is not only controlled invariant, that here means (A_E, B_1)-invariant, but also causal. In this case, the matrix that it is called M in the equation of the Theorem 11, is the previously mentioned V^*, that, however, should be normalized before the test. The results of the algorithm, shown below, confirm that this V^* is causal controlled invariant.

```
Vstar_normalized  =

!.    .   .   .   .   .   .   .   .   .   .   .   .   .   .   0   !
!                                                                 !
!.    .   .   .   .   .   .   .   .   0   .   .   .   .   .   .   !
!                                                                 !
!.    .   .   .   .   .   .   .   .   .   .   .   .   0   .   .   !
!                                                                 !
!.    .   .   .   .   .   .   .   .   .   .   0   .   .   .   .   !
!                                                                 !
!.    .   .   .   .   .   .   .   .   .   0   .   .   .   .   .   !
!                                                                 !
!.    .   .   .   .   0   .   .   .   .   .   .   .   .   .   .   !
!                                                                 !
!.    .   0   .   .   .   .   .   .   .   .   .   .   .   .   .   !
!                                                                 !
!.    .   .   .   .   .   .   .   0   .   .   .   .   .   .   .   !
!                                                                 !
!.    0   .   .   .   .   .   .   .   .   .   .   .   .   .   .   !
!                                                                 !
!.    .   .   .   .   .   .   .   .   .   .   .   0   .   .   .   !
!                                                                 !
!.    .   .   .   .   .   .   .   .   .   .   .   .   .   0   .   !
!                                                                 !
!.    .   .   0   .   .   .   .   .   .   .   .   .   .   .   .   !
!                                                                 !
!.    .   .   .   .   .   .   0   .   .   .   .   .   .   .   .   !
!                                                                 !
!0    .   .   .   .   .   .   .   .   .   .   .   .   .   .   .   !
!                                                                 !
!.    .   .   .   0   .   .   .   .   .   .   .   .   .   .   .   !
!                                                                 !
!.    .   .   .   .   .   0   .   .   .   .   .   .   .   .   .   !
!                                                                 !
!-80  .   .   .  -80  .  -80  .   .   .   .   .   .   .   .   .   !

U=

!18  .  .  .  18  .  18  .  .  .  .  .  .  .  .  .  !
!                                                    !
!36  .  .  .  36  .  36  .  .  .  .  .  .  .  .  .  !
!                                                    !
!23  .  .  .  23  .  23  .  .  .  .  .  .  .  .  .  !
Is M AE invariant ?
 F
Is P*AE*M<=(Q*AE*M)+Q*B1*U ?
 T
Is Q*AE*M<=(P*AE*M)+P*B1*U ?
 T
Is M (V*) AE-B1 invariant ?
 T
```

Figure 4.6.: Matrices V^* normalized and U, and ScicosLab output

```
H*PcR(H(-t)\otimesmin M)

!.    .  .  .  .    .  .    .  .  .  .  .  .  .  0  !
!.    .  .  .  .    .  .    .  .  0  .  .  .  .  .  !
!.    .  .  .  .    .  .    .  .  .  .  .  0  .  .  !
!.    .  .  .  .    .  .    .  .  .  .  0  .  .  .  !
!.    .  .  .  .    .  .    .  .  .  0  .  .  .  .  !
!.    .  .  .  .    0  .    .  .  .  .  .  .  .  .  !
!.    .  0  .  .    .  .    .  .  .  .  .  .  .  .  !
!.    .  .  .  .    .  .    .  0  .  .  .  .  .  .  !
!.    0  .  .  .    .  .    .  .  .  .  .  .  .  .  !
!.    .  .  .  .    .  .    .  .  .  .  .  0  .  .  !
!.    .  .  .  .    .  .    .  .  .  .  .  .  .  0  .  !
!.    .  .  0  .    .  .    .  .  .  .  .  .  .  .  !
!.    .  .  .  .    .  .    0  .  .  .  .  .  .  .  !
!0    .  .  .  .    .  .    .  .  .  .  .  .  .  .  !
!.    .  .  .  0    .  .    .  .  .  .  .  .  .  .  !
!.    .  .  .  .    .  0    .  .  .  .  .  .  .  .  !
!-80  .  .  .  -80  .  -80  .  .  .  .  .  .  .  .  !

H*PcR(H(-t)\otimesmin M) = M ?

T T T T T T T T T T T T T T T T
T T T T T T T T T T T T T T T T
T T T T T T T T T T T T T T T T
T T T T T T T T T T T T T T T T
T T T T T T T T T T T T T T T T
T T T T T T T T T T T T T T T T
T T T T T T T T T T T T T T T T
T T T T T T T T T T T T T T T T
T T T T T T T T T T T T T T T T
T T T T T T T T T T T T T T T T
T T T T T T T T T T T T T T T T
T T T T T T T T T T T T T T T T
T T T T T T T T T T T T T T T T
T T T T T T T T T T T T T T T T
T T T T T T T T T T T T T T T T
T T T T T T T T T T T T T T T T
T T T T T T T T T T T T T T T T
```

Figure 4.7.: Results of the algorithm

As it can be seen from these last lines, corresponding to the Theorem 11, the test has successfully ended, confirming that $\operatorname{Im} M = \operatorname{Im} V^*$ is causal controlled invariant, both because U is causal and all equivalences are satisfied (all comparisons are `True`).

Chapter 5.

Conclusions

In this thesis, a novel approach is introduced to model the coordinated behaviour of marine biomimetic vehicles. Specifically, the research investigates the use of max-plus algebra to effectively manage the coordination and synchronization of vehicles assigned to patrol specific areas. The application of max-plus algebra represents an innovative aspect of this work, wherein the patrolling fish robots represent one of many case studies that can be considered.

The primary aim is to address the challenges related to coordinating fish robots, engaged in confined underwater exploration. A shoal of three biomimetic vehicles is considered, each equipped with different capabilities, to conduct surveys in an underwater area via predefined paths covering specific Points of Interest in a cyclical and coordinated manner. This formulation involves diversified and repetitive tasks for each robot, with the underlying theoretical framework of max-plus algebra. The latter is renowned for its applicability in discrete event systems, and it has been exploited to develop this work, given its effectiveness in managing tasks concatenation and synchronization, and in modelling various real-world situations, including the synchronized behaviour of marine vehicles during patrolling missions.

The starting point of this thesis is rooted in an understanding of the context within which the research operates, namely marine vehicles, their mathematical models and key navigation technologies, that also lay the foundations for subsequent developments. These components are pivotal to make this work a bridge between the theoretical aspects and their practical use in simulations and real situations. In fact, this blend of theory can be connected to the practice using sensors for precise positioning to verify the vehicles' displacements and it proves valuable in simulations to study how vehicles move, using mathematical models like the Fossen model.

This thesis represents the three-year excursion of doctoral work, initially focused on a single fish robot's mathematical model and underwater technologies. The scope has then expanded to incorporate the application of max-plus algebra for the coordination of vehicles. For this reason, the structure of the thesis has a dual nature, which delves into both the individual modelling of marine vehicles and their technologies, and the broader exploration of max-plus algebra's application in cooperative vehicle control. Following the foundation of the research, in fact, the focus is then brought back to the theoretical framework, highlighting the essential role of max-plus algebra in achieving the coordinated task execution for multi-agent patrolling.

An overview with key concepts and basic results related to max-plus algebra is provided, presenting its linear systems, the concepts of controlled invariance, causality, and Model Matching Problem. The notion of causal controlled invariance for max-plus linear systems is also delved into, emphasizing its theoretical and practical implications. This notion has proven to be highly useful and applicable to a wide range of control problems in such systems, especially for online implementation of control laws. Moreover, this work contributes to the existing scientific literature by providing clarity on this topic of causal controlled invariance and introducing new equivalent sufficient conditions for a module to satisfy this property. Moreover, an algorithm has been specially developed to test such conditions, since no algorithm had so far been designed to verify the sufficient conditions defined in the literature. In other words, using the algorithm it is possible to check whether there is a causal state feedback that makes a module invariant for the closed-loop system.

The formulation of diversified and cyclic tasks for each robot, based on task-driven requirements rather than time-driven constraints, plays a central role and through a series of steps, the work leads to a complete model with the plant as a max-plus linear system. The plant is tested in simulation, providing a valuable foundation for multi-agent systems' repetitive patrolling in real underwater scenarios.

The methodology, carried out with toolboxes for both MATLAB and ScicosLab, also leads to the formalization of an appropriate "synchronization" problem for to the patrolling problem, also defined as a "Model Matching Problem (MMP)". An MMP consists in finding a suitable control law, that forces the plant, modelled as a linear system, to behave in accordance with a preestablished model of a similar kind. In this way, the shoal of fish robots can perform repetitive tasks according to a predefined strategy. Taking up the previously simulated plant, an example of resolution of an MMP is also provided. Finally, the module resulting from this solution is tested with the developed algorithm to confirm its causal controlled invariance.

While these developments mark significant contributions, the pursuit of necessary and sufficient conditions for causal controlled invariance remains a promising direction for future advancements in this field. Indeed, it is important to note that the current results are based on sufficient conditions for this property.

In summary, this research contributes to the advancement of knowledge in the field of confined underwater exploration, multi-agent patrolling, and coordinated behaviour of biomimetic marine vehicles for efficient and synchronized missions. In fact, max-plus algebra is integrated into the control framework of marine vehicles, with methodologies aimed at enhancing efficiency and effectiveness in coordinating marine vehicle patrolling. Moreover, a solution to the Model Matching Problem (MMP) is proposed, providing insights into the feasibility and effectiveness of leveraging max-plus algebra in real scenarios. A novel algorithm is also presented to test the causal controlled invariance of the module resulting from the MMP, to ensure the stability and reliability of the found solutions for vehicle control systems.

These contributions establish a synergy between theory and practice, laying the groundwork for future research and applications in the dynamic field of marine robotics and multi-agent systems.

Among different approaches for potential future developments, the investigation of using a switching system is suggested, considering parameters, such as transit and exploration times, that fluctuate within certain intervals: this would lead to an enhanced flexibility in adapting to real-world complexities. Using linear dynamics of switching type is possible to consider different interactions and configurations of the shoal with variable interactions. Moreover, this work could significantly be extended by incorporating a broader description of the patrolling problem, encompassing scenarios with varying numbers of agents and sites.

After managing the coordination aspect with max-plus algebra, particularly addressing the MMP, next steps can involve the verification and validation of the solution. This process can span real marine environments and simulated scenarios. As regards the application to a real shoal of biomimetic vehicles, further validation demands the integration of individual fish robot dynamics to confirm the proposed plan. Simulation can instead include the development of Digital Twins to have a complete simulation platform for the fish robots' path planning and modelling. Moreover, a Digital Twin can be used as a visual display of the max-plus model.

Furthermore, exploring the model's potential as a fault-detection system for identifying deviations between received data and assigned parameters is proposed to ensure the reliability of the shoal in case of unforeseen issues during operations.

In conclusion, this work has so far resulted in two publications, one for the French conference "Modélisation des Systèmes Réactifs (MSR '23)", outcome of the period spent abroad, focusing on the algorithm for causal controlled invariance verification [1], and one for "The 34th International Ocean and Polar Engineering Conference (ISOPE-2024)" as regards the modelling of the cooperating fish robots [2]. Moreover, the initial phase of research of this thesis will now be extended within the Project

"MAXFISH: Multi agents systems and Max-Plus algebra theoretical frameworks for a robot-fish shoal modelling and control" 20225RYMJE, funded by the MUR Progetti di Ricerca di Rilevante Interesse Nazionale (PRIN) Bando 2022.

Appendix A.

Examples for Causal Controlled Invariance Verification

In this appendix, some examples related to the implemented algorithm are presented. These results, developed in the ScicosLab software, are taken from [1].
Before addressing such examples, it is worth mentioning that before using the algorithm, it is, of course, necessary to add a preliminary part in the code allowing the user to define the matrices A, B, and M, in order to subsequently calculate $\begin{pmatrix} H & R & V \end{pmatrix}'$ and the generators w_i, as explained in section 3.3.2.

A.0.1. Example 1

The first example concerns the following matrices and in this case, $\operatorname{Im} M$ is controlled invariant but it is not causal and the test with P_C^R confirms this. The input data used are as follows:

$$A = \begin{pmatrix} 1 & 0 & . \\ . & 0 & . \\ 0 & . & 0 \end{pmatrix} \quad B = \begin{pmatrix} 0 & 0 \\ 4 & 5 \\ 5 & 6 \end{pmatrix} \quad M = \begin{pmatrix} 0 & 0 \\ -1 & -3 \\ 0 & 0 \end{pmatrix}$$

which lead to the following system:

$$X(k+1) = \begin{pmatrix} 1 & 0 & . \\ . & 0 & . \\ 0 & . & 0 \end{pmatrix} X(k) + \begin{pmatrix} 0 & 0 \\ 4 & 5 \\ 5 & 6 \end{pmatrix} U(k)$$

This is what was obtained with the algorithm and displayed in the ScicosLab clipboard. We've avoided showing the P and Q matrices, as they don't add any information about the results obtained.

$$U = \begin{pmatrix} -4 & -4 \\ -5 & -5 \end{pmatrix}$$

ScicosLab Output:

```
Is M A invariant?  F
Is P*A*M <= (Q*A*M) + Q*B*U?  T
Is Q*A*M <= (P*A*M) + P*B*U?  T
Is M A-B invariant?  T

H*PcR(H(-t)\otimesmin M) = M ?
 F F
 T T
 T T
```

$$H = \begin{pmatrix} -1 & -1 & -1 & -2 & -2 & -2 & -1 & -4 & -1 & -1 & -4 & -4 \\ . & . & . & -2 & . & . & . & -6 & -1 & -1 & . & . \\ . & . & . & -1 & -1 & -1 & . & -3 & . & . & -3 & -3 \end{pmatrix}$$

$$R = \begin{pmatrix} . & -5 & . & . & -6 & . & -5 & . & . & -5 & -10 & . \\ -6 & . & -6 & . & . & -7 & . & . & -6 & . & . & -11 \end{pmatrix}$$

$$V = \begin{pmatrix} 0 & 0 & 0 & -1 & -1 & -1 & 0 & . & 0 & 0 & . & . \\ 0 & . & . & . & . & . & 0 & -3 & . & . & -3 & -3 \end{pmatrix}$$

$$H * P_C^R(H^{-T} \otimes' M) = \begin{pmatrix} -1 & -1 \\ -1 & -3 \\ 0 & 0 \end{pmatrix}$$

As it can be seen from the last lines, which correspond to the result of Theorem 11, it is confirmed that $\operatorname{Im} M$ is not causal controlled invariant, both because U is not causal and because some equivalences are not satisfied: there are indeed False (`F`) values, whereas, to have causal controlled invariance, all components should be True (`T`).

A.0.2. Example 2

In this example, different matrices A and B are considered, compared to the Example 1 of Section A.0.1. However, the same matrix M was used, and in this case, $\operatorname{Im} M$ is both controlled invariant and causal. The input data used are as follows:

$$A = \begin{pmatrix} 0 & 1 & 0 \\ . & 0 & . \\ 0 & . & 0 \end{pmatrix} \quad B = \begin{pmatrix} 1 & 0 \\ 0 & 1 \\ . & 3 \end{pmatrix} \quad M = \begin{pmatrix} 0 & 0 \\ -1 & -3 \\ 0 & 0 \end{pmatrix}$$

In this case, here is what was obtained with the algorithm :

$$U = \begin{pmatrix} 6 & 6 \\ 4 & 4 \end{pmatrix}$$

ScicosLab Output:

```
Is M A invariant?  T

Is P*A*M <= (Q*A*M) + Q*B*U?  T

Is Q*A*M <= (P*A*M) + P*B*U?  T

Is M A-B invariant?  T
```

```
H*PcR(H(-t)\otimesmin M) = M ?
  T T
  T T
  T T
```

$$H = \begin{pmatrix} . & -1 & . & -1 & . & . & . & 0 & . & . & . & 0 & . & -1 & -1 & . \\ . & -4 & -4 & . & . & -1 & . & . & . & -1 & . & . & . & -2 & . & -2 \\ . & . & -1 & . & -1 & . & -1 & . & 0 & . & . & . & 0 & . & . & -1 \end{pmatrix}$$

$$R = \begin{pmatrix} -1 & . & . & -4 & -4 & . & -2 & . & . & . & -1 & . & . & . & -2 & . \\ -3 & . & . & . & . & -3 & . & -4 & -4 & -3 & -3 & -3 & -3 & . & . & . \end{pmatrix}$$

$$V = \begin{pmatrix} 0 & . & . & . & . & 0 & -1 & . & . & 0 & 0 & -1 & -1 & -1 & -1 & -1 \\ 0 & -1 & -1 & -1 & -1 & 0 & . & 0 & 0 & . & . & 0 & 0 & . & . & . \end{pmatrix}$$

$$H * P_C^R(H^{-T} \otimes' M) = \begin{pmatrix} 0 & 0 \\ -1 & -3 \\ 0 & 0 \end{pmatrix}$$

A.0.3. Example 3

In this example, there are different matrices A, B, and M. This case represents a situation where there exists a causal control law U, but only a part of the state is used. In fact, looking at the matrix A, it is noticed that it has a column composed only of ϵ elements, and here, even though the matrix U is causal and the image $\operatorname{Im} M$ is controlled invariant, the latter does not satisfy the criterion of causal invariance as defined in this thesis. The input data are here as follows:

$$A = \begin{pmatrix} 2 & . & 4 \\ 1 & . & 0 \\ 0 & . & 1 \end{pmatrix} \quad B = \begin{pmatrix} 0 & 2 \\ 4 & 1 \\ 0 & 0 \end{pmatrix} \quad M = \begin{pmatrix} -2 & -1 \\ 0 & 0 \\ 0 & -3 \end{pmatrix}$$

The algorithm's responses are shown below:

$$U = \begin{pmatrix} 5 & 5 \\ 6 & 6 \end{pmatrix}$$

ScicosLab Output:

```
Is M A invariant?  F

Is P*A*M <= (Q*A*M) + Q*B*U?  T

Is Q*A*M <= (P*A*M) + P*B*U?  T

Is M A-B invariant?  T
```

```
H*PcR(H(-t)\otimesmin M) = M ?

  F F

  T T

  T F
```

$$H * P_C^R(H^{-T} \otimes' M) = \begin{pmatrix} . & . \\ 0 & 0 \\ 0 & . \end{pmatrix}$$

This is an example of a causal controlled invariant module, but the equality (4.3) of Theorem 11 is not satisfied: this illustrates that the conditions of Proposition 3 are only sufficient.

Appendix B.

Alternative Proof for Theorem 10

In order to avoid the the hypothesis $A_E \geq I_{n+1}$, or just the hypothesis $A_P \geq I_{n_P}$ within the Theorem 5 [70], an alternative proof is provided as follows.

Proof Given an alternative system of the form $x(k+1) = A_E x(k) \oplus B_1 u(k+1) \oplus B_2 w(k+1)$, where u is a control input, and w is a disturbance, together with a submodule $\mathcal{K}$ of the state-space, the request is to check whether, for every disturbance w, there exists a control u such that $x(k)$ lies in $\mathcal{K}$. Actually, the answer depends only on the initial condition $x(0)$. The set of such admissible initial conditions is the set, called e.g. $\mathcal{W}^\star$, for which for every w, there exists a control u such that x remains in $\mathcal{K}$. This set can be seen as the supremal element of the family of modules $\mathcal{W}$ that satisfy the inclusion $A_E \mathcal{W} \oplus \operatorname{Im} B_2 \subset W \ominus \operatorname{Im} B_1$. This inclusion is equivalent to the couple of conditions $A_E \mathcal{W} \subset W \ominus \operatorname{Im} B_1$ and $\operatorname{Im} B_2 \subset W \ominus \operatorname{Im} B_1$. Since the latter is just the condition of controlled invariance, the conclusion is that the problem is solvable if and only if $\operatorname{Im} B_2 \subset \mathcal{V}^\star_{\mathcal{K}}(A_E, B_1) \ominus \operatorname{Im} B_1$.

When this is applied to a system for the Model Matching Problem, Theorem 5 is then obtained, without the hypothesis $A_E \geq I_{n+1}$. In this way, the problem is solved with the provided additional hypothesis. □

Bibliography

[1] V. Bartolucci, J. J. Loiseau, C. Martinez, and D. Scaradozzi, “Invariance causale contrôlée pour les systèmes max-plus linéaires,” in *Modélisation des Systèmes Réactifs (MSR ’23)*, Toulouse, France, 2023. [Online]. Available: https://msr2023.sciencesconf.org/504078/document

[2] V. Bartolucci, D. Scaradozzi, E. Zattoni, J. J. Loiseau, C. Martinez, and G. Conte, “A max-plus algebra-based approach for modelling shoals of fish robots during underwater exploration,” in *The 34th International Ocean and Polar Engineering Conference (ISOPE-2024)*, 2024, submitted.

[3] A. Fukuhara, M. Gunji, and Y. Masuda, “Comparative anatomy of quadruped robots and animals: a review,” *Advanced Robotics*, vol. 36, no. 13, pp. 612–630, 2022.

[4] A. Stuttaford-Fowler, H. Samani, and C.-Y. Yang, “Biomimicry in soft robotics actuation and locomotion,” in *2022 International Conference on System Science and Engineering (ICSSE)*. IEEE, 2022, pp. 017–021.

[5] Z. Gao, Q. Shi, T. Fukuda, C. Li, and Q. Huang, “An overview of biomimetic robots with animal behaviors,” *Neurocomputing*, vol. 332, pp. 339–350, 2019.

[6] S. Zimmerman and A. Abdelkefi, “Review of marine animals and bioinspired robotic vehicles: Classifications and characteristics,” *Progress in Aerospace Sciences*, vol. 93, pp. 95–119, 2017.

[7] F. Xie, Q. Zuo, Q. Chen, H. Fang, K. He, R. Du, Y. Zhong, and Z. Li, “Designs of the biomimetic robotic fishes performing body and/or caudal fin (BCF) swimming locomotion: A review,” *Journal of Intelligent & Robotic Systems*, vol. 102, pp. 1–19, 2021.

[8] D. Scaradozzi, G. Palmieri, D. Costa, and A. Pinelli, “BCF swimming locomotion for autonomous underwater robots: a review and a novel solution to improve control and efficiency,” *Ocean Engineering*, vol. 130, pp. 437–453, 2017.

[9] G. Li, G. Liu, D. Leng, X. Fang, G. Li, and W. Wang, “Underwater undulating propulsion biomimetic robots: A review,” *Biomimetics*, vol. 8, no. 3, p. 318, 2023.

[10] D. S. Barrett, “The design of a flexible hull undersea vehicle propelled by an oscillating foil,” Ph.D. dissertation, Massachusetts Institute of Technology, 1994.

[11] J. M. Anderson and N. K. Chhabra, “Maneuvering and stability performance of a robotic tuna,” *Integrative and comparative biology*, vol. 42, no. 1, pp. 118–126, 2002.

[12] J. M. Kumph, “Maneuvering of a robotic pike,” Ph.D. dissertation, Massachusetts Institute of Technology, 2000.

[13] K. Hirata, T. Takimoto, and K. Tamura, “Study on turning performance of a fish robot,” in *First International Symposium on Aqua Bio-Mechanisms.* Mitaka, 2000, pp. 287–292.

[14] M. Nakashima, “Development of a two-joint dolphin robot,” *Neurotechnology for biomimetic robots*, pp. 309–324, 2002.

[15] M. Nakashima, Y. Takashi, T. Tsubaki, and K. Ono, “Three-dimensional maneuverability of the dolphin robot, bio-mechanisms of swimming and flying (edited by kato, n., ayers, j. and morikawa, h.),” 2004.

[16] G. Dogangil, E. Ozcicek, and A. Kuzucu, “Design, construction, and control of a robotic dolphin,” in *2005 IEEE International Conference on Robotics and Biomimetics-ROBIO.* IEEE, 2005, pp. 51–56.

[17] H. Hu, “Biologically inspired design of autonomous robotic fish at Essex,” in *IEEE SMC UK-RI Chapter Conference, on Advances in Cybernetic Systems.* Citeseer, 2006, pp. 3–8.

[18] J. Liang, T. Wang, S. Wang, D. Zou, and J. Sun, “Experiment of robofish aided underwater archaeology,” in *2005 IEEE International Conference on Robotics and Biomimetics-ROBIO.* IEEE, 2005, pp. 499–504.

[19] T. Wang, L. Wen, J. Liang, and G. Wu, “Fuzzy vorticity control of a biomimetic robotic fish using a flapping lunate tail,” *Journal of Bionic Engineering*, vol. 7, no. 1, pp. 56–65, 2010.

[20] R. K. Katzschmann, J. DelPreto, R. MacCurdy, and D. Rus, “Exploration of underwater life with an acoustically controlled soft robotic fish,” *Science Robotics*, vol. 3, no. 16, p. eaar3449, 2018.

[21] O. Moreno Mayz, C. Sanoja, and N. Certad, “Design, modelling, control and simulation of biomimetic underwater robot,” in *2019 Latin American Robotics Symposium (LARS), 2019 Brazilian Symposium on Robotics (SBR) and 2019 Workshop on Robotics in Education (WRE)*, 2019, pp. 216–221.

[22] D. Costa, G. Palmieri, D. Scaradozzi, and M. Callegari, “Experimental validation of a bio-inspired thruster,” *Journal of Dynamic Systems, Measurement, and Control*, vol. 143, no. 8, p. 081004, 2021.

[23] D. Costa, G. Palmieri, M.-C. Palpacelli, M. Callegari, and D. Scaradozzi, “Design of a bio-inspired underwater vehicle,” in *2016 12th IEEE/ASME International Conference on Mechatronic and Embedded Systems and Applications (MESA)*. IEEE, 2016, pp. 1–6.

[24] D. Costa, G. Palmieri, M.-C. Palpacelli, D. Scaradozzi, and M. Callegari, “Design of a carangiform swimming robot through a multiphysics simulation environment,” *Biomimetics*, vol. 5, no. 4, p. 46, 2020.

[25] R. Blake, “The mechanics of labriform locomotion: I. labriform locomotion in the angelfish (pterophyllum eimekei): an analysis of the power stroke,” *Journal of Experimental Biology*, vol. 82, no. 1, pp. 255–271, 1979.

[26] D. Costa, C. Scoccia, M. Palpacelli, M. Callegari, and D. Scaradozzi, “Design of a labriform-steering underwater robot using a multiphysics simulation environment,” *Robotics*, vol. 11, no. 1, 2022.

[27] P. Langley, “Cognitive architectures and general intelligent systems,” *AI magazine*, vol. 27, no. 2, pp. 33–33, 2006.

[28] K. P. Sycara, “Multiagent systems,” *AI magazine*, vol. 19, no. 2, pp. 79–79, 1998.

[29] J. Yan, X. Lin, Z. Ren, S. Zhao, J. Yu, C. Cao, P. Yin, J. Zhang, and S. Scherer, “MUI-TARE: Cooperative multi-agent exploration with unknown initial position,” *IEEE Robotics and Automation Letters*, 2023.

[30] H. F. Wang, “Multi-agent co-ordination for the secondary voltage control in power-system contingencies,” *IEE Proceedings-Generation, Transmission and Distribution*, vol. 148, no. 1, pp. 61–66, 2001.

[31] S. D. McArthur, S. M. Strachan, and G. Jahn, “The design of a multi-agent transformer condition monitoring system,” *IEEE Transactions on Power Systems*, vol. 19, no. 4, pp. 1845–1852, 2004.

[32] T. Nagata and H. Sasaki, “A multi-agent approach to power system restoration,” *IEEE transactions on power systems*, vol. 17, no. 2, pp. 457–462, 2002.

[33] Y. Tomita, C. Fukui, H. Kudo, J. Koda, and K. Yabe, “A cooperative protection system with an agent model,” *IEEE Transactions on Power Delivery*, vol. 13, no. 4, pp. 1060–1066, 1998.

[34] M. Pipattanasomporn, H. Feroze, and S. Rahman, “Multi-agent systems in a distributed smart grid: Design and implementation,” in *2009 IEEE/PES Power Systems Conference and Exposition*. IEEE, 2009, pp. 1–8.

[35] A. Dimeas and N. Hatziargyriou, “A multi-agent system for microgrids,” in *Hellenic Conference on Artificial Intelligence*. Springer, 2004, pp. 447–455.

[36] G. Conte and D. Scaradozzi, “An approach to home automation by means of MAS theory,” in *Modeling and Control of Complex Systems*. CRC Press, 2007, pp. 477–500.

[37] Z. Wang, X. Liu, and S. Wu, “BACnet intelligent home supervisory control system based on multi-agent,” in *The 7th International Conference on Advanced Communication Technology, 2005, ICACT 2005.*, vol. 2. IEEE, 2005, pp. 761–764.

[38] M. Ruta, F. Scioscia, G. Loseto, and E. Di Sciascio, “Semantic-based resource discovery and orchestration in home and building automation: A multi-agent approach,” *IEEE Transactions on Industrial Informatics*, vol. 10, no. 1, pp. 730–741, 2013.

[39] D. Mahmood, N. Javaid, and M. Ilahi, “Home energy management using multi agent system for web based grids,” in *2016 International Conference on Frontiers of Information Technology (FIT)*. IEEE, 2016, pp. 342–347.

[40] W. Li, T. Logenthiran, W. L. Woo, V.-T. Phan, and D. Srinivasan, “Implementation of demand side management of a smart home using multi-agent system,” in *2016 IEEE Congress on Evolutionary Computation (CEC)*. IEEE, 2016, pp. 2028–2035.

[41] M. Tornow, A. Al-Hamadi, and V. Borrmann, “A multi-agent mobile robot system with environment perception and HMI capabilities,” in *2013 IEEE International Conference on Signal and Image Processing Applications*, 2013, pp. 252–257.

[42] C. C. Sotzing, J. Evans, and D. M. Lane, “A multi-agent architecture to increase coordination efficiency in multi-auv operations,” in *OCEANS 2007 - Europe*, 2007, pp. 1–6.

[43] X. Q. Bian, T. Chen, J. Zhou, and Z. Yan, “Research of autonomous control based on multi-agent for auv,” in *2009 International Workshop on Intelligent Systems and Applications*, 2009, pp. 1–4.

[44] M. Moarref and H. Sayyaadi, “Facility location optimization via multi-agent robotic systems,” in *2008 IEEE International Conference on Networking, Sensing and Control*, 2008, pp. 287–292.

[45] G. Franck, C. Vincent, and C. Francois, “A reactive multi-agent system for localization and tracking in mobile robotics,” in *16th IEEE International Conference on Tools with Artificial Intelligence*, 2004, pp. 431–435.

[46] A. Husain, H. Jones, B. Kannan, U. Wong, T. Pimentel, S. Tang, S. Daftry, S. Huber, and W. L. Whittaker, “Mapping planetary caves with an autonomous, heterogeneous robot team,” in *2013 IEEE Aerospace Conference*, 2013, pp. 1–13.

[47] A. Howard, L. E. Parker, and G. S. Sukhatme, “Experiments with a large heterogeneous mobile robot team: Exploration, mapping, deployment and detection,” *The International Journal of Robotics Research*, vol. 25, no. 5-6, pp. 431–447, 2006.

[48] M. C. G. Quintero, J. A. O. López, and R. F. A. Bertel, “Coordination mechanisms for a multi-agent robotic system applied to search and target location,” in *IX Latin American Robotics Symposium and IEEE Colombian Conference on Automatic Control, 2011 IEEE*, 2011, pp. 1–6.

[49] A. Marjovi, J. G. Nunes, L. Marques, and A. de Almeida, “Multi-robot exploration and fire searching,” in *2009 IEEE/RSJ International Conference on Intelligent Robots and Systems*, 2009, pp. 1929–1934.

[50] F. Ehlers, “Multi-agent teams for underwater surveillance,” in *2010 International Conference on Emerging Security Technologies*, 2010, pp. 136–141.

[51] S. Zheng, X. Zhang, and S. Sheng, “Simultaneous fault detection and control protocol design for coordination of multi-agent systems,” in *2017 29th Chinese Control And Decision Conference (CCDC)*, 2017, pp. 6425–6430.

[52] H. Su, X. Wang, and Z. Lin, “Flocking of multi-agents with a virtual leader,” *IEEE Transactions on Automatic Control*, vol. 54, no. 2, pp. 293–307, 2009.

[53] J. C. Varughese, R. Thenius, P. Leitgeb, F. Wotawa, and T. Schmickl, “A model for bio-inspired underwater swarm robotic exploration,” *IFAC-PapersOnLine*, vol. 51, no. 2, pp. 385–390, 2018, 9th Vienna International Conference on Mathematical Modelling.

[54] H. J. He, A. Koppel, A. S. Bedi, D. J. Stilwell, M. Farhood, and B. Biggs, “Decentralized multi-agent exploration with limited inter-agent communications,” in *2023 IEEE International Conference on Robotics and Automation (ICRA)*, 2023, pp. 5530–5536.

[55] M. Cococcioni, L. Fiaschi, and P. F. J. Lermusiaux, “Game theory for unmanned vehicle path planning in the marine domain: State of the art and new possibilities,” *Journal of Marine Science and Engineering*, vol. 9, no. 11, 2021.

[56] M. Dorigo, G. Theraulaz, and V. Trianni, "Swarm robotics: Past, present, and future [point of view]," *Proceedings of the IEEE*, vol. 109, no. 7, pp. 1152–1165, 2021.

[57] A. Marino, G. Antonelli, A. P. Aguiar, A. Pascoal, and S. Chiaverini, "A decentralized strategy for multirobot sampling/patrolling: Theory and experiments," *IEEE Transactions on Control Systems Technology*, vol. 23, no. 1, pp. 313–322, 2015.

[58] P. Abreu, G. Antonelli, F. Arrichiello, A. Caffaz, A. Caiti, G. Casalino, N. C. Volpi, I. B. de Jong, D. De Palma, H. Duarte, J. P. Gomes, J. Grimsdale, G. Indiveri, S. Jesus, K. Kebkal, E. Kelholt, A. Pascoal, D. Polani, L. Pollini, E. Simetti, and A. Turetta, "Widely Scalable Mobile Underwater Sonar Technology: An Overview of the H2020 WiMUST Project," *Marine Technology Society Journal*, vol. 50, no. 4, pp. 42–53, 2016.

[59] B. Allotta, G. Antonelli, A. Bongiovanni, A. Caiti, R. Costanzi, D. De Palma, P. Di Lillo, M. Franchi, P. Gjanci, G. Indiveri, C. Petrioli, A. Ridolfi, and E. Simetti, "Underwater acoustic source localization using a multi-robot system: the DAMPS project," in *2021 International Workshop on Metrology for the Sea; Learning to Measure Sea Health Parameters (MetroSea)*, 2021, pp. 388–393.

[60] A. Caiti, E. Ciaramella, G. Conte, G. Cossu, D. Costa, S. Grechi, R. Nuti, D. Scaradozzi, and A. Sturniolo, "OptoCOMM: Introducing a new optical underwater wireless communication modem," in *2016 IEEE Third Underwater Communications and Networking Conference (UComms)*, 2016, pp. 1–5.

[61] G. Cohen, D. Dubois, J. Quadrat, and M. Viot, "A linear-system-theoretic view of discrete-event processes and its use for performance evaluation in manufacturing," *IEEE transactions on Automatic Control*, vol. 30, no. 3, pp. 210–220, 1985.

[62] F. Baccelli, G. Cohen, G. J. Olsder, and J.-P. Quadrat, *Synchronization and linearity.* Wiley New York, 1992, vol. 1.

[63] G. Cohen, S. Gaubert, and J.-P. Quadrat, "Max-plus algebra and system theory: where we are and where to go now," *Annual reviews in control*, vol. 23, pp. 207–219, 1999.

[64] J. Komenda, S. Lahaye, J.-L. Boimond, and T. van den Boom, "Max-plus algebra in the history of discrete event systems," *Annual Reviews in Control*, vol. 45, pp. 240–249, 2018.

[65] W. Chen, H. Liu, and E. Qi, "Discrete event-driven model predictive control for real-time work-in-process optimization in serial production systems," *Journal of Manufacturing Systems*, vol. 55, pp. 132–142, 2020.

[66] P. Majdzik, “Feasible schedule under faults in the assembly system,” in *2020 16th International Conference on Control, Automation, Robotics and Vision (ICARCV)*. IEEE, 2020, pp. 1049–1054.

[67] G. F. Oliveira, R. M. F. Candido, V. M. Gonçalves, C. A. Maia, B. Cottenceau, and L. Hardouin, “Discrete event system control in max-plus algebra: Application to manufacturing systems,” *IFAC-PapersOnLine*, vol. 53, no. 4, pp. 143–150, 2020.

[68] G. Basile, G. Marro, and J. Schumacher, “Controlled and conditioned invariants in linear system theory,” *IEEE Transactions on Automatic Control*, vol. 39, no. 1, pp. 250–250, 1994.

[69] W. M. Wonham, *Linear Multivariable Control: A Geometric Approach*, 3rd ed. New York: Springer-Verlag, 1985.

[70] D. Animobono, D. Scaradozzi, E. Zattoni, A. M. Perdon, and G. Conte, “The model matching problem for max-plus linear systems: A geometric approach,” *IEEE Transactions on Automatic Control*, vol. 68, no. 6, pp. 3581–3587, 2023.

[71] J.-L. Ferrier, S. Lahaye, L. Hardouin, and J.-L. Boimond, “MAISTeR: a user friendly software package for performance analysis and decision, based on (max,+) algebra,” in *IEEE international conference on systems, man and cybernetics*, vol. 3, 2000, pp. 2132–2137.

[72] S. Lahaye, L. Hardouin, and J.-L. Boimond, “Models combination in (max,+) algebra for the implementation of a simulation and analysis software,” *Kybernetika*, vol. 39, no. 2, pp. 143–154, 2003.

[73] B. Cottenceau, L. Hardouin, and I. Ouerghi, “Evolution of Kanban systems thanks to a (max,+)-algebra analysis,” *IFAC Proceedings Volumes*, vol. 39, no. 3, pp. 265–270, 2006.

[74] B. Heidergott, G. J. Olsder, and J. Van Der Woude, *Max Plus at work: modeling and analysis of synchronized systems: a course on Max-Plus algebra and its applications*. Princeton University Press, 2006, vol. 13.

[75] L. Houssin, S. Lahaye, and J.-L. Boimond, “Modelling and control of urban bus networks in dioids algebra,” in *WODES 04*, 2004, pp. IFAC–proceedings.

[76] U. Wikborg and T.-E. Lee, “Noncyclic scheduling for timed discrete-event systems with application to single-armed cluster tools using pareto-optimal optimization,” *IEEE Transactions on Automation Science and Engineering*, vol. 10, no. 3, pp. 699–710, 2012.

[77] J.-H. Kim and T.-E. Lee, “Schedule stabilization and robust timing control for time-constrained cluster tools,” in *IEEE International Conference on Robotics and Automation*, vol. 1, 2003, pp. 1039–1044.

[78] J.-H. Kim, M. Zhou, and T.-E. Lee, “Schedule restoration for single-armed cluster tools,” *IEEE Transactions on Semiconductor Manufacturing*, vol. 27, no. 3, pp. 388–399, 2014.

[79] S.-G. Ko, T.-S. Yu, and T.-E. Lee, “Scheduling dual-armed cluster tools for concurrent processing of multiple wafer types with identical job flows,” *IEEE Transactions on Automation Science and Engineering*, vol. 16, no. 3, pp. 1058–1070, 2018.

[80] B. Addad, S. Amari, and J.-J. Lesage, “Analytic calculus of response time in networked automation systems,” *IEEE Transactions on Automation Science and Engineering*, vol. 7, no. 4, pp. 858–869, 2010.

[81] C. Paya, E. Le Corronc, Y. Pencolé, and P. Vialletelle, “Observer-based detection and localization of time shift failures in (max,+)-linear systems,” in *2021 IEEE 17th International Conference on Automation Science and Engineering (CASE)*. IEEE, 2021, pp. 545–550.

[82] A. Sahuguède, E. Le Corronc, and Y. Pencolé, “Design of indicators for the detection of time shift failures in (max,+)-linear systems,” *IFAC-PapersOnLine*, vol. 50, no. 1, pp. 6813–6818, 2017.

[83] E. Le Corronc, A. Sahuguède, Y. Pencolé, and C. Paya, “Localization of time shift failures in (max,+)-linear systems,” *IFAC-PapersOnLine*, vol. 51, no. 7, pp. 186–191, 2018.

[84] L. Hardouin, B. Cottenceau, S. Lagrange, and E. Le Corronc, “Performance analysis of linear systems over semiring with additive inputs,” in *2008 9th International Workshop on Discrete Event Systems*. IEEE, 2008, pp. 43–48.

[85] H. Al Bermanei, J. M. Böling, and G. Högnäs, “Modeling and scheduling of production systems by using max-plus algebra,” *Flexible Services and Manufacturing Journal*, pp. 1–22, 2023.

[86] S. Gaubert and J. Mairesse, “Modeling and analysis of timed Petri nets using heaps of pieces,” in *1997 European Control Conference (ECC)*. IEEE, 1997, pp. 754–759.

[87] T. J. van den Boom and B. De Schutter, “Modelling and control of discrete event systems using switching max-plus-linear systems,” *Control engineering practice*, vol. 14, no. 10, pp. 1199–1211, 2006.

[88] B. Kersbergen, J. Rudan, T. van den Boom, and B. De Schutter, “Towards railway traffic management using switching max-plus-linear systems,” *Discrete Event Dynamic Systems*, vol. 26, no. 2, pp. 183–223, 2016.

[89] S. Aberkane, R. Kara, and S. Amari, “Modelling and feedback control for a class of Petri nets with shared resources subject to strict time constraints using max-plus algebra,” *International Journal of Systems Science*, vol. 52, no. 14, pp. 3060–3075, 2021.

[90] D. Animobono, “A structural geometric approach to the model matching problem for max-plus linear systems,” Ph.D. dissertation, Università Politecnica delle Marche, 2023.

[91] D. Animobono, D. Scaradozzi, E. Zattoni, A. M. Perdon, and G. Conte, “The model matching problem for switching max-plus systems: a geometric approach,” *IFAC-PapersOnLine*, vol. 55, no. 40, pp. 7–12, 2022, 1st IFAC Workshop on Control of Complex Systems (COSY 2022).

[92] K. L. Hitz, “Scheduling of flexible flowshops,” 1979.

[93] J.-S. Song and T.-E. Lee, “Petri net modeling and scheduling for cyclic job shops with blocking,” *Computers & Industrial Engineering*, vol. 34, no. 2, pp. 281–295, 1998.

[94] T.-E. Lee, “Stable earliest starting schedules for cyclic job shops: a linear system approach,” *International Journal of Flexible Manufacturing Systems*, vol. 12, no. 1, pp. 59–80, 2000.

[95] H. P. Hillion and J.-M. Proth, “Performance evaluation of job-shop systems using timed event-graphs,” *IEEE transactions on automatic control*, vol. 34, no. 1, pp. 3–9, 1989.

[96] S. Lahaye, J. L. Boimond, and L. Hardouin, “Linear periodic systems over dioids,” *Discrete Event Dynamic Systems*, vol. 14, no. 2, pp. 133–152, 2004.

[97] B. Cottenceau, S. Lahaye, and L. Hardouin, “Modeling of time-varying (max,+) systems by means of weighted timed event graphs,” *IFAC Proceedings Volumes*, vol. 47, no. 2, pp. 465–470, 2014.

[98] B. Cottenceau, L. Hardouin, and J. Trunk, “Modèles à base d’opérateurs pour les systèmes (max,+) cycliques,” in *MSR 2019-12ème Colloque sur la Modélisation des Systèmes Réactifs, Nov 2019, Angers, France*, 2019.

[99] J. Trunk, “On the modeling and control of extended timed event graphs in dioids,” Ph.D. dissertation, Angers, 2019.

[100] X. David-Henriet, J. Raisch, L. Hardouin, and B. Cottenceau, "Modeling and control for max-plus systems with partial synchronization," *IFAC Proceedings Volumes*, vol. 47, no. 2, pp. 105–110, 2014.

[101] J. Trunk, B. Cottenceau, L. Hardouin, and J. Raisch, "Model decomposition of timed event graphs under partial synchronization in dioids," *IFAC-PapersOnLine*, vol. 51, no. 7, pp. 198–205, 2018.

[102] S. Gaubert and R. Katz, "Rational semimodules over the max-plus semiring and geometric approach to discrete event systems," *Kybernetika*, vol. 40, pp. 153–180, 2004.

[103] R. D. Katz, "Max-plus (A, B)-invariant spaces and control of timed discrete-event systems," *IEEE Transactions on Automatic Control*, vol. 52, no. 2, pp. 229–241, 2007.

[104] M. Di Loreto, S. Gaubert, R. D. Katz, and J.-J. Loiseau, "Duality between invariant spaces for max-plus linear discrete event systems," *SIAM Journal on Control and Optimization*, vol. 48, no. 8, pp. 5606–5628, 2010.

[105] L. Hardouin, M. Lhommeau, and Y. Shang, "Towards geometric control of max-plus linear systems with applications to manufacturing systems," in *2011 50th IEEE Conference on Decision and Control and European Control Conference*. IEEE, 2011, pp. 1149–1154.

[106] B. De Schutter, T. van den Boom, J. Xu, and S. S. Farahani, "Analysis and control of max-plus linear discrete-event systems: An introduction," *Discrete Event Dynamic Systems*, vol. 30, no. 1, pp. 25–54, 2019.

[107] L. Houssin, S. Lahaye, and J.-L. Boimond, "Control of (max,+)-linear systems minimizing delays," *Discrete Event Dynamic Systems*, vol. 23, no. 3, pp. 261–276, 2013.

[108] E. Menguy, J.-L. Boimond, L. Hardouin, and J.-L. Ferrier, "Just-in-time control of timed event graphs: update of reference input, presence of uncontrollable input," *IEEE Transactions on Automatic Control*, vol. 45, no. 11, pp. 2155–2159, 2000.

[109] B. Cottenceau, L. Hardouin, J.-L. Boimond, and J.-L. Ferrier, "Model reference control for timed event graphs in dioids," *Automatica*, vol. 37, no. 9, pp. 1451–1458, 2001.

[110] B. De Schutter and T. Van Den Boom, "Model predictive control for max-plus-linear discrete event systems," *Automatica*, vol. 37, no. 7, pp. 1049–1056, 2001.

[111] P. Declerck and A. Guezzi, "Predictive control of timed event graphs with specifications defined by p-time event graphs," *Discrete Event Dynamic Systems*, vol. 24, no. 3, pp. 261–273, 2014.

[112] S. Masuda, "A model predictive control for max-plus-linear systems with interval parameters," in *2006 SICE-ICASE International Joint Conference*. IEEE, 2006, pp. 1096–1099.

[113] P. Declerck, "Trajectory tracking control of a timed event graph with specifications defined by a P-time event graph: On-line control and off-line preparation." *IFAC Proceedings Volumes*, vol. 43, no. 12, pp. 155–160, 2010.

[114] H. Takahashi, H. Goto, and M. Kasahara, "Application of a critical chain project management based framework on max-plus linear systems," in *International Conference on Complex, Intelligent and Software Intensive Systems*. IEEE, 2009, pp. 898–903.

[115] L. Hardouin, C. A. Maia, B. Cottenceau, and M. Lhommeau, "Observer design for $(max, +)$ linear systems," *IEEE Transactions on Automatic Control*, vol. 55, no. 2, pp. 538–543, 2010.

[116] V. M. Gonçalves, C. A. Maia, L. Hardouin, and Y. Shang, "An observer for tropical linear event-invariant dynamical systems," in *53rd IEEE Conference on Decision and Control*. IEEE, 2014, pp. 5967–5972.

[117] P. Declerck, "Estimation, prediction and control in (max,+) systems," *IFAC Proceedings Volumes*, vol. 34, no. 13, pp. 849–854, 2001.

[118] R. Jacob and S. Amari, "Output feedback control of discrete processes under time constraint: application to cluster tools," *International Journal of Computer Integrated Manufacturing*, vol. 30, no. 8, pp. 880–894, 2017.

[119] M. L. J. Hautus, "Controlled invariance in systems over rings," in *Feedback Control of Linear and Nonlinear Systems: Proceedings of the Joint Workshop on Feedback and Synthesis of Linear and Nonlinear Systems*, ser. Lecture Notes in Control and Information Sciences, D. Hinrichsen and A. Isidori, Eds., vol. 39. Springer Berlin Heidelberg, 1982, pp. 107–122.

[120] G. Basile and G. Marro, "Controlled and conditioned invariant subspaces in linear system theory," *Journal of Optimization Theory and Applications*, vol. 3, pp. 306–315, 1969.

[121] W. M. Wonham and A. S. Morse, "Decoupling and pole assignment in linear multivariable systems: a geometric approach," *SIAM J. Control*, vol. 8, pp. 1–18, 1970.

[122] G. Conte and A. M. Perdon, "The disturbance decoupling problem for systems over a ring," *SIAM Journal on Control and Optimization*, vol. 33, no. 3, pp. 750–764, 1995.

[123] C. Cárdenas, J. J. Loiseau, and C. Martinez, "Controlled invariance and dynamic feedback for systems over semirings," in *2015 Proceedings of the Conference on Control and its Applications*. SIAM, 2015, pp. 1–8.

[124] N. Ito and H. Inaba, "Dynamic feedback (A,B)-invariance of submodules for linear systems over commutative Noetherian domains," *Lin. Algebra Appl.*, vol. 282, pp. 123–129, 1998.

[125] S. Amari, I. Demongodin, J. J. Loiseau, and C. Martinez, "Max-plus control design for temporal constraints meeting in timed event graphs," *IEEE Transactions on Automatic Control*, vol. 57, pp. 462–467, 2012.

[126] C. Cárdenas, J. Cardillo, J. J. Loiseau, and C. Martinez, "Control problem in max plus linear model with temporal constraints," *Revista Iberoamericana de Automatica e Informatica Industrial*, vol. 13, pp. 438–449, 2016.

[127] C. A. Maia, C. Andrade, and L. Hardouin, "On the control of max-plus linear system subject to state restriction," *Automatica*, vol. 47, no. 5, pp. 988–992, 2011.

[128] V. M. M. Gonçalves, C. A. Maia, and L. Hardouin, "On max-plus dynamical system theory: the regulation problem," *Automatica*, vol. 75, pp. 202–209, 2017.

[129] V. M. Gonçalves, C. A. Maia, and L. Hardouin, "On the steady-state control of timed event graphs with firing date constraints," *IEEE Transactions on Automatic Control*, vol. 61, pp. 2187–2202, 2016.

[130] C. Kim and T.-E. Lee, "Feedback control of cluster tools for regulating wafer delays," *IEEE Transactions on Automation Science and Engineering*, vol. 13, no. 2, pp. 1189–1199, 2016.

[131] M. Ahmane and L. Truffet, "State feedback control via positive invariance for max-plus linear systems using γ-algorithm," in *IEEE Conference on Emerging Technologies and Factory Automation*, 2006, pp. 217–224.

[132] L. Hardouin, Y. Shang, C. Maia, and B. Cottenceau, "Observer-based controllers for max-plus linear systems," *IEEE Trans. Automatic Control*, vol. 62, pp. 2153–2165, 2017.

[133] V. Gonçalves, C. Maia, and L. Hardouin, "On max-plus linear dynamical system theory: The observation problem," *Automatica*, vol. 105, pp. 103–111, 2019.

[134] L. Hardouin, C. Maia, B. Cottenceau, and R. S. Mendes, "Max-plus linear observer: Application to manufacturing systems," pp. 171–176, 2010.

[135] C. Martinez, R. Kara, A. N. Abdesselam, and J. J. Loiseau, "Systems synchronisation in max-plus algebra: a controlled invariance perspective in memoriam édouard Wagneur," in *1st IFAC Workshop on Control of Complex Systems, COSY)*, vol. 55, no. 40, Bologna, Italy, 2022, pp. 1–6.

[136] C. Cárdenas, J. J. Loiseau, and C. Martinez, "Invariance par retour d'état sur le demi-anneau max-plus," *Modélisation des Systèmes Réactifs (MSR 2017)*, Marseille, France, 2017.

[137] T. Bousch, "Fonctions topicales et causalité," *Bulletin of the Belgian Mathematical Society – Simon Stevin*, vol. 13, pp. 489–498, 2006.

[138] B. Cottenceau, L. Hardouin, J.-L. Boimond, and J.-L. Ferrier, "Synthesis of greatest linear feedback for timed-event graphs in dioid," *IEEE Trans. Automatic Control*, vol. 44, pp. 1258–1262, 1999.

[139] X. Allamigeon and S. Gaubert, "The tropical double description method," in *Proceedings of the 27th Annual Symposium on Theoretical Aspects of Computer Science STACS*, 2010, pp. 47–58.

[140] X. Allamigeon, S. Gaubert, and Goubault, "Computing the vertices of tropical polyhedra using directed hypergraphs," *Discrete & Computational Geometry*, vol. 49, p. 247–279, 2013.

[141] P. Declerck, "Causality phenomenon and compromise technique for predictive control of timed event graphs with specifications defined by P-time event graphs," *12th IFAC International Workshop on Discrete Event Systems*, vol. 47, no. 2, pp. 99–104, 2014.

[142] G. Conte, A. Perdon, and E. Zattoni, "Model matching problems for positive systems," vol. 53, no. 2, pp. 4648–4653, 2020.

[143] G. Conte and A. M. Perdon, "Problems and results in a geometric approach to the theory of systems over rings," in *Linear algebra for control theory.* Springer, 1994, pp. 61–74.

[144] M. Lhommeau, L. Hardouin, and B. Cottenceau, "About disturbance decoupling of timed event graphs in dioids," in *Sixth International Workshop on Discrete Event Systems, 2002. Proceedings.* IEEE, 2002, pp. 203–208.

[145] Y. Shang, L. Hardouin, M. Lhommeau, and C. A. Maia, "An integrated control strategy in disturbance decoupling of max-plus linear systems with applications to a high throughput screening system in drug discovery," in *53rd IEEE Conference on Decision and Control.* IEEE, 2014, pp. 5143–5148.

[146] Y. Shang, L. Hardouin, M. Lhommeau and C.A. Maia, "Open loop controllers to solve the disturbance decoupling problem for max-plus linear systems," in *2013 European Control Conference (ECC)*. IEEE, 2013, pp. 125–130.

[147] Y. Shang, L. Hardouin, M. Lhommeau, and C. A. Maia, "Robust controllers in disturbance decoupling of uncertain max-plus linear systems: an application to a high throughput screening system for drug discovery," in *2016 13th International Workshop on Discrete Event Systems*. IEEE, 2016, pp. 404–409.

[148] A. Oke, L. Hardouin, M. Lhommeau, and Y. Shang, "Observer-based controller for disturbance decoupling of max-plus linear systems with applications to a high throughput screening system in drug discovery," in *2017 IEEE 56th Annual Conference on Decision and Control (CDC)*, 2017, pp. 4242–4247.

[149] M. Lhommeau, L. Hardouin, and B. Cottenceau, "Disturbance decoupling of timed event graphs by output feedback controller," *WODES 2002, Workshop on Discrete Event Systems*, Zaragoza, 2002.

[150] R. Santos-Mendes, B. Cottenceau, and L. Hardouin, "Adaptive feedback control for (max,+)-linear systems," in *2005 IEEE Conference on Emerging Technologies and Factory Automation*, vol. 2. IEEE, 2005, pp. 6–pp.

[151] L. Libeaut and J. J. Loiseau, "Model matching for timed event graphs," *IFAC Proceedings Volumes*, vol. 29, no. 1, pp. 4807–4812, 1996, 13th World Congress of IFAC, 1996, San Francisco USA, 30 June - 5 July.

[152] C. A. Maia, L. Hardouin, R. Santos-Mendes, and B. Cottenceau, "On the model reference control for max-plus linear systems," in *Proceedings of the 44th IEEE Conference on Decision and Control*. IEEE, 2005, pp. 7799–7803.

[153] V. Kucera, *Analysis and Design of Discrete Linear Control Systems*. Prague: Academia, 1991.

[154] D. Animobono, D. Scaradozzi, E. Zattoni, A. M. Perdon, and G. Conte, "The model matching problem for periodic max-plus systems," Submitted.

[155] T. I. Fossen, "Marine control systems–guidance. navigation, and control of ships, rigs and underwater vehicles," *Marine Cybernetics, Trondheim, Norway, Org. Number NO 985 195 005 MVA, www. marinecybernetics. com*, 2002.

[156] T. I. Fossen, *Handbook of marine craft hydrodynamics and motion control*. John Wiley & Sons, 2011.

[157] D. Costa, "Development of biomimetic propulsiv systems in a multiphysics environment," Ph.D. dissertation, Università Politecnica delle Marche, 2019.

[158] N. Ciuccoli, "Intelligent systems for the exploration of structured and complex environments," Ph.D. dissertation, Università Politecnica delle Marche, 2019.

[159] W. Ali Waqar, "Studio e simulazioni di sistemi NGC per robot marini biomorfi," Master's thesis, Università Politecnica delle Marche, 2019.

[160] J. Stuelpnagel, "On the parametrization of the three-dimensional rotation group," *SIAM Review*, vol. 6, no. 4, pp. 422–430, 1964.

[161] E. Omerdic, *Thruster fault diagnosis and accommodation for overactuated open-frame underwater vehicles.* University of South Wales (United Kingdom), 2004.

[162] G. Antonelli, *Modelling of underwater robots.* Springer, 2014.

[163] D. Scaradozzi, N. Ciuccoli, A. Pugliese, V. Bartolucci, S. M. Egi, M. Memişoğlu, and T. Özyiğit, "A novel DPV as a holistic platform for real-time physiological status assessment of divers," in *2021 29th Mediterranean Conference on Control and Automation (MED).* IEEE, 2021, pp. 280–285.

[164] V. Bartolucci, N. Ciuccoli, F. Prendi, L. Screpanti, and D. Scaradozzi, "A digital twin infrastructure for designing an underwater survey with a professional DPV," in *2022 30th Mediterranean Conference on Control and Automation (MED).* IEEE, 2022, pp. 829–834.

[165] L. Paull, S. Saeedi, M. Seto, and H. Li, "AUV navigation and localization: A review," *IEEE Journal of oceanic engineering*, vol. 39, no. 1, pp. 131–149, 2013.

[166] G. Fukuda, D. Hatta, X. Guo, and N. Kubo, "Performance evaluation of IMU and DVL integration in marine navigation," *Sensors*, vol. 21, no. 4, p. 1056, 2021.

[167] P. Butkovic and G. Hegedüs, "An elimination method for finding all solutions of the system of linear equations over an extremal algebra," *Ekonomicko-matematicky Obzor*, vol. 20, no. 2, pp. 203–215, 1984.

[168] M. Michael, C. Guy, G. Stéphane, and Q. Jean-Pierre, "Max-Plus Toolbox of Scilab," http://www.cmap.polytechnique.fr/~gaubert/MaxplusToolbox.html, 2009, accessed: 2023-11-27.

[169] J. Stańczyk, "Max-plus algebra toolbox for Matlab," 2016.

[170] ScicosLab, "ScicosLab," http://scicoslab.org, 2007, accessed: 2023-11-27.